

SMR 1302 - 17

WINTER SCHOOL ON LASER SPECTROSCOPY AND APPLICATIONS

19 February - 2 March 2001

***Photoelectron Spectroscopy
with and without Photoelectrons***

Martin COCKETT
Department of Chemistry, University of York
Heslington, York, U.K.

These are preliminary lecture notes, intended only for distribution to participants.



THE UNIVERSITY *of York*

**Photoelectron Spectroscopy with
and without photoelectrons:
*From the photoelectric effect to ZEKE
spectroscopy***

Martin Cockett

*Department of Chemistry
University of York
Heslington, York
UK.*

Outline

- 1) The origins of photoelectron spectroscopy
 - Photoelectric effect*
 - Development of UVPES & XPS*
 - Experimental methods*
 - Factors affecting Resolution*
- 2) Applications
 - Atoms*
 - Diatom Molecules*
 - Molecular Orbital Theory*
 - Koopmans' Theorem – closed and open shell*
 - Autoionisation*
 - Polyelectronic molecules*
- 3) The quest for improved resolution
 - Refinement of experimental conditions*
 - Laser REMPI-PES – state selection*
- 4) Dispensing with energy analysis
 - Threshold Photoelectron Spectroscopy*
 - Autoionisation revisited*
- 5) The next step: ZEKE spectroscopy
 - Concepts*
 - Comparisons to PES*
 - Rydberg states and Field Ionisation*
 - Experimental details*
 - Improving resolution*
- 6) Case Studies: *Electronically excited states, autoionisation, Rydberg excited van der Waals complexes.*

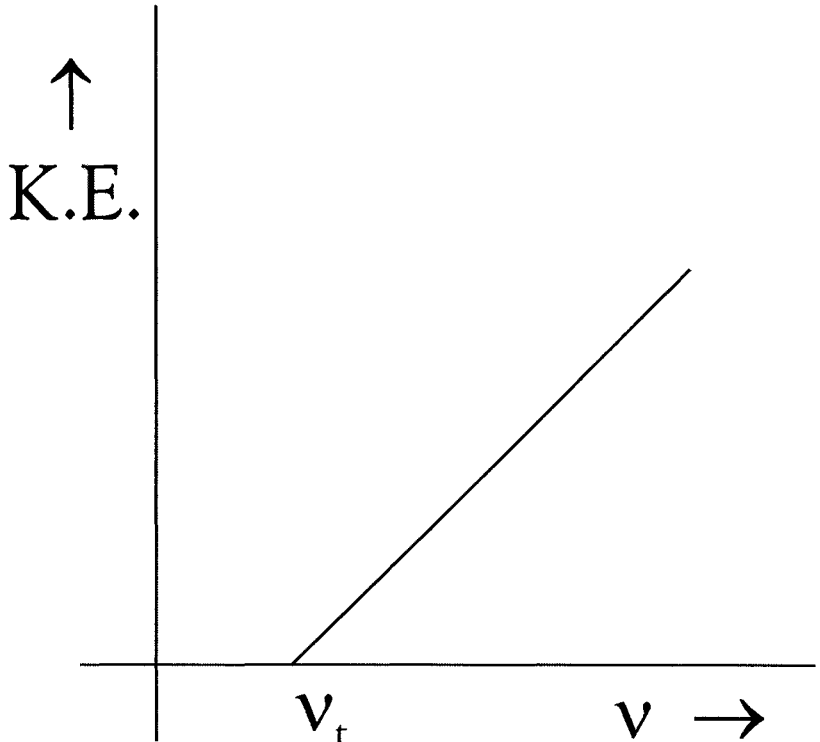
Origins of Photoelectron Spectroscopy

(a) The Photoelectric Effect

- First observed on surfaces of easily ionisable metals (e.g. Alkali metals).

$$h\nu = \frac{1}{2}m_e v^2 + \Phi$$

$$\text{K.E.} \propto h\nu.$$



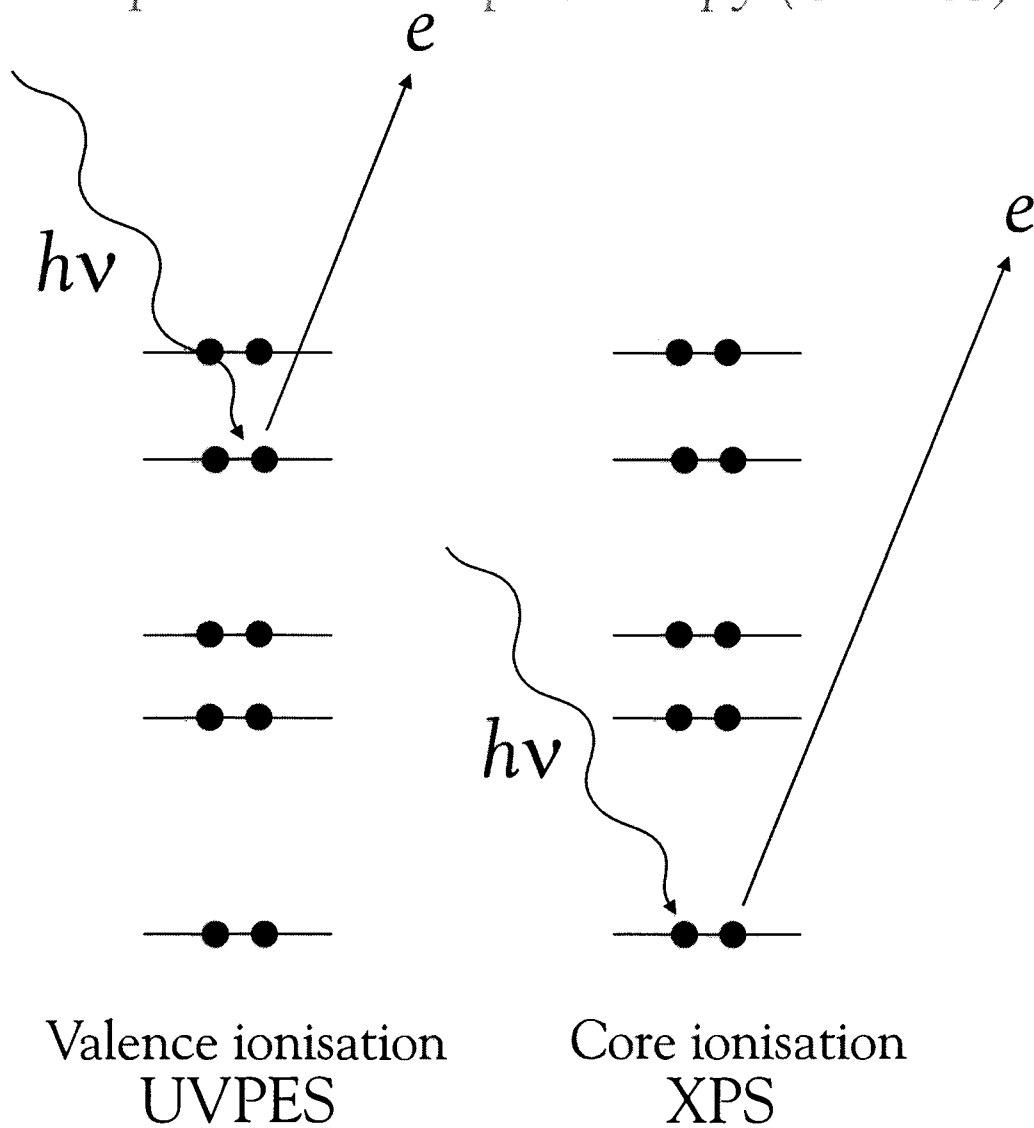
- Einstein¹ developed theory in 1905

For alkali metal surfaces, Φ is of the order of a few eV which requires near UV radiation.

¹ A. Einstein, Ann. Physik., 31 (1905) 132.

(b) The development of Photoelectron spectroscopy

- 1956 Siegbahn² invents X-ray photoelectron spectroscopy (XPS).
- 1962 Turner et al.³ and Vilesov et al.⁴ develop ultraviolet photoelectron spectroscopy (UVPES).



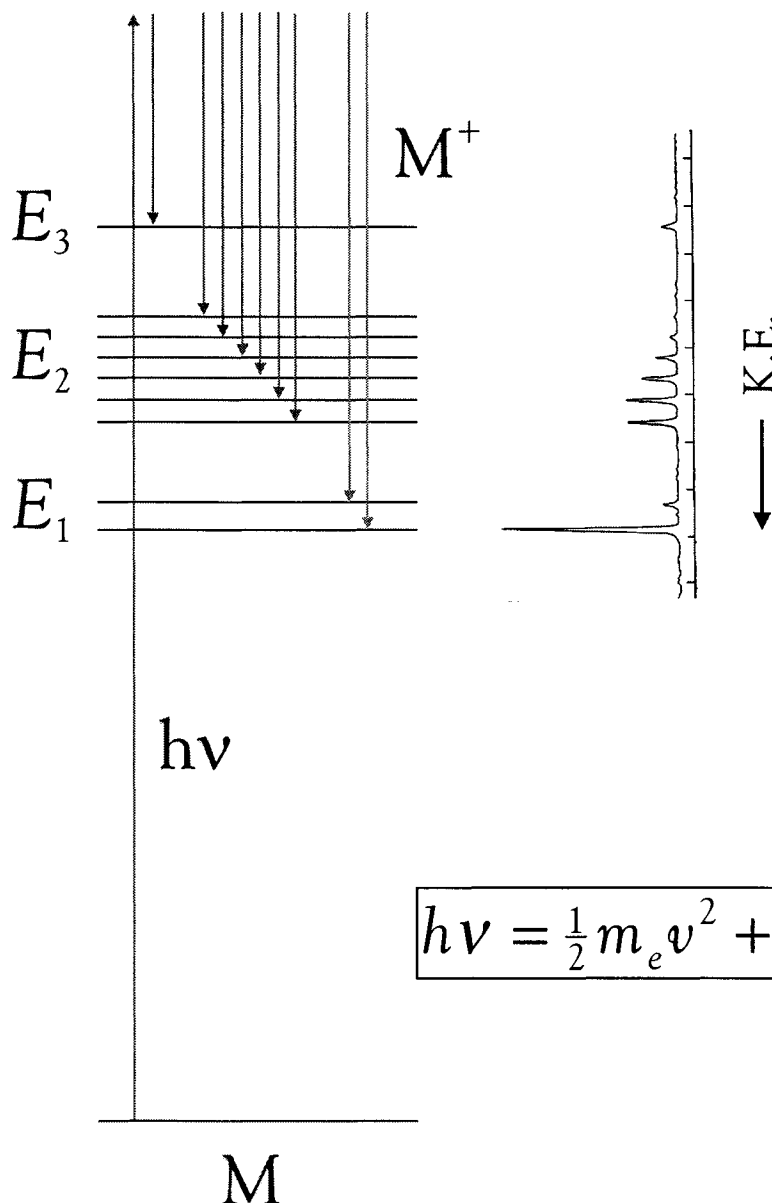
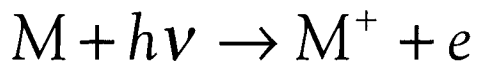
² K. Seibgahn and K. Everson, *Nucl. Phys.*, **1** (1956) 137

³ M.I. Al-Joboury and D.W. Turner, *J. Chem. Phys.*, **37**, (1962) 3007.

⁴ F.I. Vilesov, B.L. Kurbatov and A.N. Terenin, *Dokl. Akad. Nauk SSSR*, **138** (1961) 1329.

How does it work?

UVPES (gas phase) and XPS (solid state & gas phase) both involve the following process:

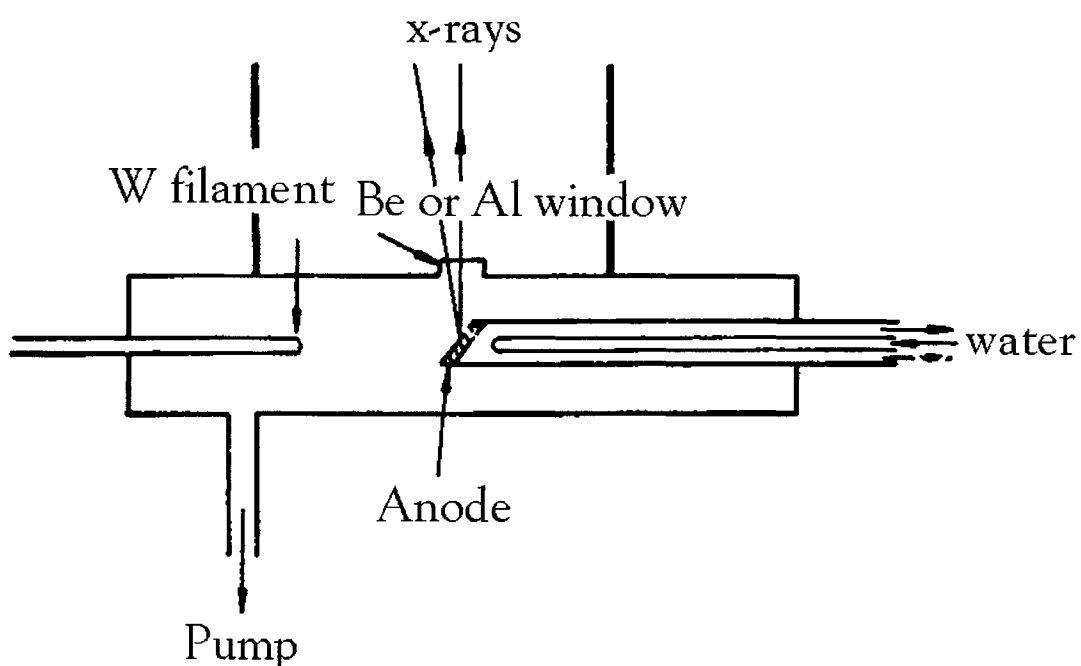
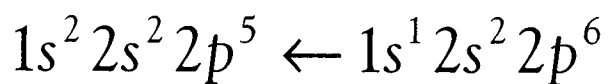


The kinetic energy of the photoelectrons depends on the photon energy and the final state of the ion.

Experimental Methods

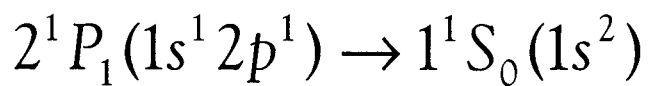
(a) Photon Source (preferably *monochromatic*)

XPS AlK α (1487 eV) or MgK α (1253 eV)

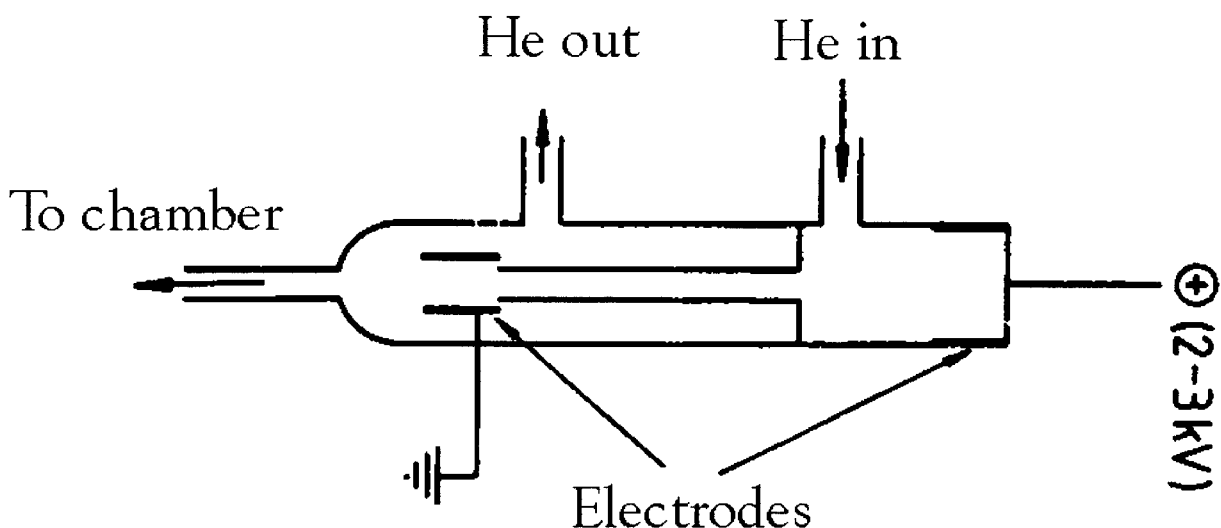
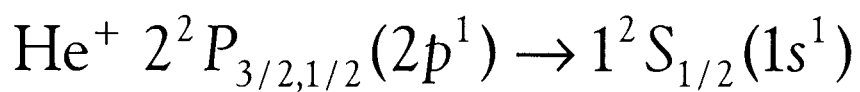


UVPES

- HeI (21.22 eV)



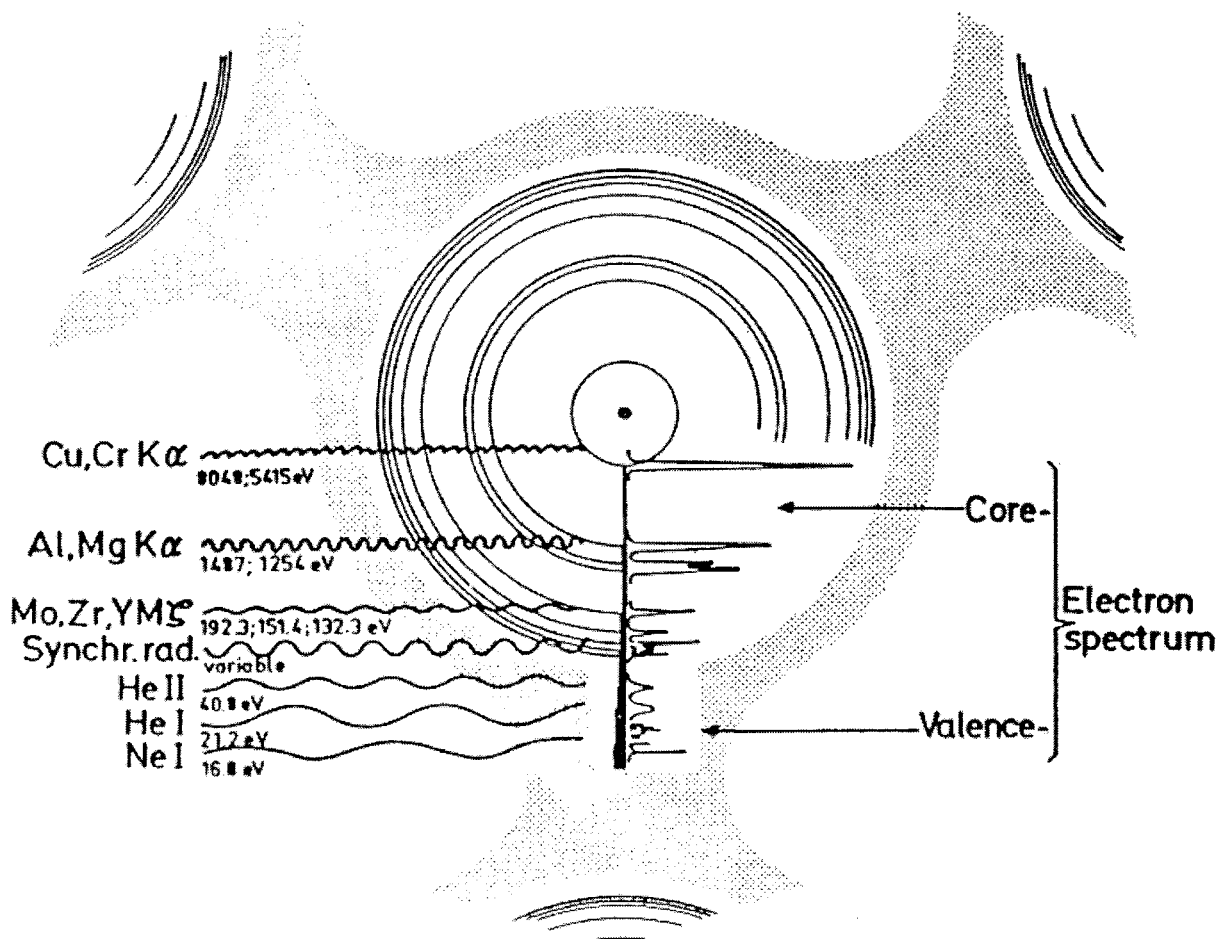
- HeII (40.8 eV)



- NeI (16.67 and 16.85 eV)



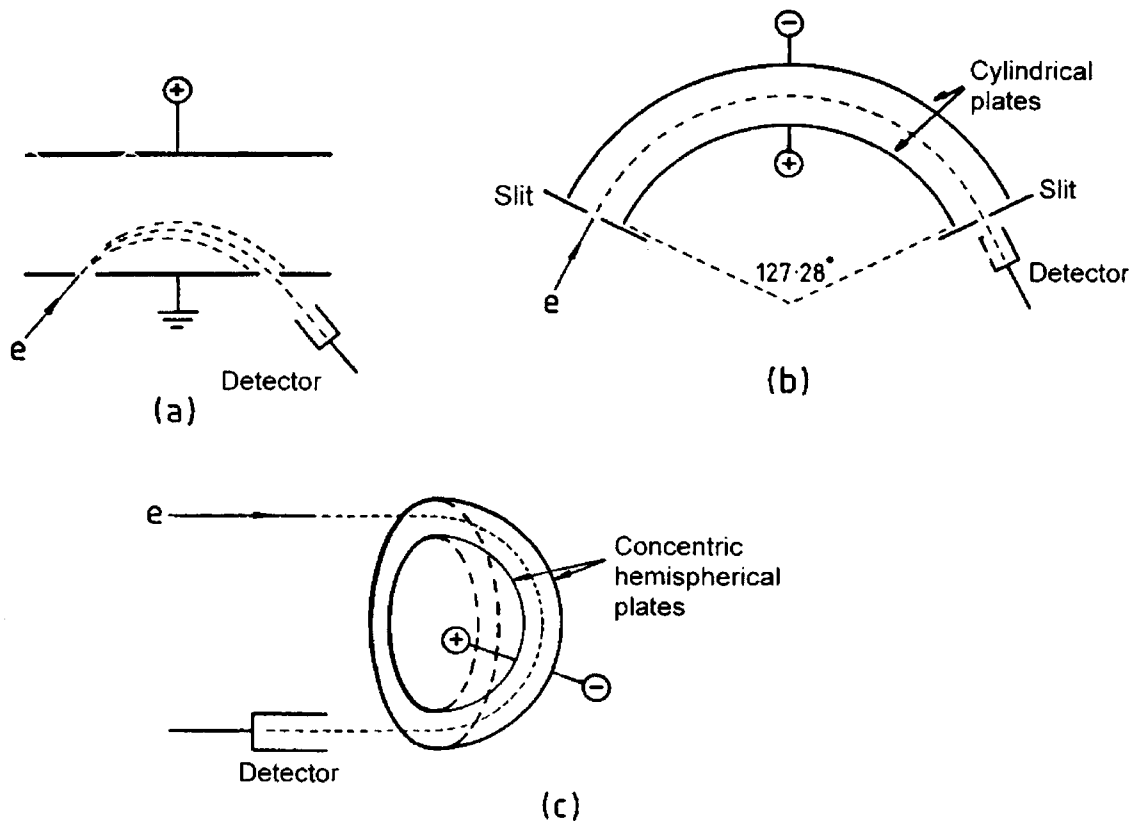
Summary



Types of radiation used in PES correlated to the regions of electronic structure probed.

(b) Kinetic energy analysis

Deflection analysers: *Electrons with different energies follow different paths when subject to magnetic or electric fields*



(a) Parallel plate, (b) 127° cylindrical and (c) hemispherical analysers

Electrons of a kinetic energy E will reach the detector when

$$V = \frac{E}{e} \left(\frac{R_2}{R_1} - \frac{R_1}{R_2} \right)$$

for plates of radii R_1 and R_2 ($R_2 > R_1$).

(c) Resolution

(i) Radiation linewidth $\approx 3\text{--}4 \text{ meV (He I)}$
 $\approx 0.2\text{--}1 \text{ eV (AlK}\alpha\text{)}$

(ii) Doppler broadening $\approx 4 \text{ meV}$ ($m=100$,
 $T=300 \text{ K}$, $eKE = 10 \text{ eV}$)

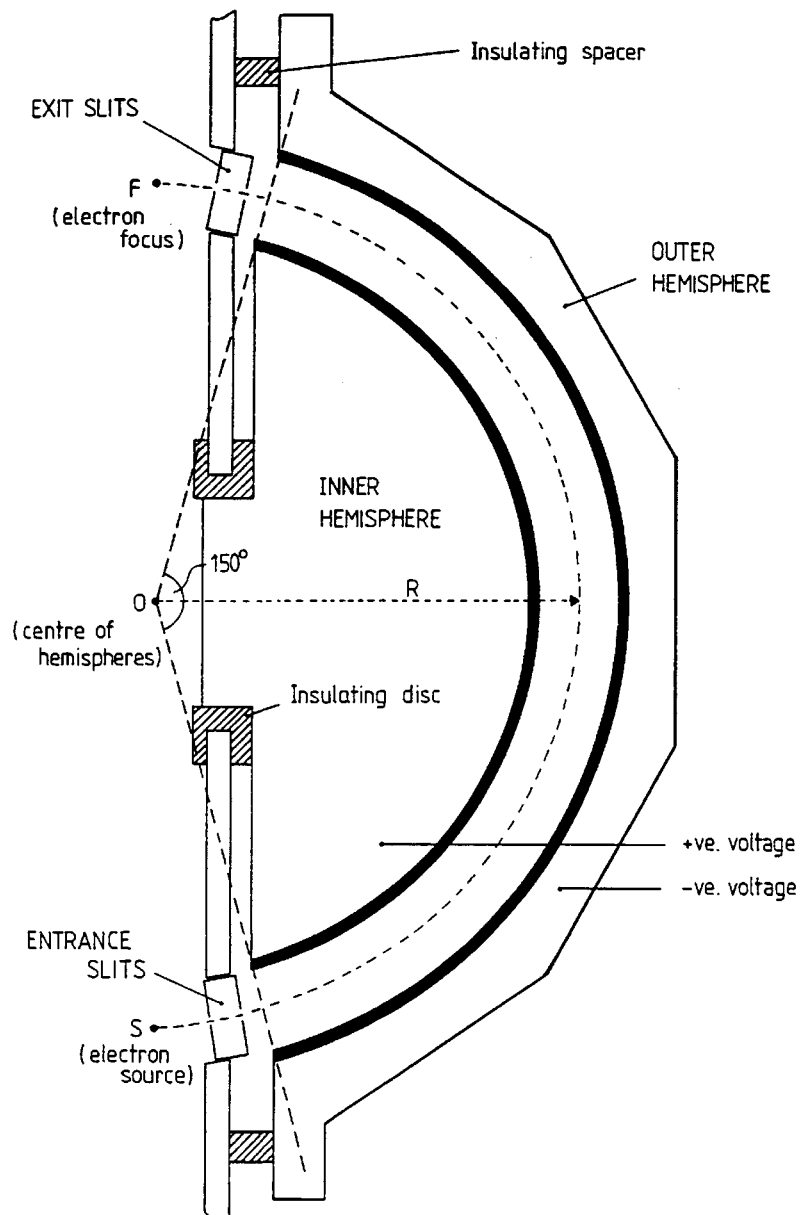
(iii) The analyser

$$\Delta E = \frac{1}{2}e \frac{V}{(R_2 - R_1)} \Delta R$$

where

$$\Delta R \approx S/2$$

is the variation in R
and S is the total slit
width.



Other factors affecting resolution

$$\Delta E = \frac{1}{2} e \frac{V}{(R_2 - R_1)} \quad \Delta R = \frac{E}{R} \Delta R \approx \frac{E S}{R^2}$$

- The resolution improves as S is reduced (but transmission suffers).
- Resolution improves as the kinetic energy is reduced (but transmission suffers).
- ΔR depends on other factors such as stray electric/magnetic fields, local point charges (dirt!).

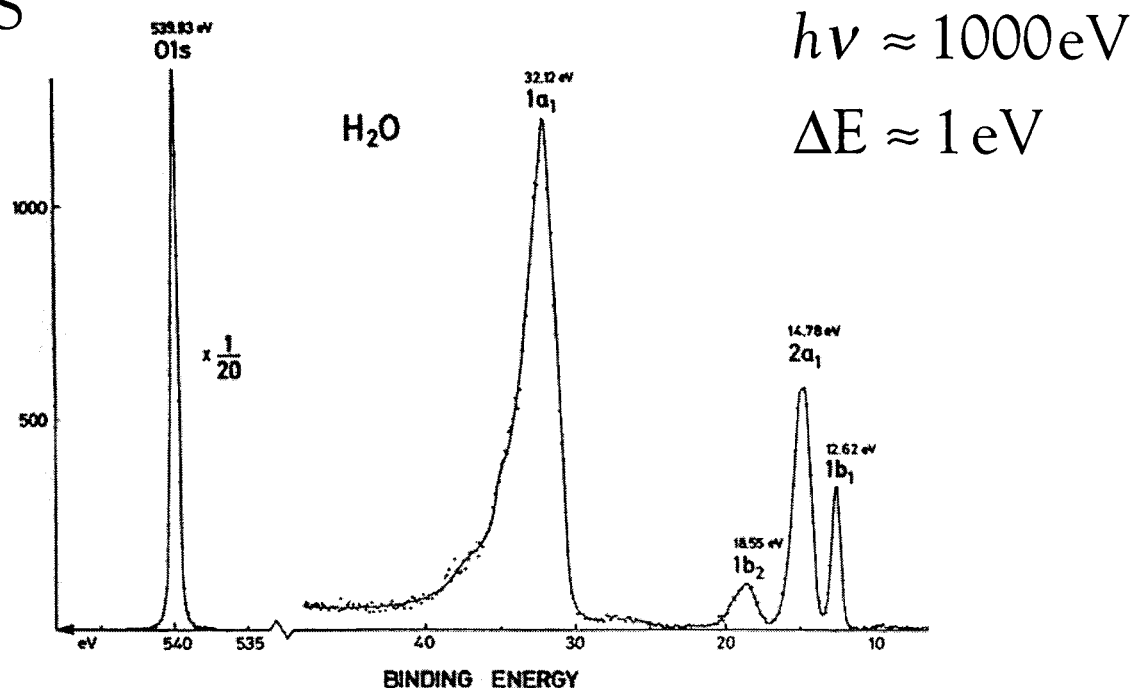
PES *always involves a compromise between resolution and transmission.*

- Typical resolution $\approx 10\text{-}20 \text{ meV} = 80\text{-}160 \text{ cm}^{-1}$

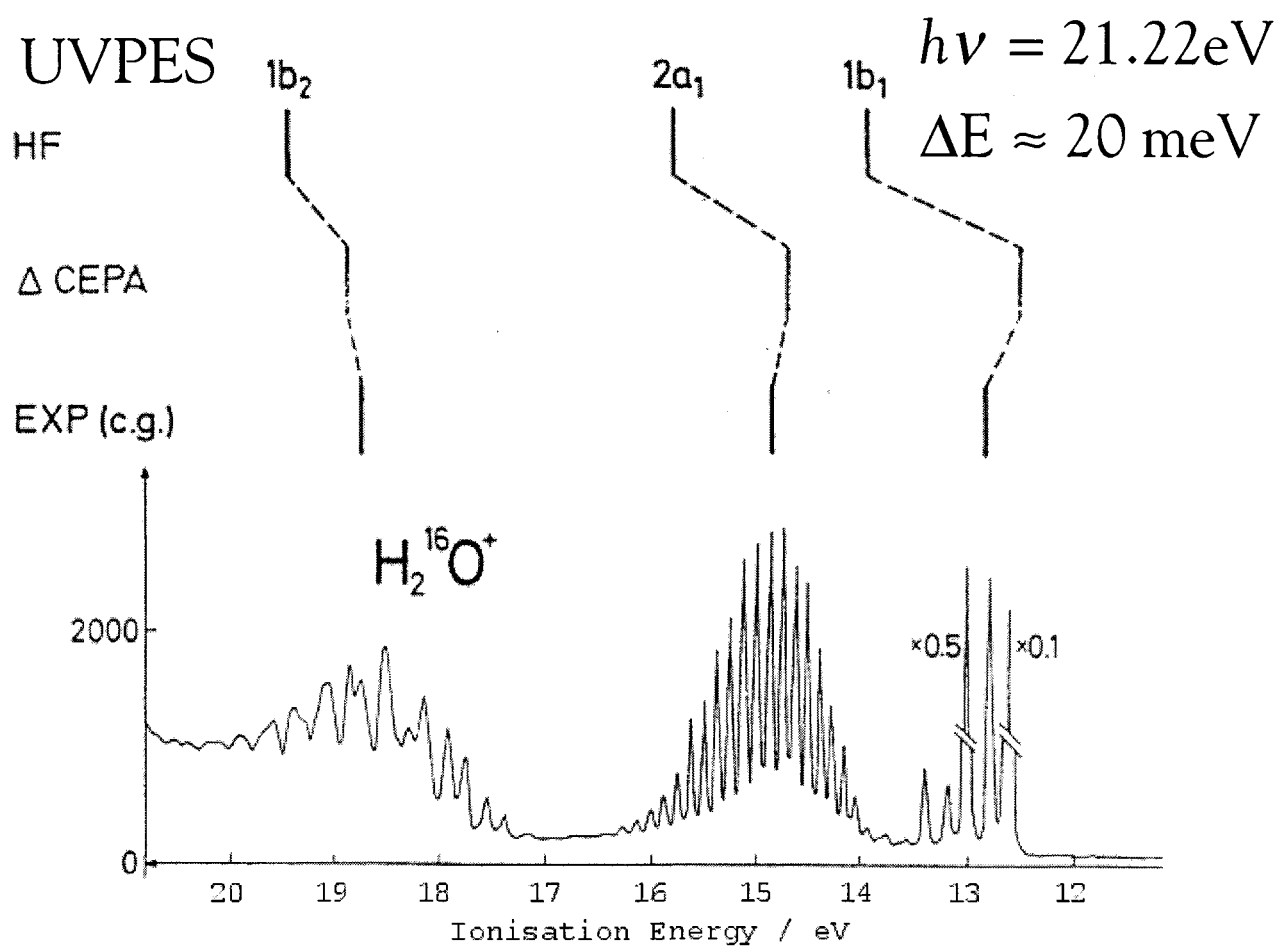
Vibrations – YES (mostly)
Rotations – NO!

XPS vs UV-PES

(a) XPS



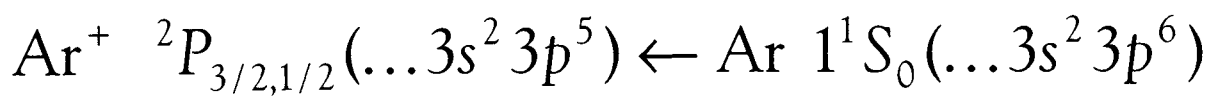
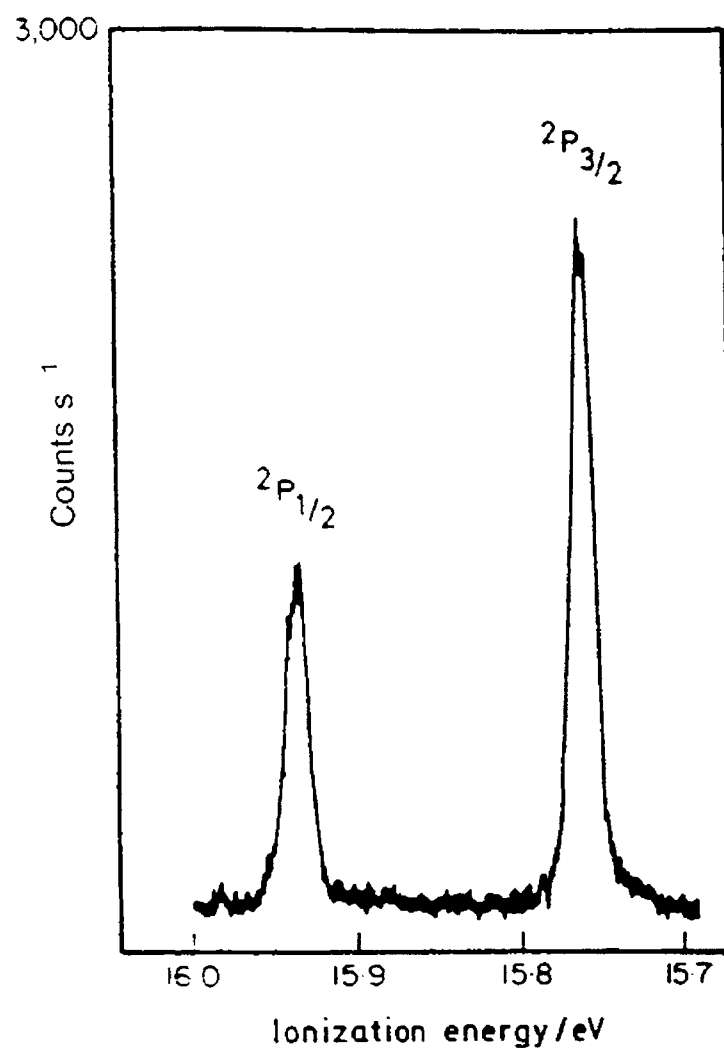
(b) UV-PES



UVPES of Atoms

PES of atoms provides little additional information over higher resolution techniques

$$KE = h\nu - IE_i$$



UVPES of Diatomic Molecules

$$KE = h\nu - IE_i - \Delta E_{vib} - \Delta E_{rot}$$

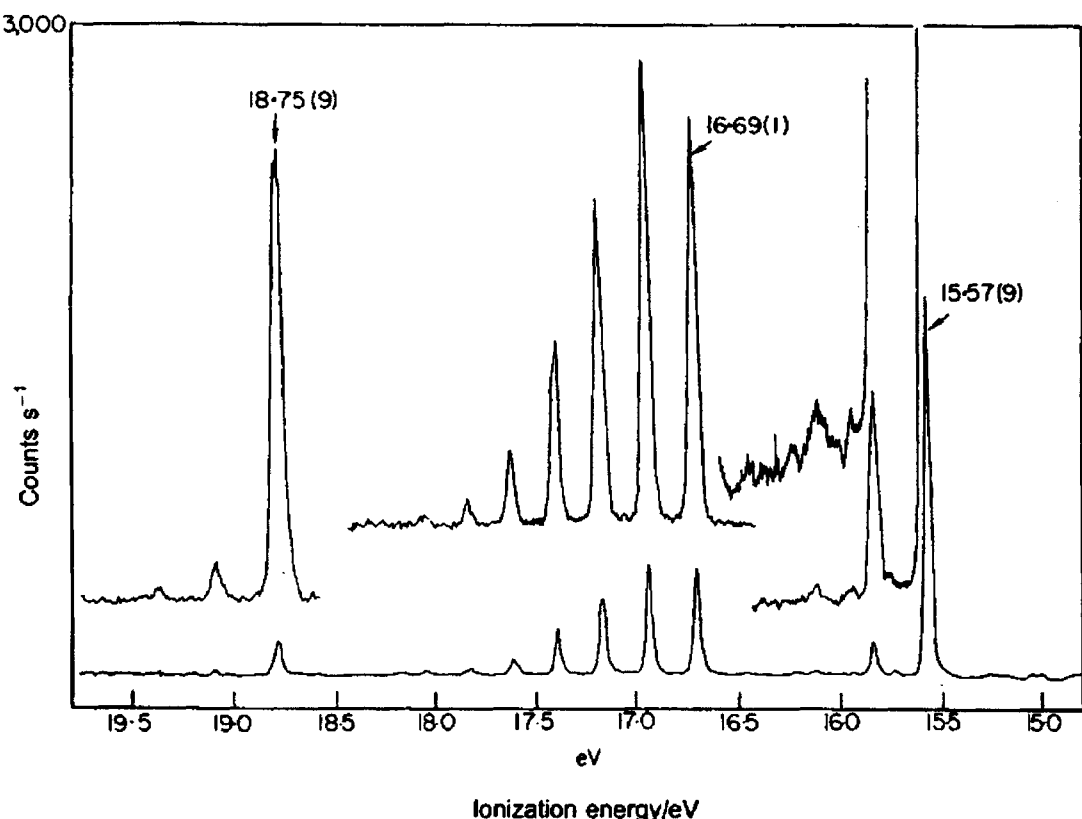
where ΔE_{vib} and ΔE_{rot} represent the internal vibrational and rotational energy of the ion.

How are molecular photoelectron spectra different from atomic PE spectra?



ΔE_{vib} and ΔE_{rot}

The Photoelectron Spectrum of Nitrogen



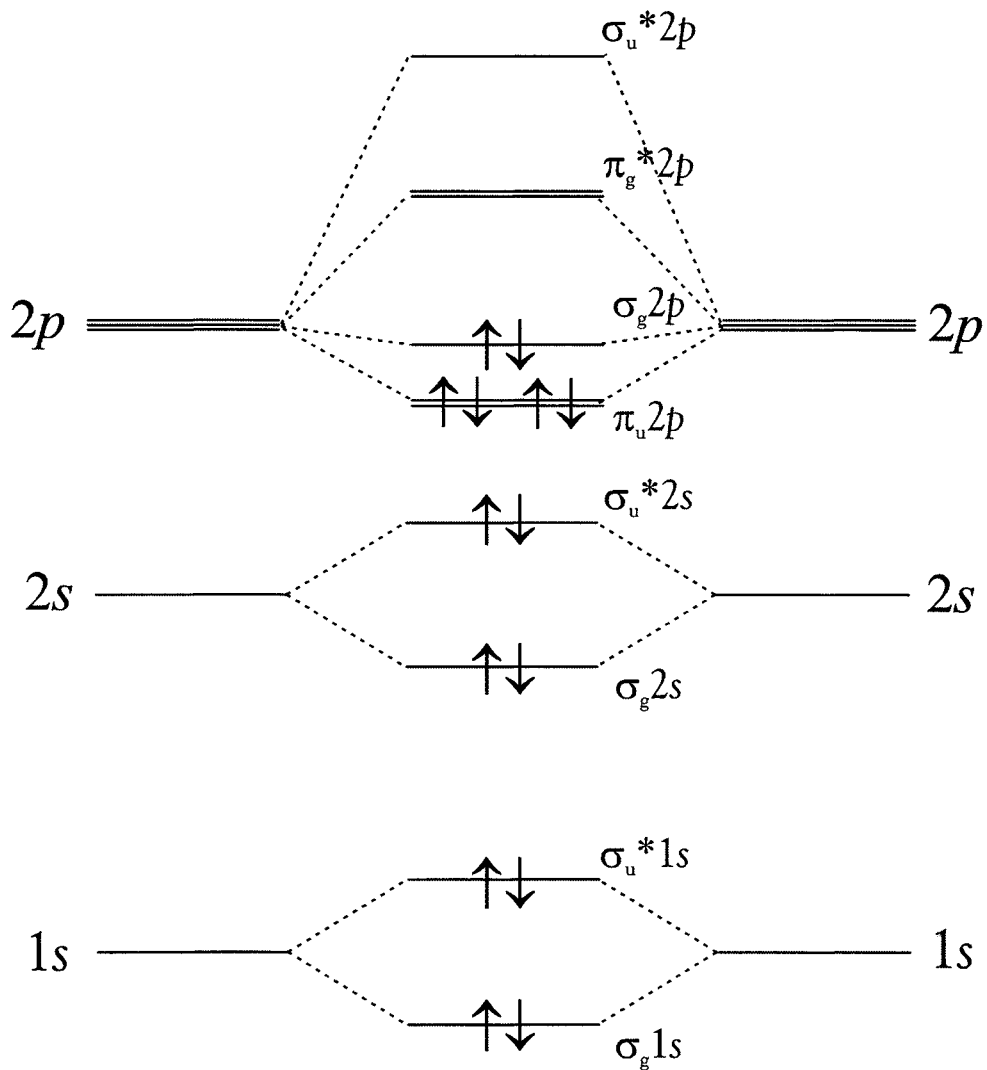
How can we explain the structure in a PE spectrum?

Molecular Orbital Theory

Molecular orbitals are constructed from linear combinations of atomic orbitals (LCAO)

$$\psi = \sum_i c_i \phi_i$$

MO diagram for N₂

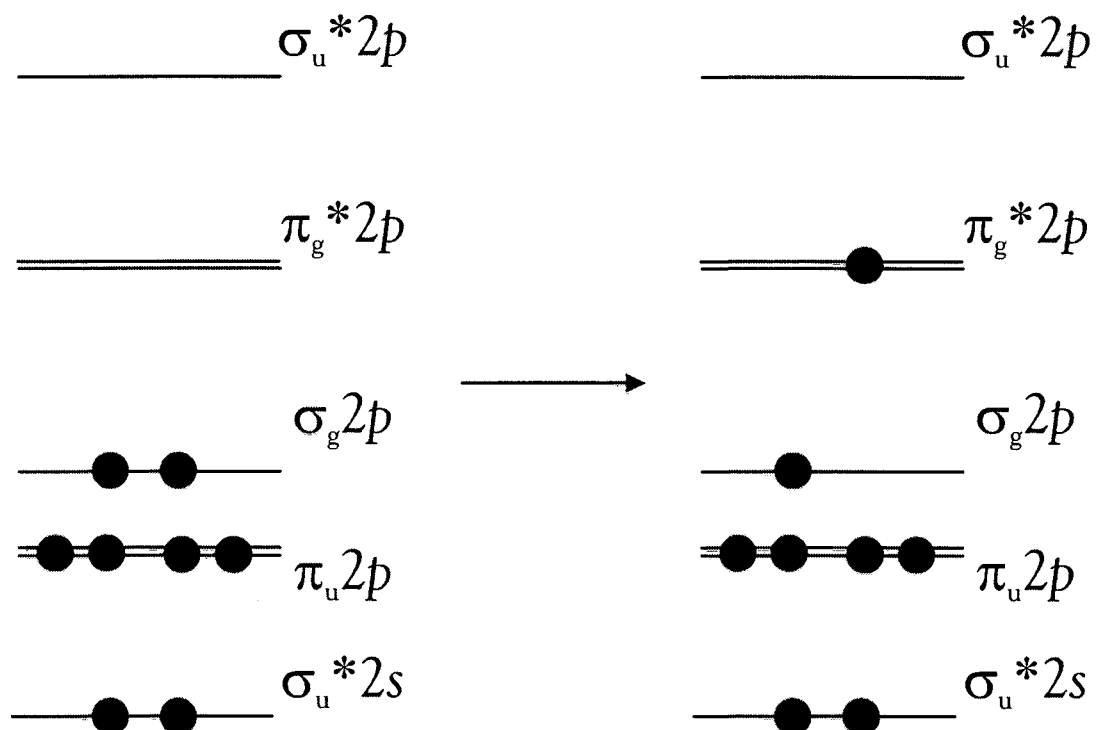


What is an electronic transition?

(a) The One-electron description

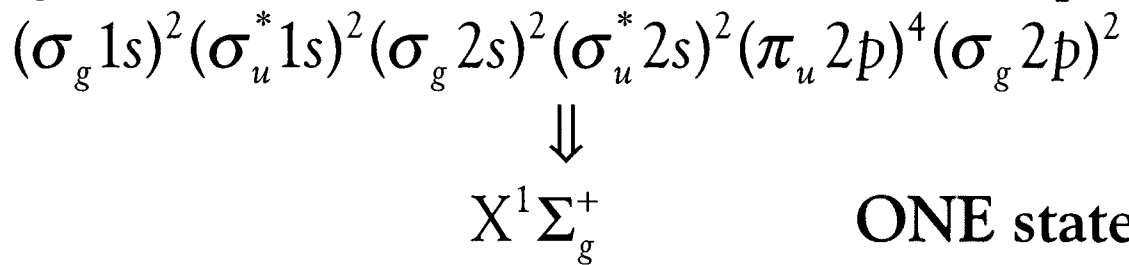
The excitation of an electron from an occupied MO to an unoccupied MO.

e.g. N_2

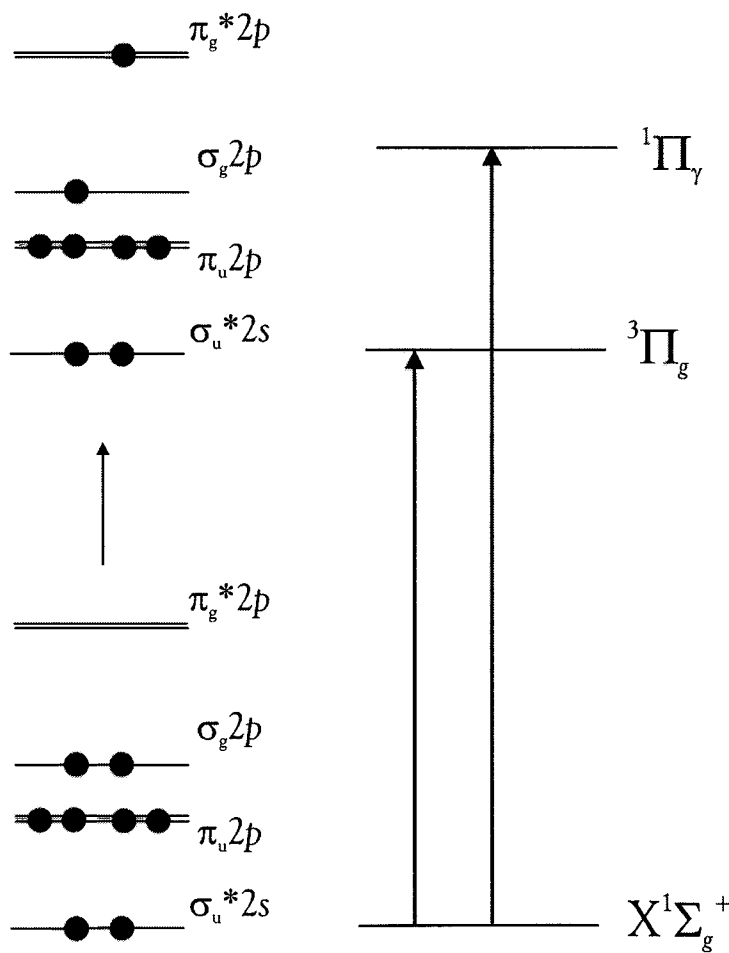
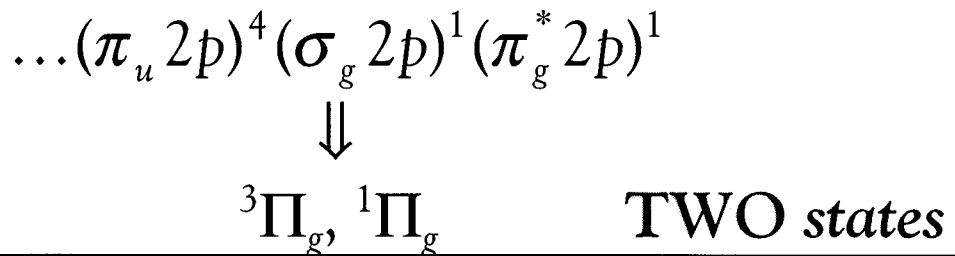


(b) Electronic transitions really occur between states!

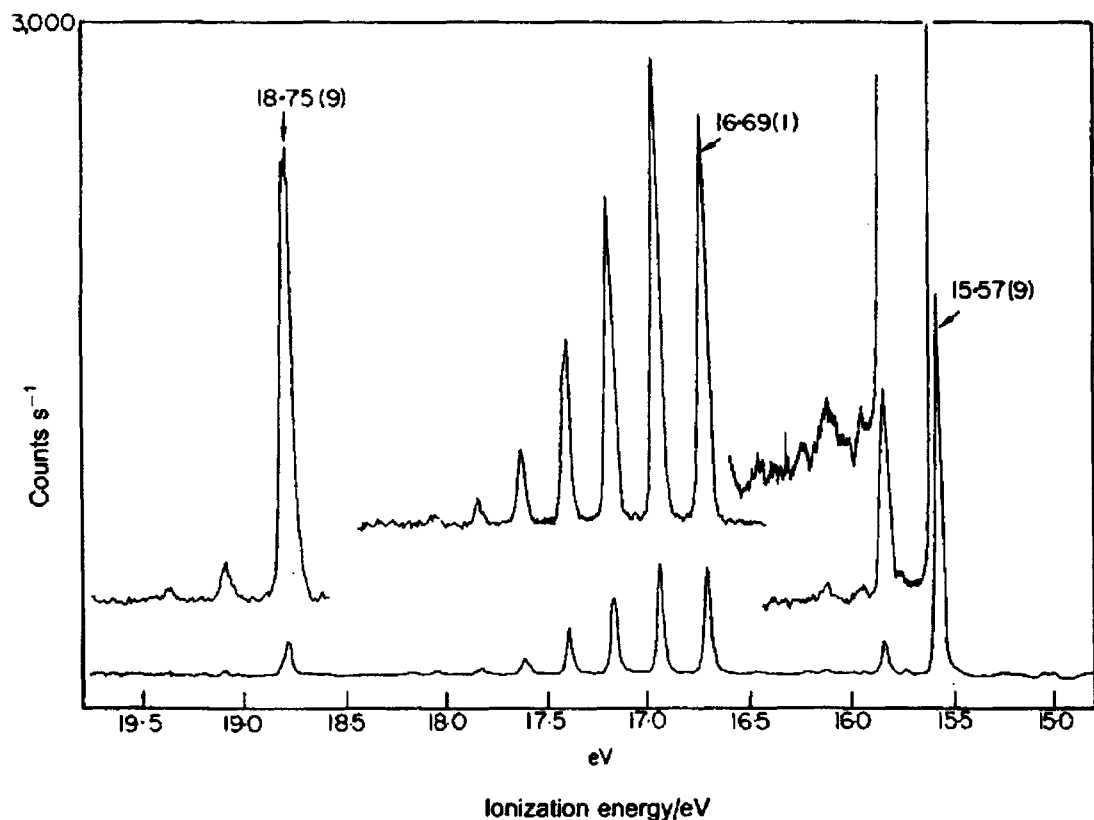
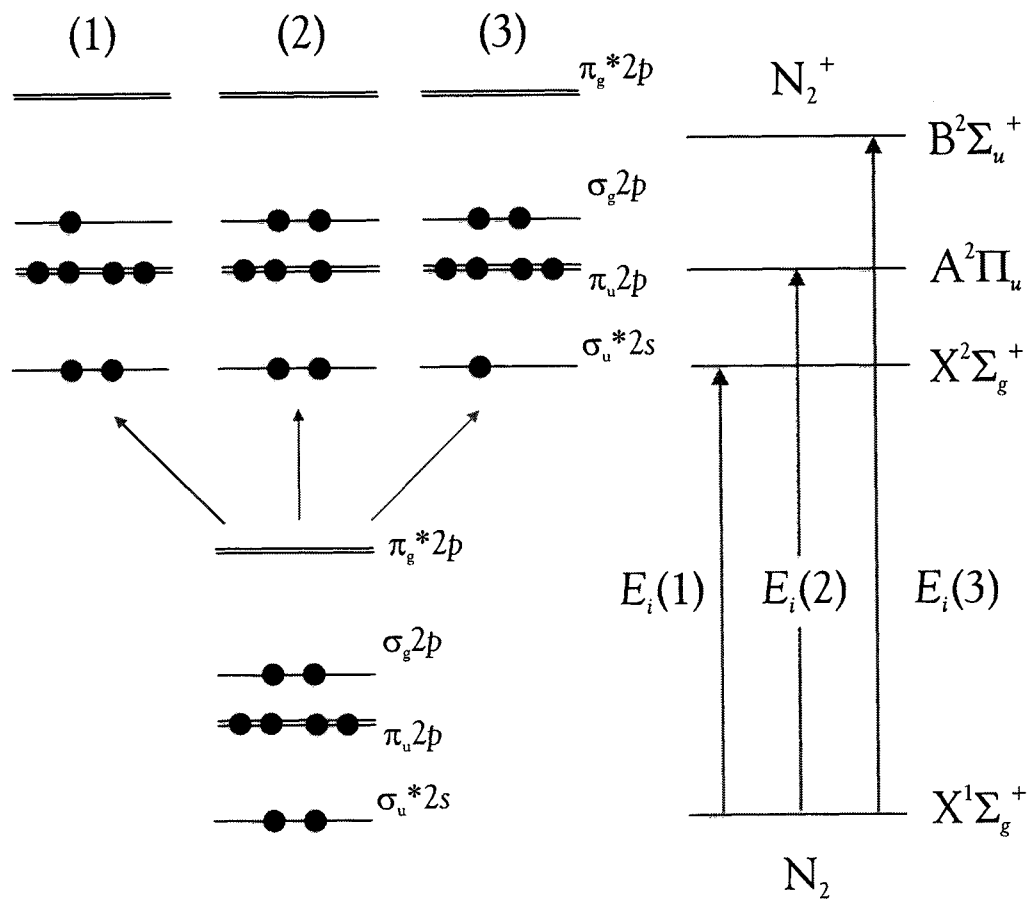
The ground electronic state configuration of N₂:



The excited configuration of N₂



(c) The one-electron description provides a good representation of ionisation in most closed shell molecules



Koopmans' Theorem

'For a closed shell molecule, the ionisation energy for an electron in a particular orbital is approximately equal to the negative of the orbital energy'

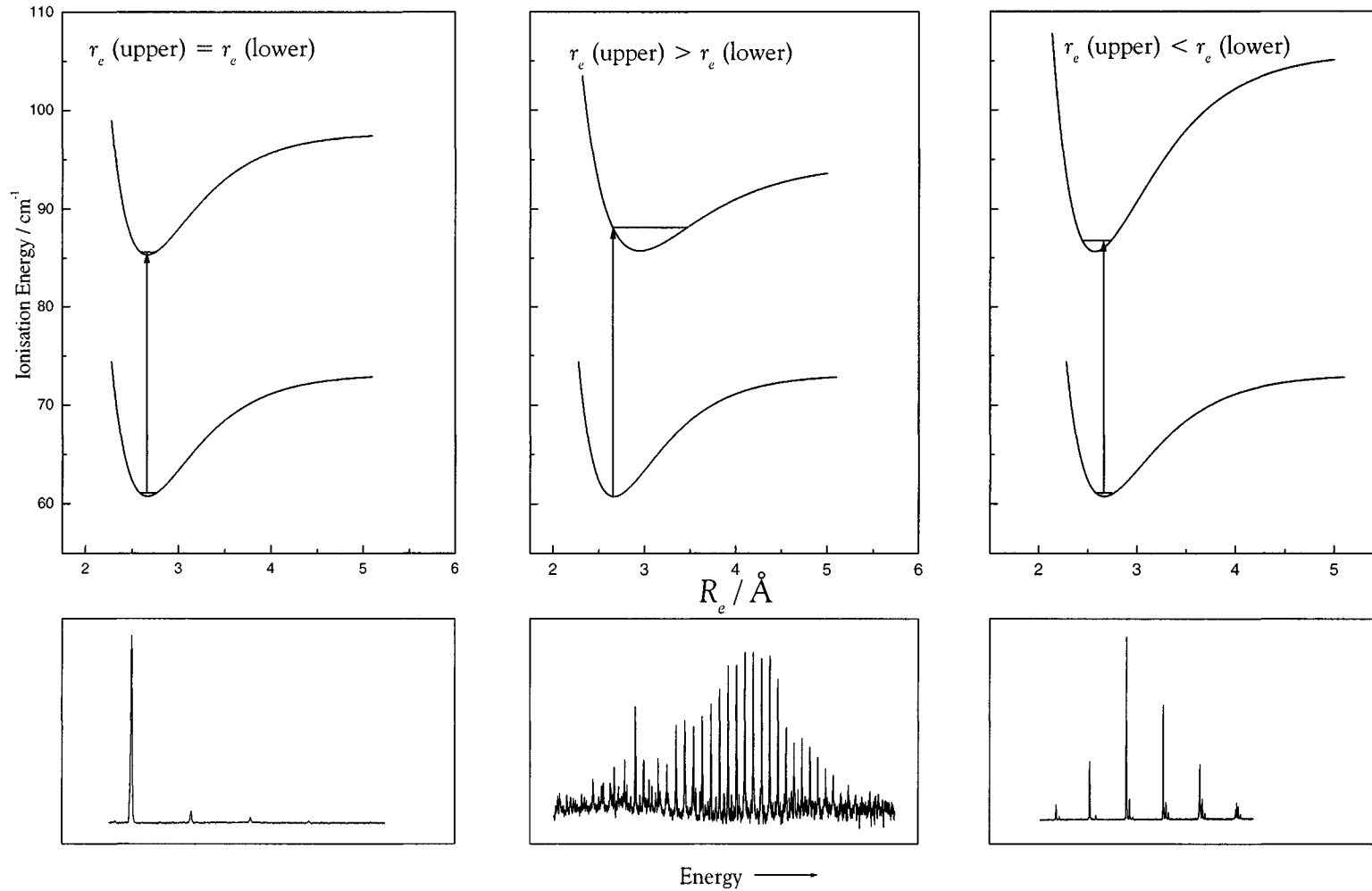
$$I.E. \approx -\epsilon_i$$

- (1) Orbitals are an entirely theoretical concept.
- (2) Their energies can only be obtained by calculation.
- (3) Experimental ionisation energies are the measureable quantity which most closely corresponds to the orbital energy.

Understanding the origin of Vibrational Structure

The Franck-Condon Principle

RC



Limitations of Koopmans' theorem:

(a) Neglect of electron reorganisation

Orbital relaxation, or reorganisation, may occur following ionisation.

$$I.E. \approx -\epsilon_i + E_R$$

(b) Neglect of electron correlation

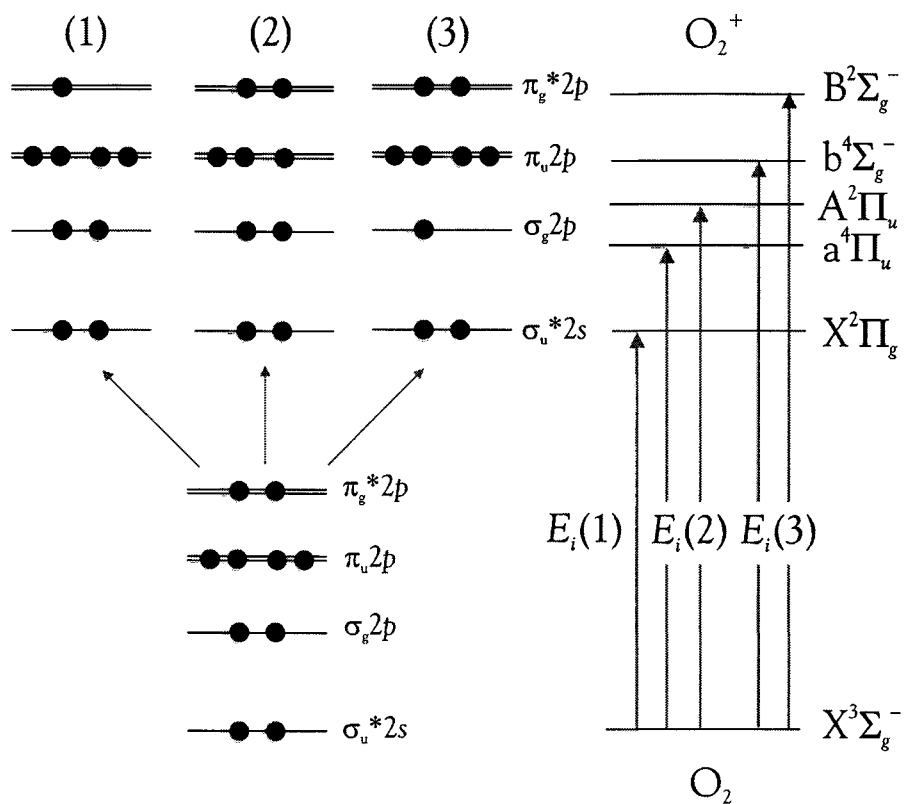
Electronic motion is **correlated** – electrons do not see an ‘averaged out’ charge of all the other electrons.

Both effects can be small, and fortuitously, in many cases cancel out!

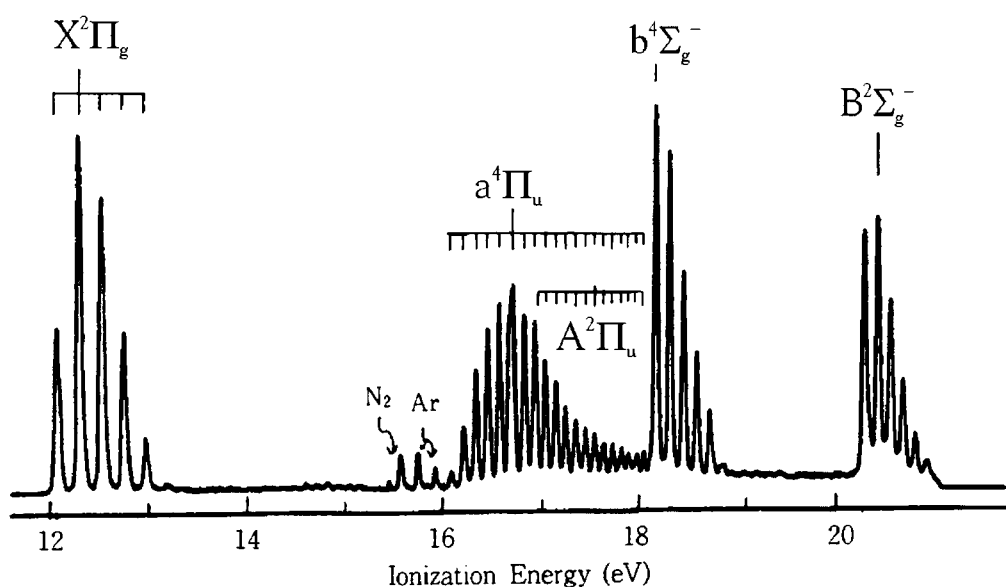
(c) Fails to account for open shell molecules

(c) Koopmans' theorem fails for open shell molecules

Oxygen



O_2 Oxygen



Autoionisation in PES

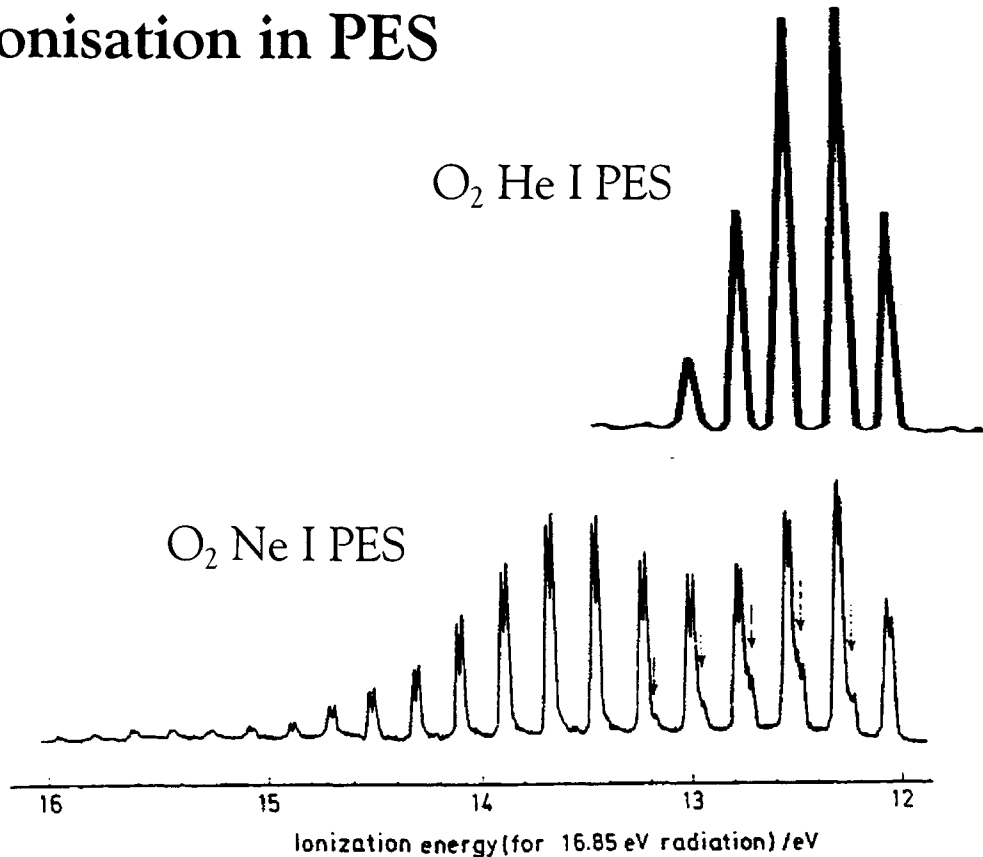
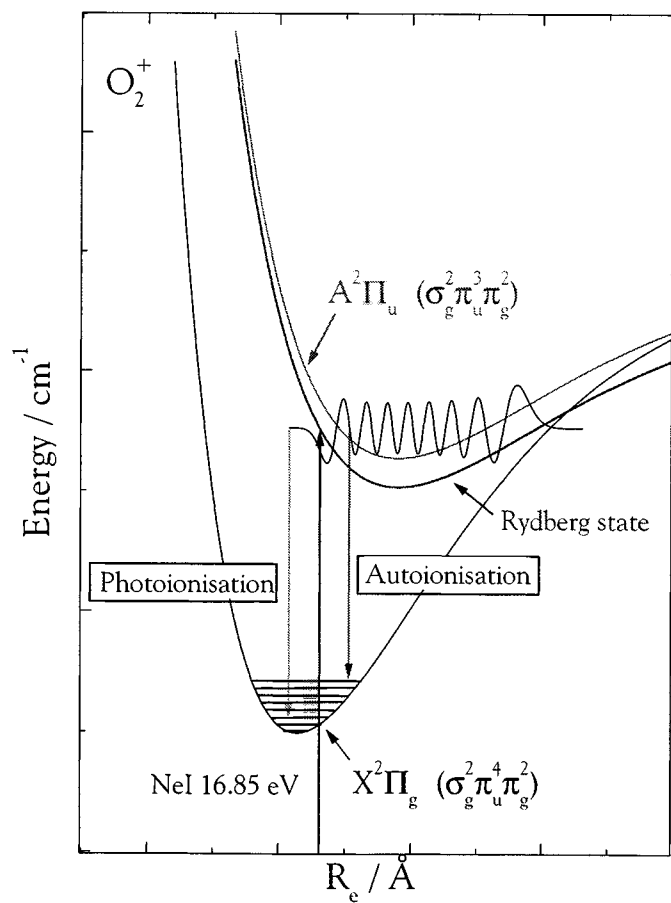


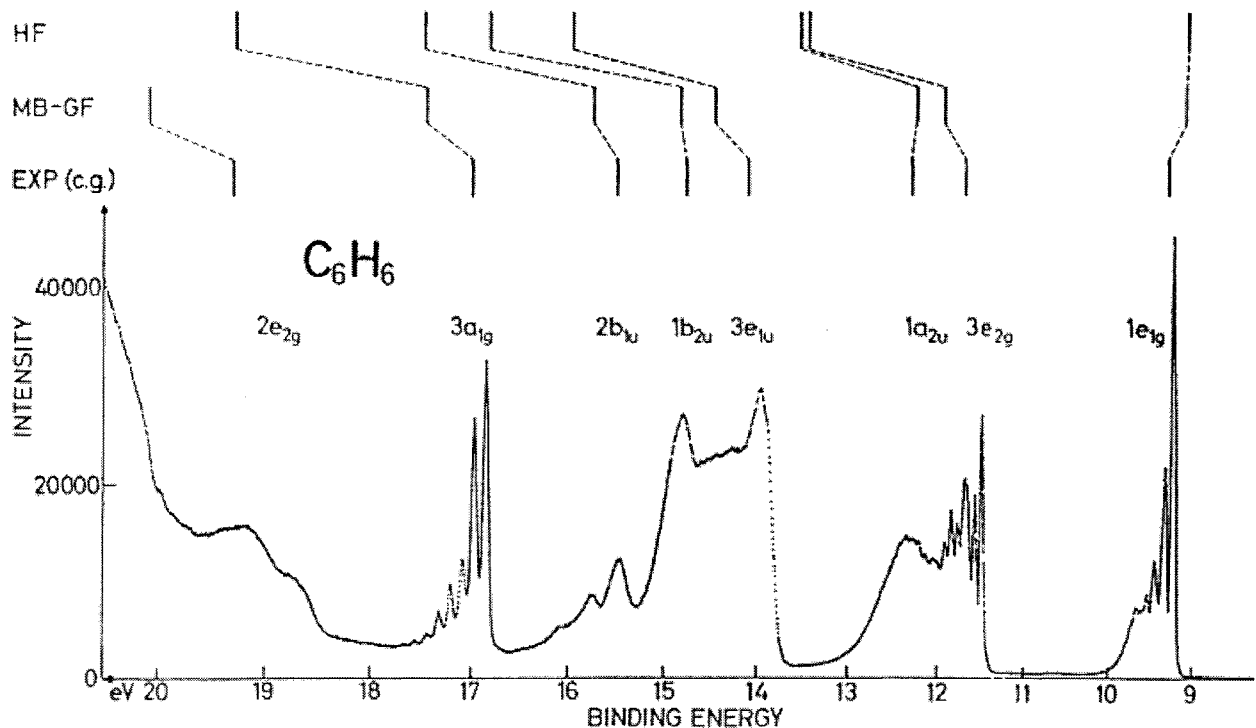
Figure 7.19 Autoionization in the $\text{O}_2^+(\text{X}^2\Pi_g) \leftarrow \text{O}_2 (\text{X}^3\Sigma_g^-)$ band system using a NeI source. The bands marked with arrows are due to the 16.67 eV radiation and do not show autoionization
[Reproduced, with permission, from Eland, J. H. D. (1974). *Photoelectron Spectroscopy*, p. 63, Butterworths, London]



Polyelectronic Molecules

Benzene

- Partially resolved vibrational structure
e.g. ν_1 (ring breathing mode) in $3a_{1g}$ band.
- Bands arise from ionisation from σ and π MO's.



The quest for higher resolution

- In the 1960's and 70's typical resolution no better than 10 meV (80 cm^{-1}).
- 1992 Baltzer, Karlsson and Wannberg⁵ improved to 4.5 meV (36 cm^{-1}) using mw electron-cyclotron-resonance source (linewidth 1.2 meV)

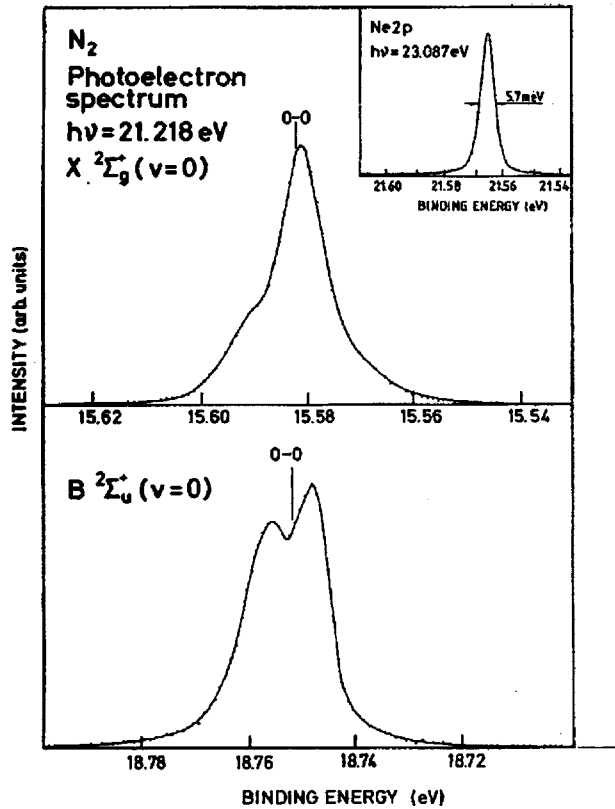


FIG. 1. The upper part shows the He I excited photoelectron spectrum corresponding to the $X^1\Sigma_g^+(N_2, v=0) \rightarrow X^2\Sigma_g^+(N_2^+, v=0)$ transition. The lower part shows the He I excited photoelectron spectrum corresponding to the $X^1\Sigma_g^+(N_2, v=0) \rightarrow B^2\Sigma_u^+(N_2^+, v=0)$ transition. In the upper right part the Ne 2P_{3/2} line excited with the He I β radiation at 23.087 eV is inserted. The lines connecting the experimental points are drawn as guides to the eye.

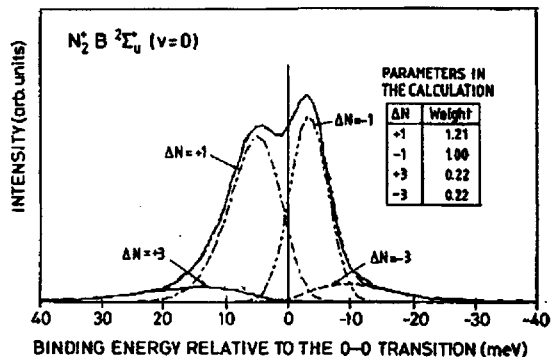
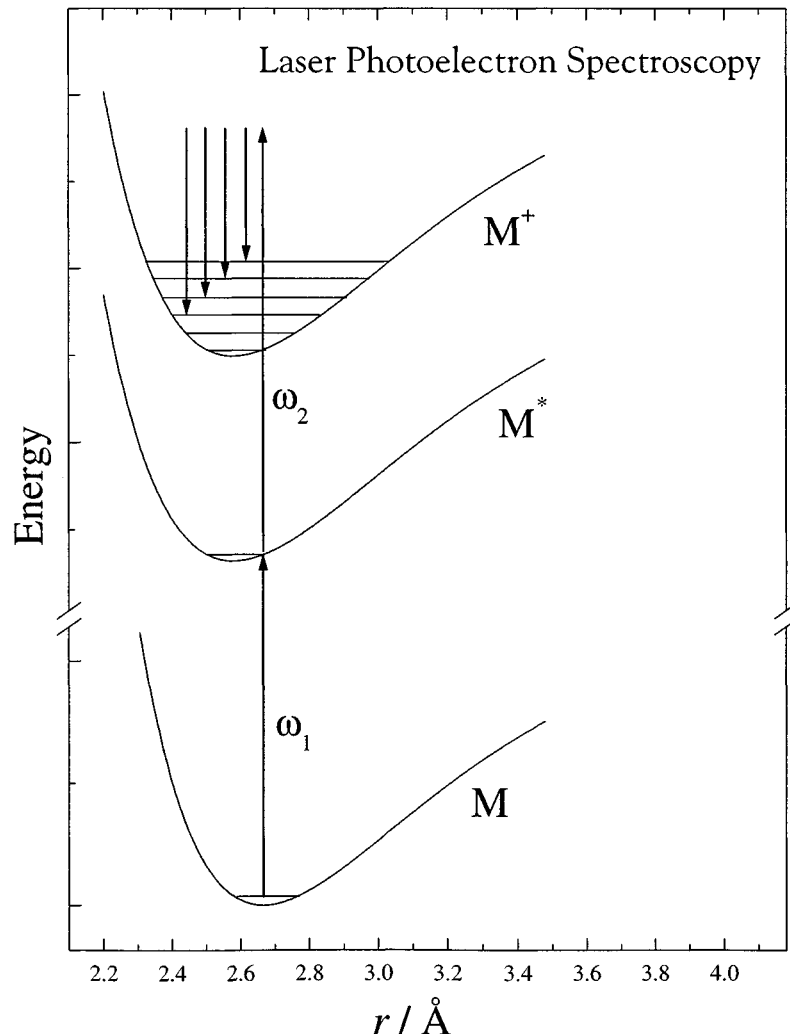


FIG. 3. The experimental (full line) and fitted theoretical (dashed line) $X^1\Sigma_g^+(N_2, v=0) \rightarrow B^2\Sigma_u^+(N_2^+, v=0)$ spectra shown together. The spectra are very similar and an obvious difference can be seen only at -12 meV from the zero level, where the intensity of the experimental spectrum is somewhat higher. For clarity, the subbands corresponding to transitions with $\Delta N = \pm 1$ and ± 3 are included. Also the weights used in the fitting of the theoretical spectrum are shown in the figure normalized to 1.00 for $\Delta N = -1$ subband. The energy scale refers to zero at the (unobserved) 0-0 transition.

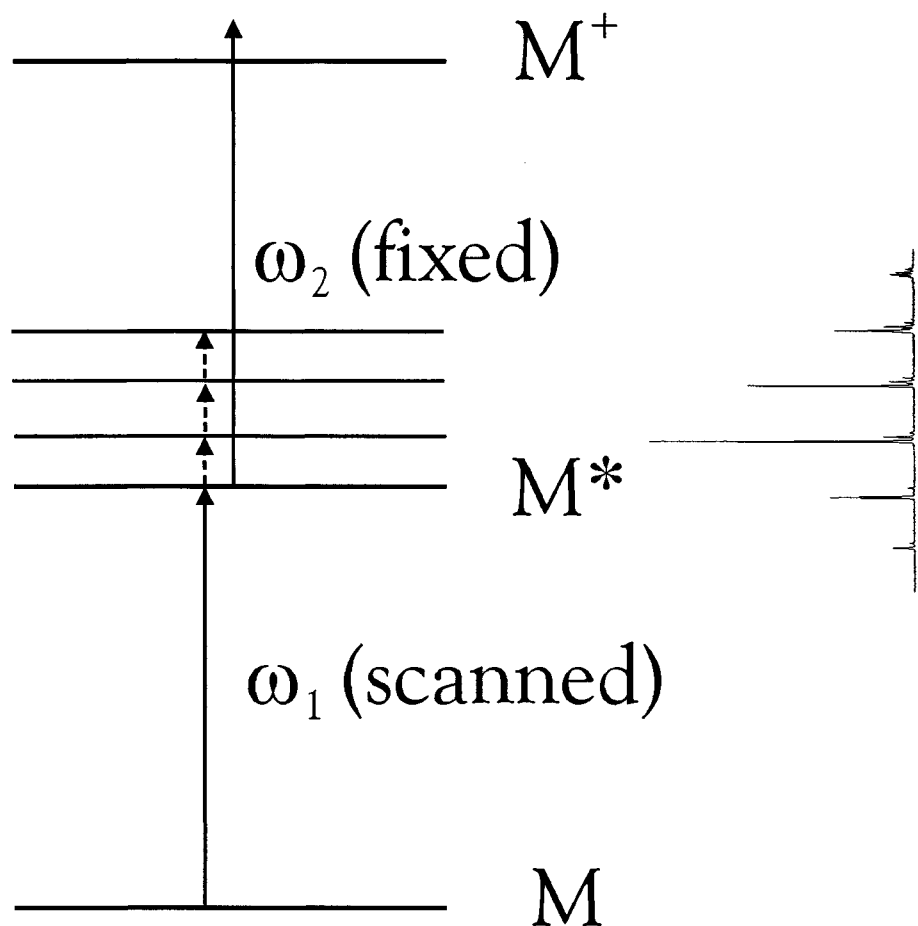
⁵ P. Baltzer, L. Karlsson and B. Wannberg, Phys. Rev A, **46** (1992)
315

Laser Photoelectron Spectroscopy (1980's)

- Employs resonance enhanced multiphoton ionisation (REMPI) – a two step process.
- State selection
- Supersonic jets and molecular beams ($T_{trans} \approx 1 \text{ K}$, $T_{rot} \approx 10 \text{ K}$, $T_{vib} \approx 100 \text{ K}$)
- Narrow laser linewidth ($< 1 \text{ cm}^{-1}$)
- Molecule specificity



REMPI spectroscopy characterises the intermediate state



A Case Study: The Ar-NO van der Waals Complex

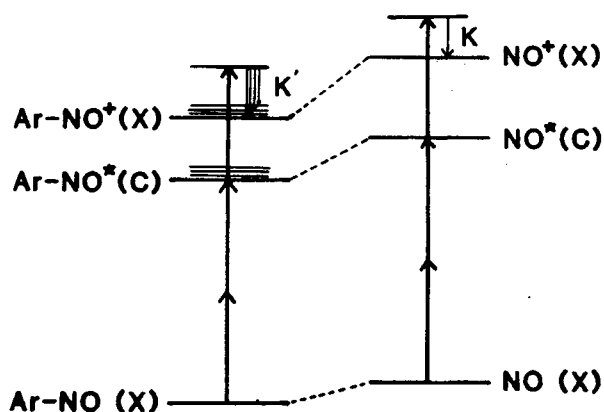


FIG. 5. Schematic energy level diagrams of NO and Ar-NO, relevant to $(2+1)$ resonant multiphoton ionization through their Rydberg C states.

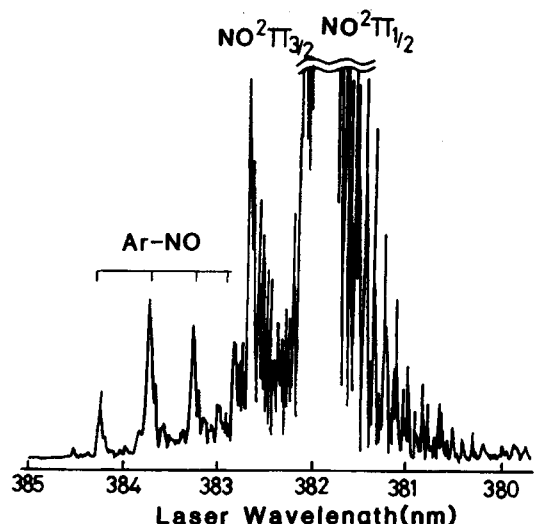


FIG. 1. An MPI ion-current spectrum obtained with a free jet of a mixture of 5% NO in Ar in the laser wavelength region 380–385 nm. The stagnation pressure was 1 atm.

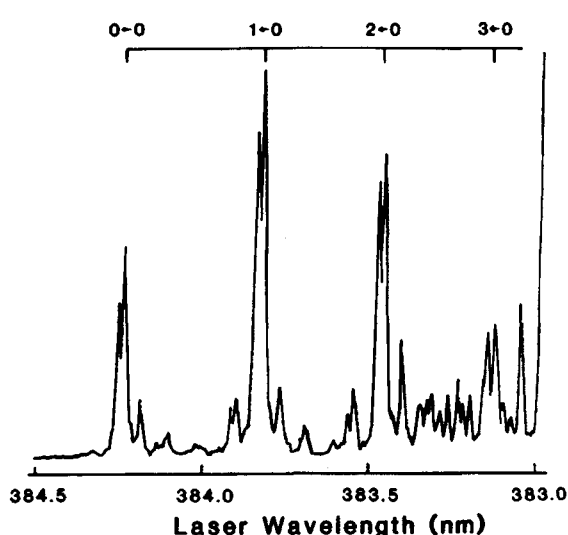


FIG. 2. An MPI ion-current spectrum attributed to the Ar-NO van der Waals complex, shown in an extended scale. The experimental conditions are the same as in Fig. 1.

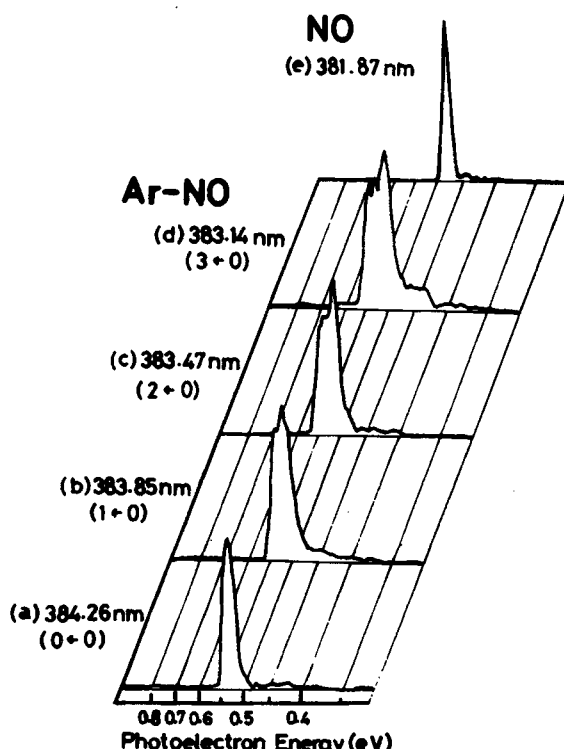


FIG. 4. Photoelectron spectra obtained by the $(2+1)$ resonant multiphoton ionization of a free jet of the Ar-NO (5%) mixture at the ion-current peaks of the Ar-NO van der Waals complex [spectra (a)–(d)] and of the free NO molecule [spectrum (e)].

Resolution of 20 meV, but molecule specificity!

K. Sato, Y. Achiba and K. Kimura,
J. Chem. Phys., **81** (1984) 57

Magnetic bottles, supersonic jets and lasers

- Late 1990's de Lange *et al.* obtained a resolution of 8 meV (64 cm^{-1}) using magnetic bottle electron energy analysis.

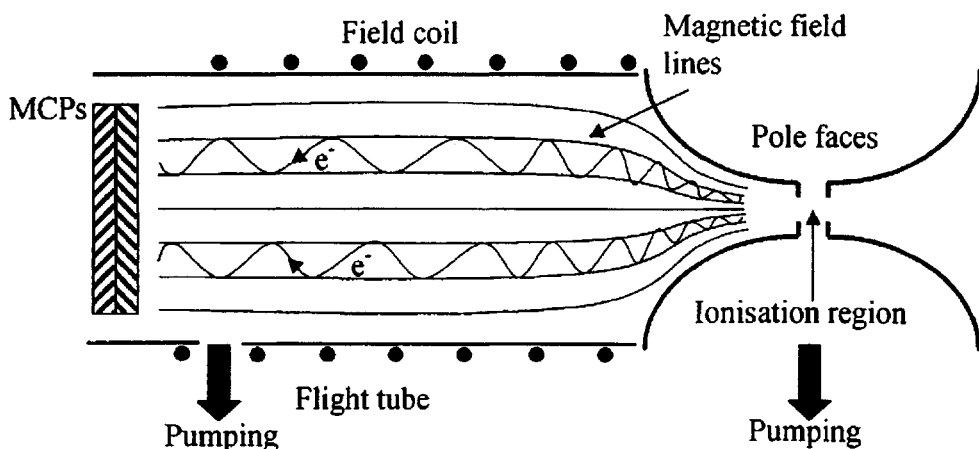


Fig. 1. Schematic of 'magnetic bottle' spectrometer showing the key functional elements.

A.M. Rijs *et al.* / Journal of Electron Spectroscopy and Related Phenomena 112 (2000) 151–162

161

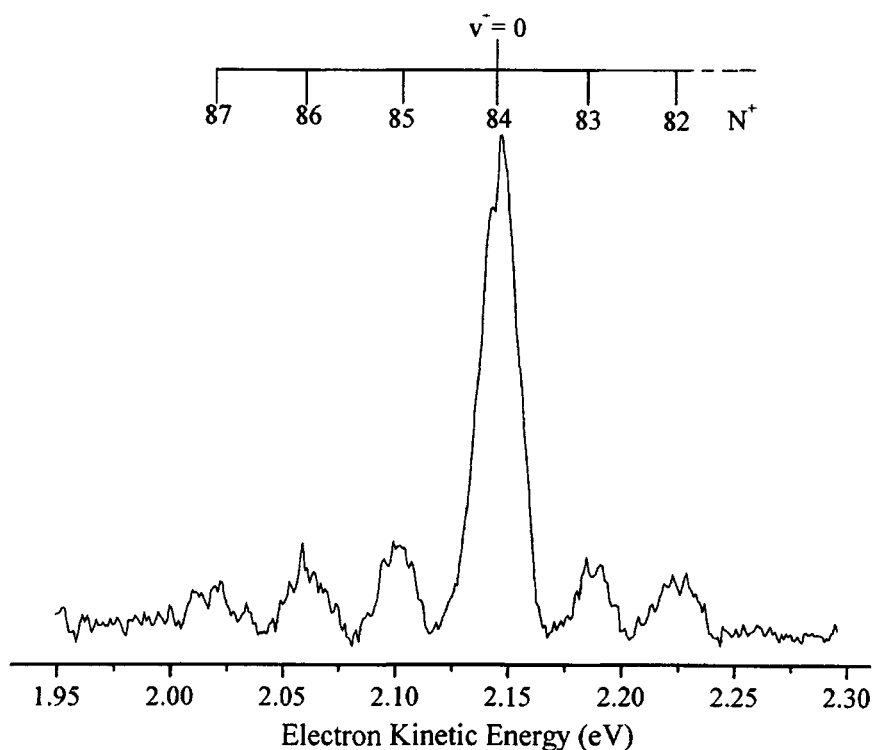


Fig. 4. Rotationally resolved photoelectron spectrum obtained by a one-photon ionisation from the Q(84) level of the intermediate $B^1\Sigma^+$ ($v' = 0$) state of rotationally excited CO.

Laser limited Photoelectron Spectroscopy?

Weinkauf *et al*⁶ achieve $4 - 8 \text{ cm}^{-1}$ resolution

- Minimising excess energy ($< 300 \text{ meV}$)
- Careful reduction of point charges in ionisation region
- REMPI state selection & time-of-flight energy analysis

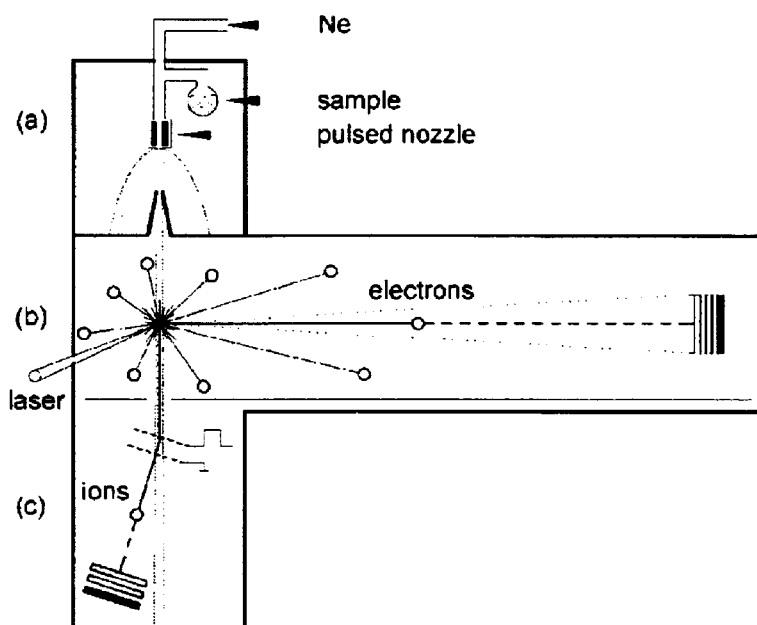
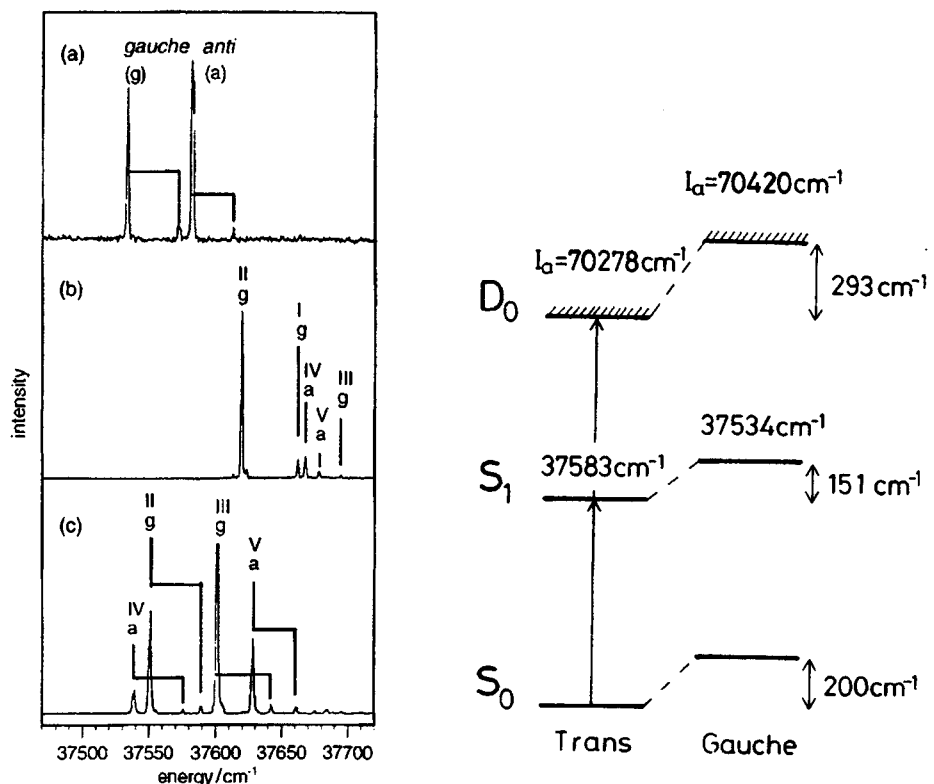


Fig. 2 Experimental setup of the MPI high-resolution photoelectron spectrometer: (a) inlet chamber, (b) field-free photoelectron spectrometer, (c) pulsed time-of-flight mass spectrometer. Note that MPI, MPI-PE and mass spectra can be recorded in the same instrument.

⁶ R. Weinkauf, F. Lehrer, E.W. Schlag and A. Metsala, *Faraday Discuss.* **115** (2000) 363

Photoelectron Spectrum of *n*-propylbenzene

(a) REMPI spectrum



(b) REMPI-PE spectrum

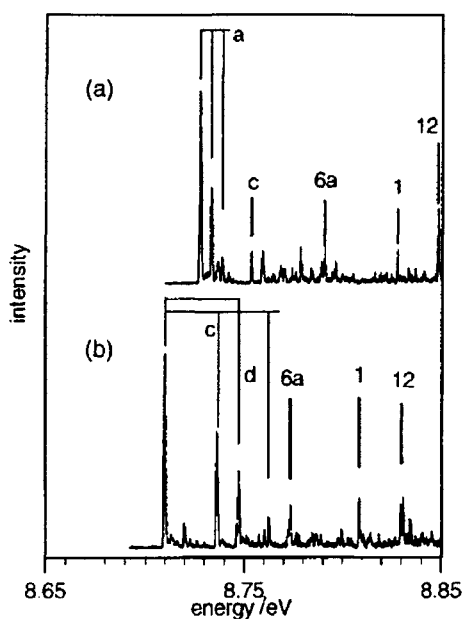
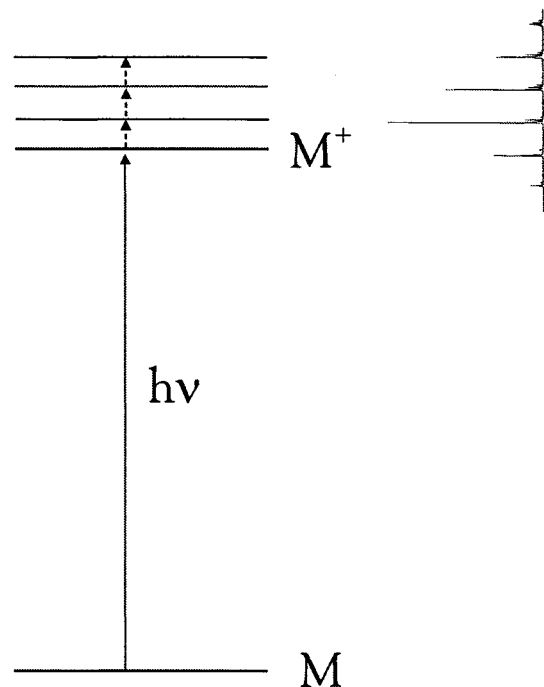


Fig. 6 The MPI-PE spectra of *n*-propylbenzene: (a) *gauche* and (b) *anti* conformer. The very different vibronic transition pattern allows a clear conformer assignment. The transition intensities show a relative small structural change upon ionization. The resolution of the MPI-PE spectrum is better than 8 cm⁻¹.

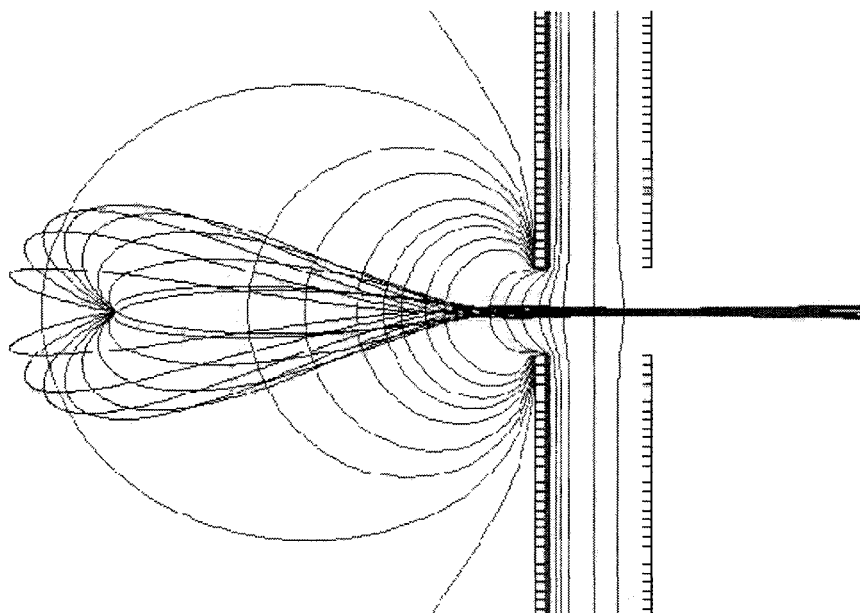
Dispensing with kinetic energy analysis

Threshold Photoelectron Spectroscopy (TPES)

- Collects threshold photoelectrons ('zero' energy) emitted when a resonant transition is excited.

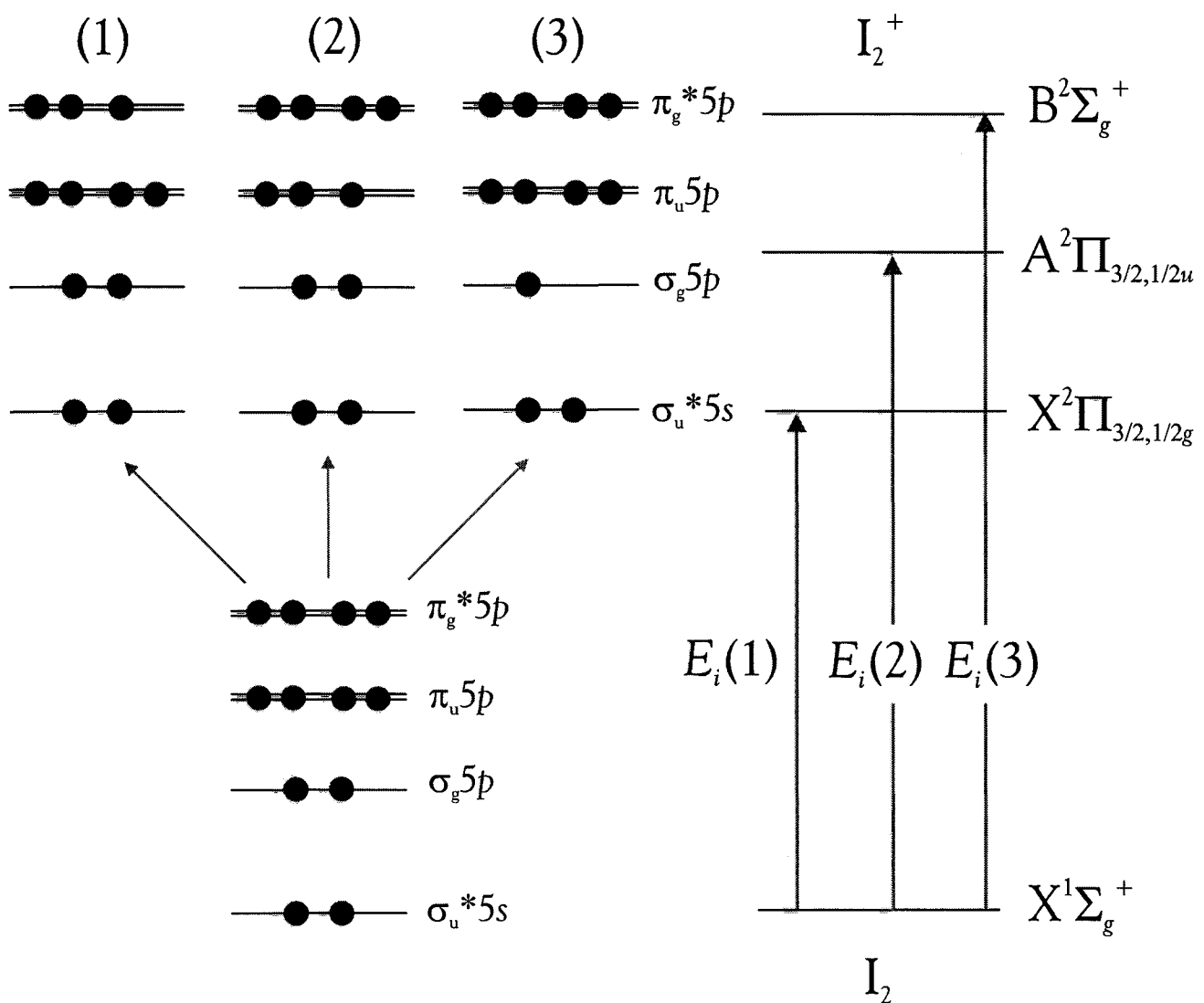


- Synchrotron radiation
- Penetrating field electron lens



Trajectories of 0.001eV electrons emitted from a point source are focused and collimated by the weak electric field from an 'extractor' electrode that penetrates through the 0 Volt aperture.

A Case Study: Molecular Iodine

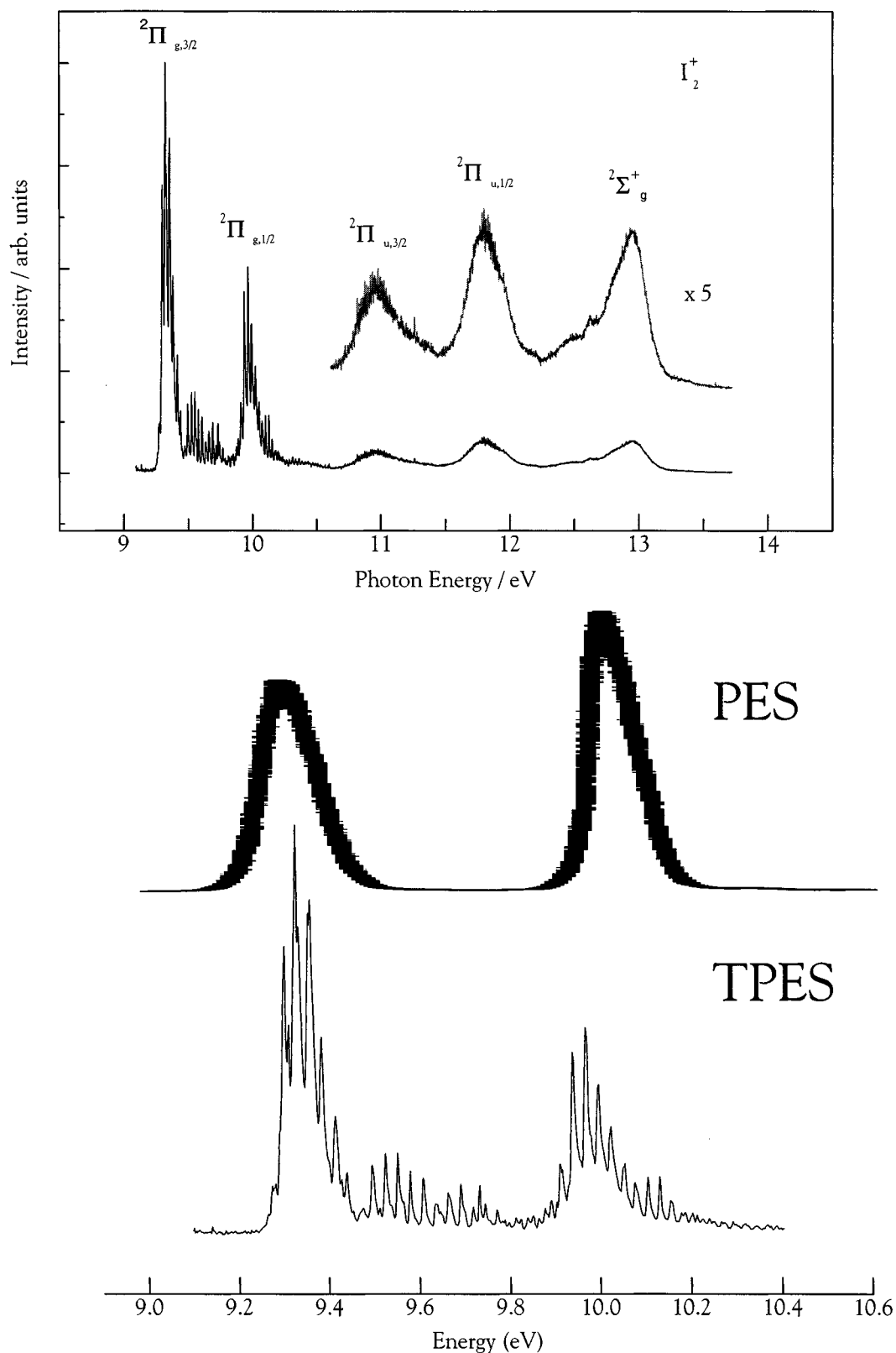


Each $^2\Pi$ state is split into two spin-orbit states

$$(\pi_g^* 5p)^3 \ ^2\Pi_{3/2,1/2,g} \leftarrow (\pi_g^* 5p)^4 \ ^1\Sigma_g^+$$

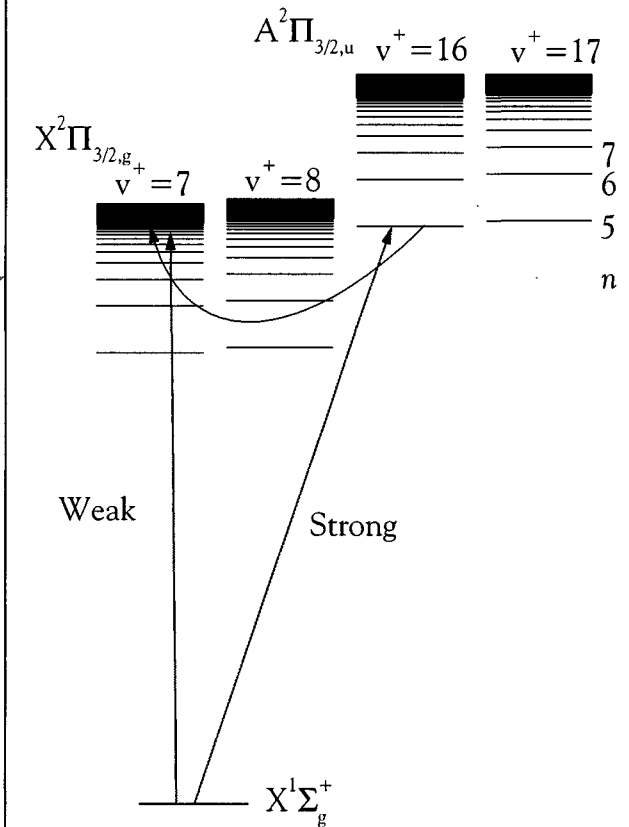
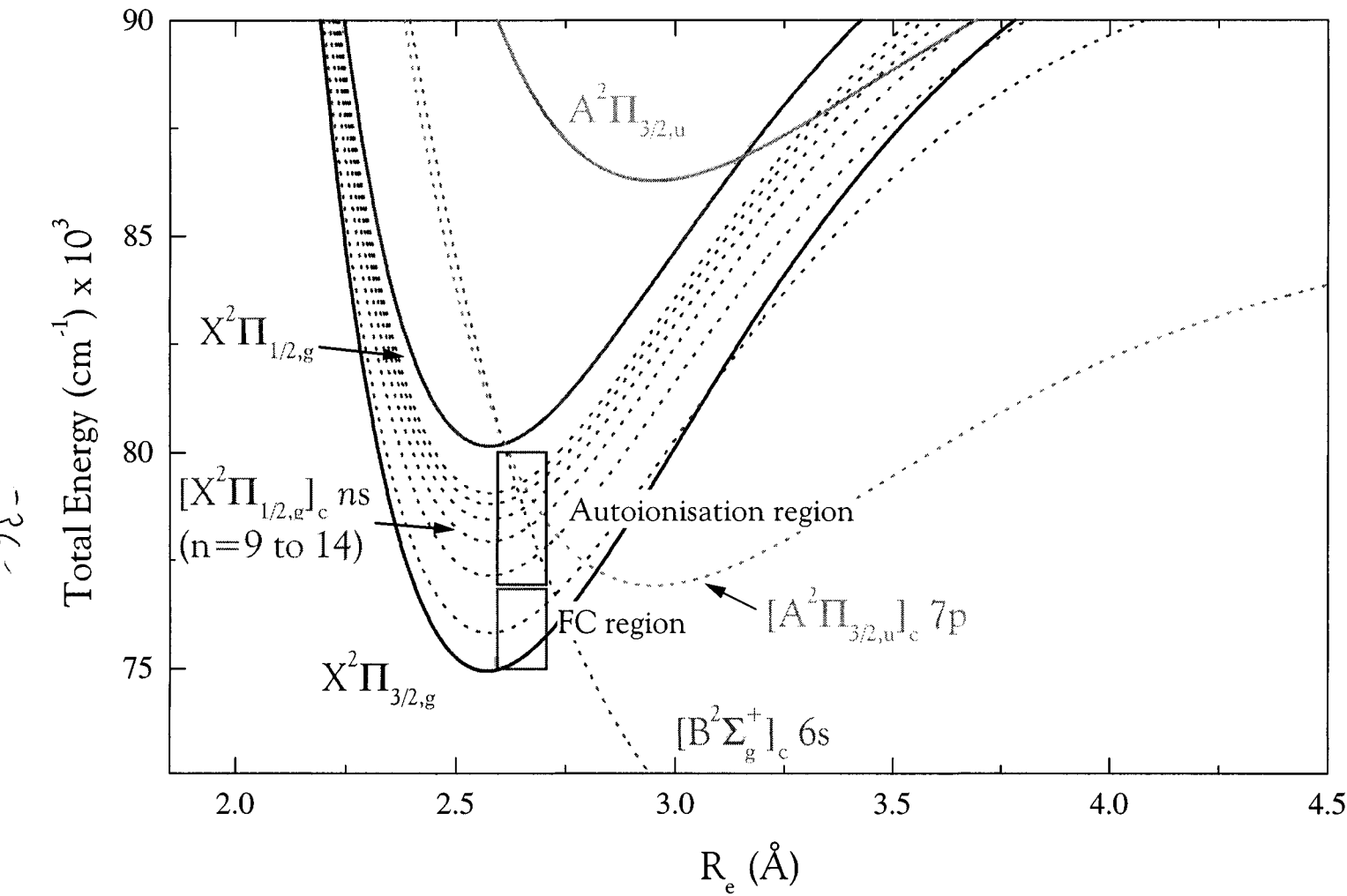
TPES of Molecular Iodine⁷

- Resolution ≈ 5 meV (40 cm^{-1})



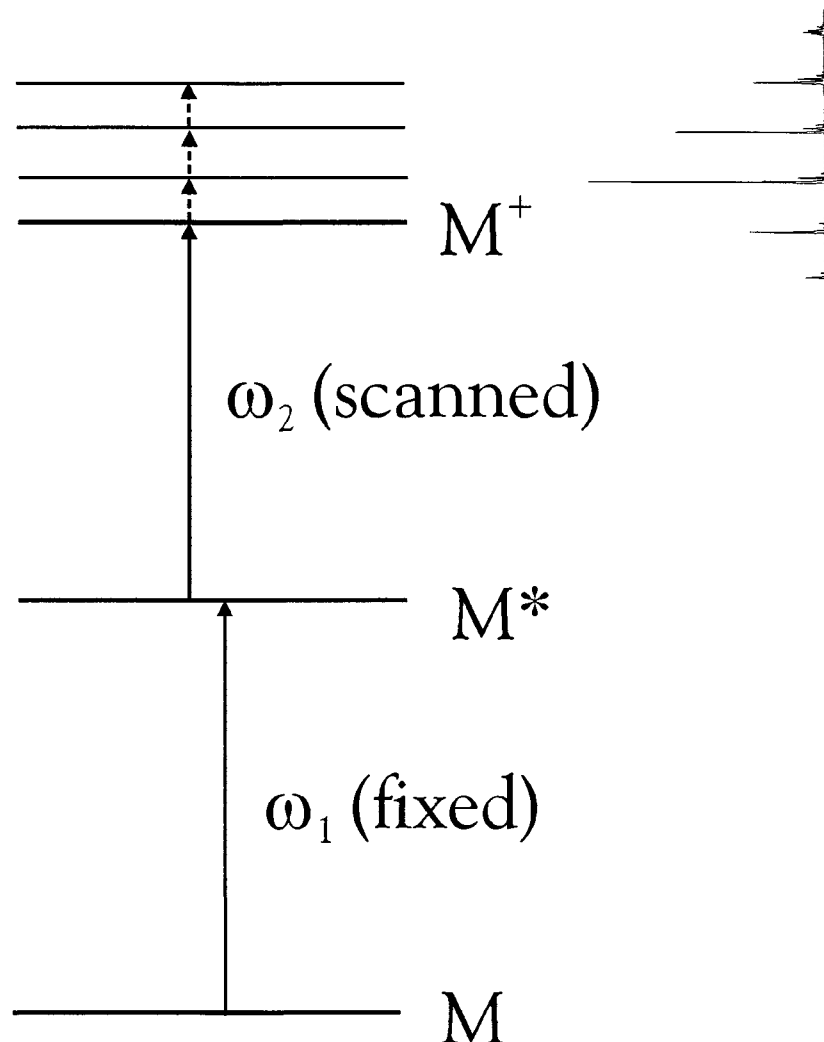
⁷ A.J. Yencha, M.C.R. Cockett, J.G. Goode, R.J. Donovan, A. Hopkirk and G.C. King, *Chem. Phys. Lett.*, **229** (1994) 347.

Autoionisation Revisited



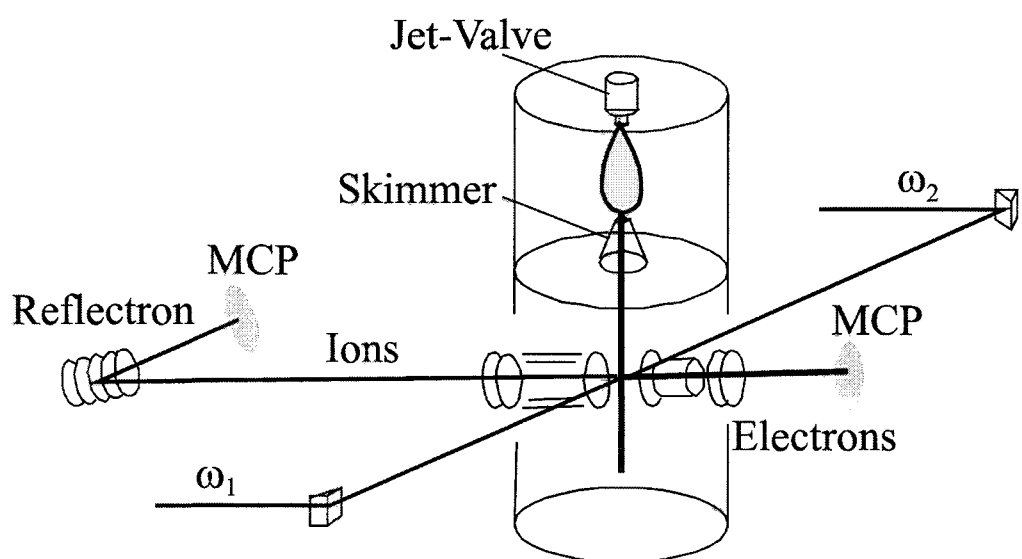
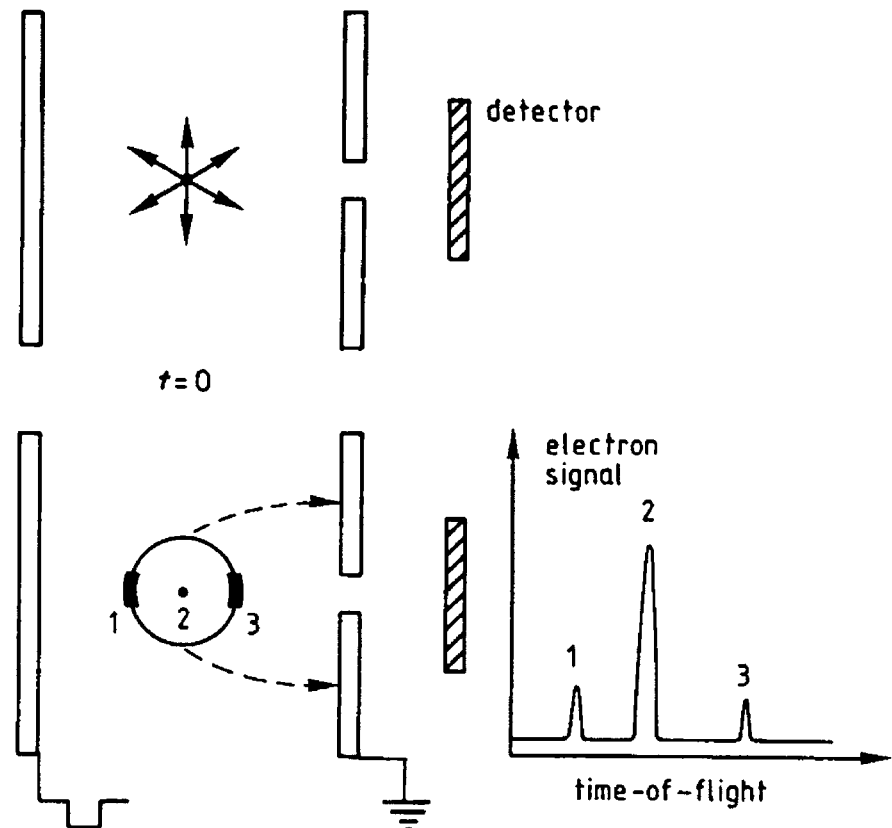
The next step: Zero Electron Kinetic Energy
(ZEKE) (photoelectron) spectroscopy
Lasers, delay, long life and Rydberg states

- REMPI+TPES=ZEKE



How do we separate ‘ZEKE’ electrons from ‘fast’ electrons?

We do nothing!



1984 The first ZEKE spectrum⁸

- Resolution better than $\approx 2 \text{ cm}^{-1}$
- Rotational structure

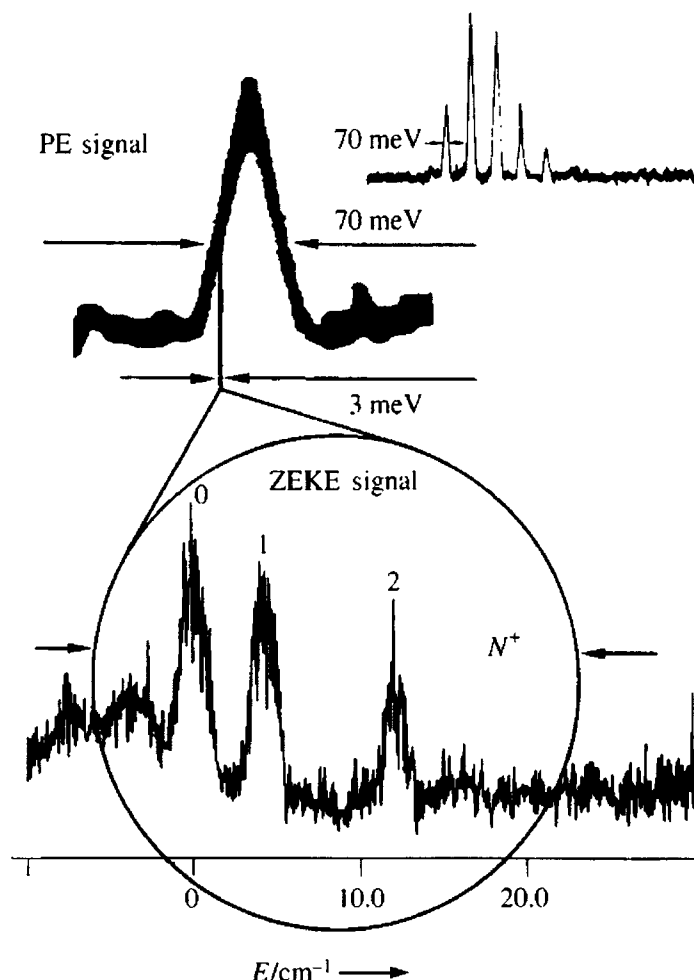
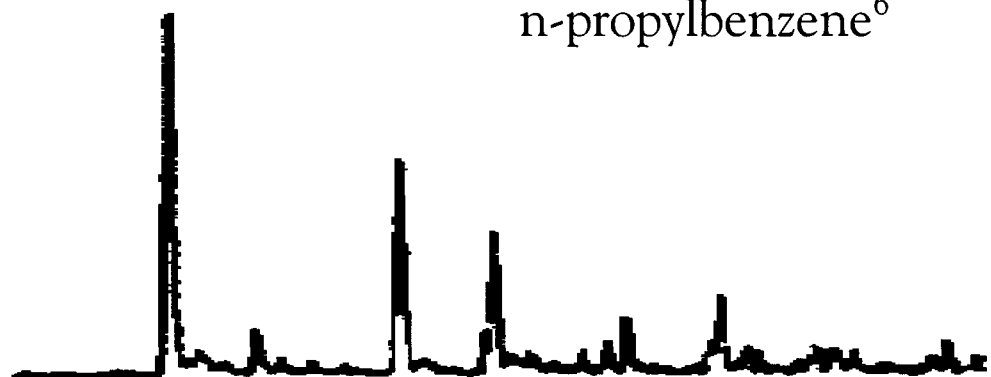


Figure 2. The first VUV photoelectron spectrum of NO^{14+} (top) with a vibrational progression from $v^- = 0$ to $v^+ = 4$ of the ${}^1\Sigma^+$ electronic ground state of NO^+ and comparison of the $v^+ = 0$ peak with the first ZEKE spectrum obtained.^[14] The ZEKE spectrum shows the lowest rotational states in the vibrational state $v^+ = 0$ with $N^+ = 0 - 2$.

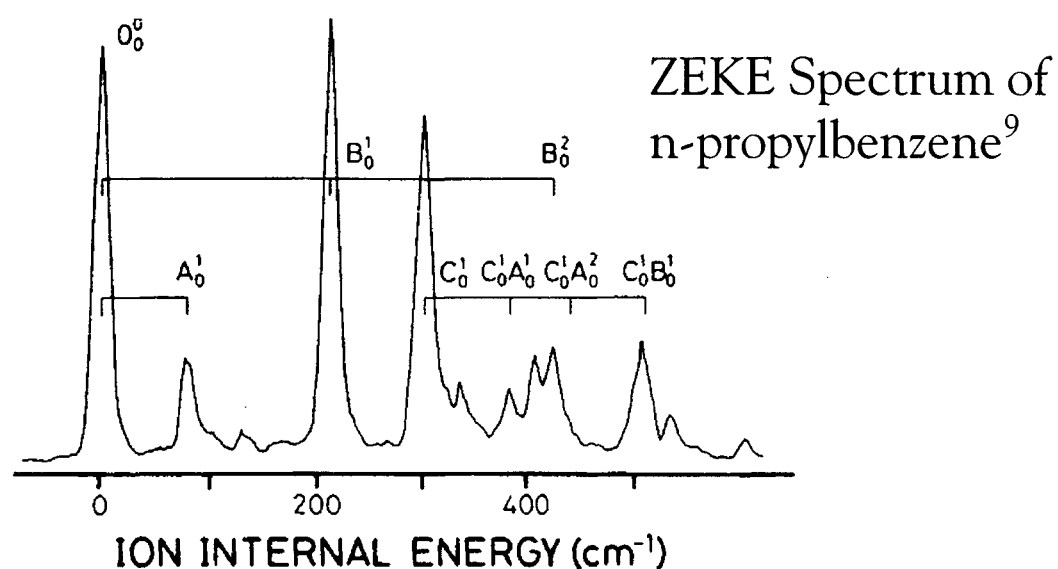
⁸ K. Müller-Dethlefs, M. Sander and E.W. Schlag, *Chem. Phys. Lett.*, **112** (1984) 291.

Is ZEKE spectroscopy ‘real’ photoelectron spectroscopy?

Photoelectron Spectrum of
n-propylbenzene⁶



ZEKE Spectrum of
n-propylbenzene⁹



⁶R. Weinkauf, F. Lehrer, E.W. Schlag and A. Metsala, *Faraday Discuss.* **115** (2000) 363

⁹M. Takahashi and K. Kimura, *J. Chem. Phys.*, **97** (1992) 2920.

It looks like a duck, and walks like a duck but ...

- Late 1980's: ZEKE spectra are not equivalent to PE spectra.
- Each band is shifted by a few cm^{-1} to lower energy.

Are we really detecting ‘ZEKE’ electrons?

- ZEKE spectra frequently exhibit autoionisation.

Band intensities cannot be trusted!

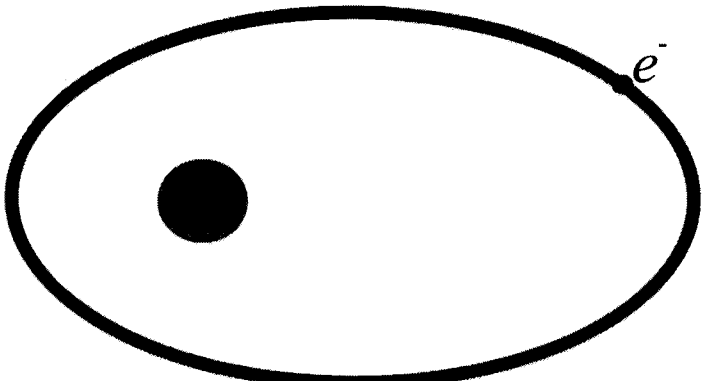
ZEKE electrons are not really photoelectrons

The Role of Rydberg States and Field Ionisation

What are Rydberg States?

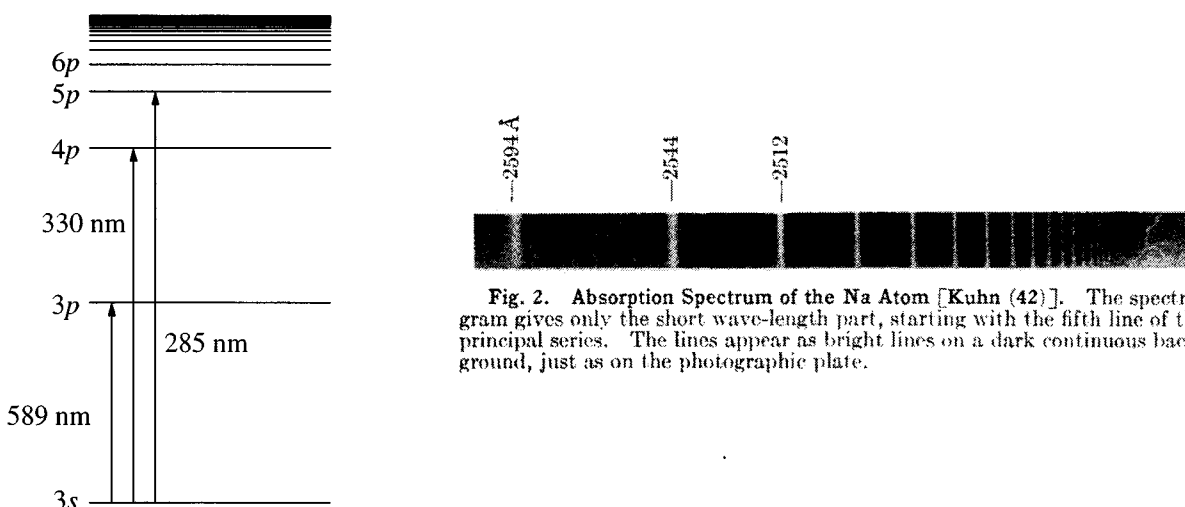
- Rydberg states are electronic states of high principal quantum number n .

- The electron occupies an orbital whose size is large relative to the dimensions of the ionic core.



Atoms:

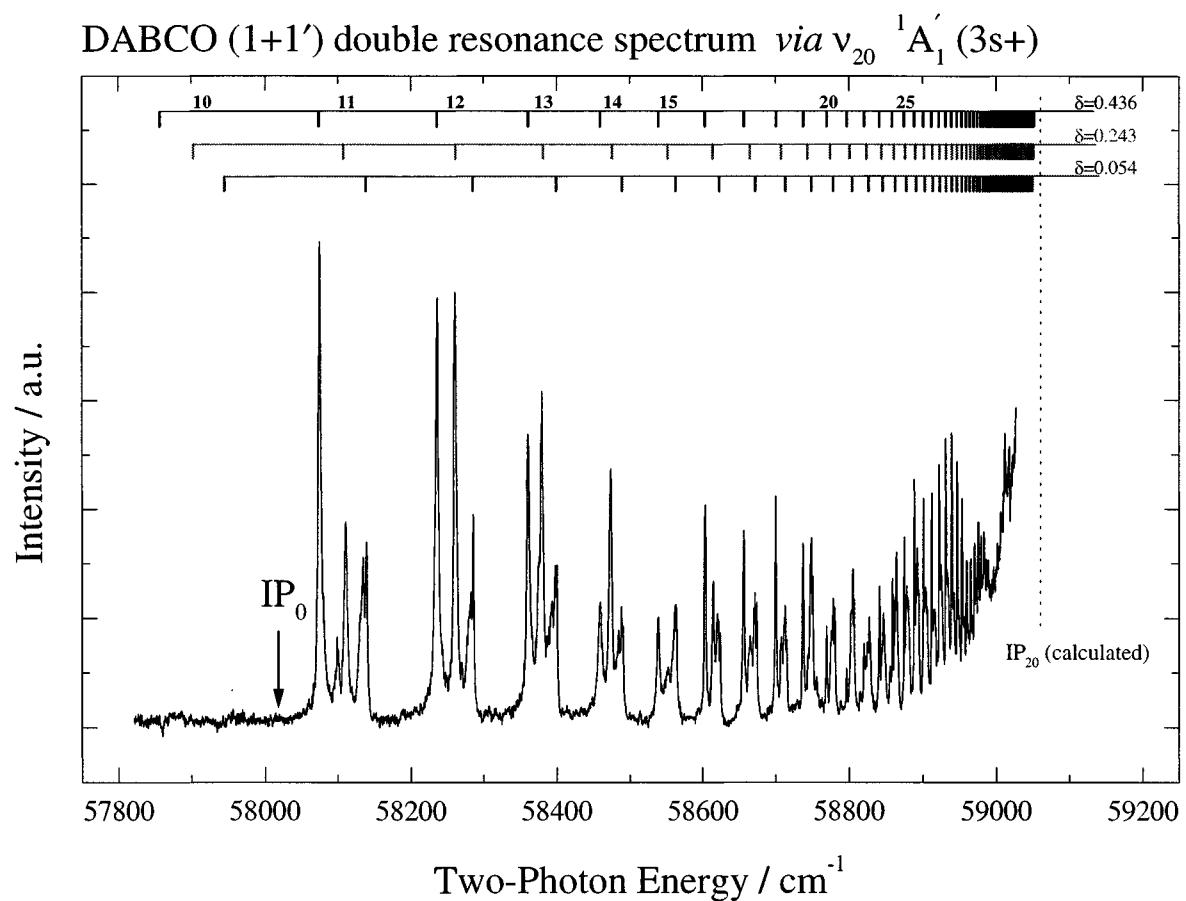
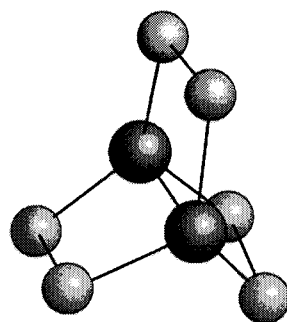
Sodium $1s^2 2s^2 2p^6 4p^{1/2} P_{3/2,1/2} \leftarrow 1s^2 2s^2 2p^6 3s^1 2S_{1/2}$



Molecular Rydberg States

When is a molecule an atom?

- At sufficiently high levels of electronic excitation, all molecules eventually resemble the hydrogen atom.



Lifetimes

Rydberg states are potentially **HUGE**.

$$r = \frac{n^2 \hbar^2 4\pi \epsilon_0}{Ze^2 m}$$

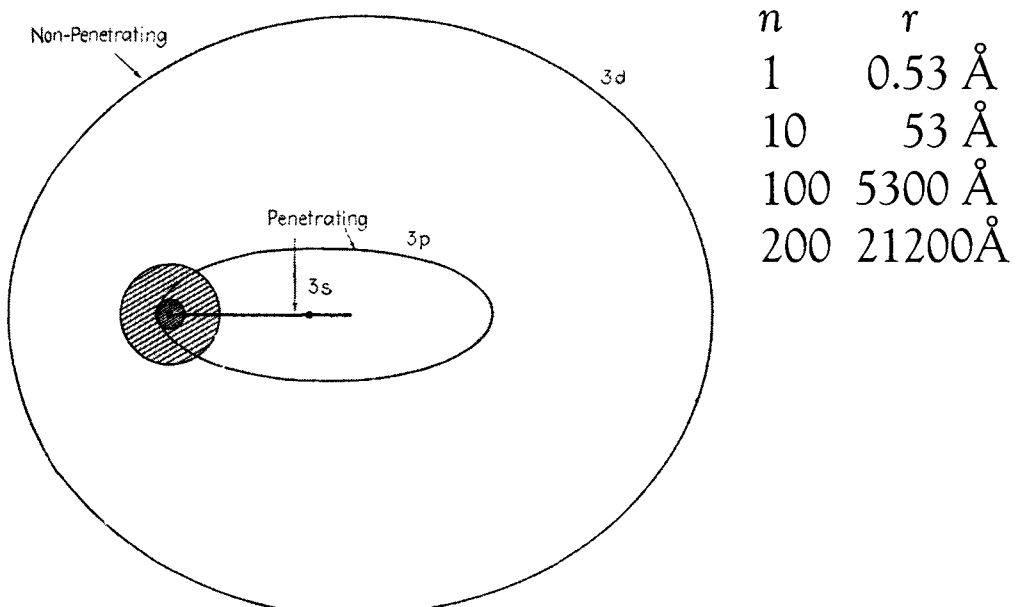


FIG. 7.3.—Comparison of the quantum-mechanical with the classical model of the neutral sodium atom. Three of the lowest possible states for the single valence electron are also shown.

Lifetimes

For low- ℓ , $\tau \propto n^3$

For high- ℓ , $\tau \propto n^5$

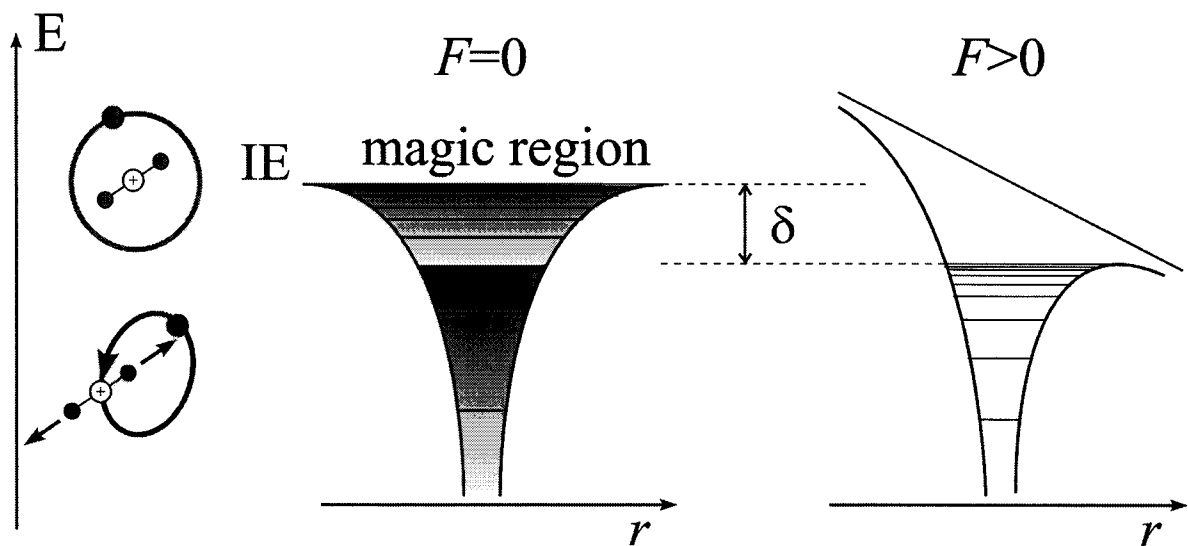
In sodium

$$n = 30; \ell = 0; \tau = 32 \mu\text{s.}$$

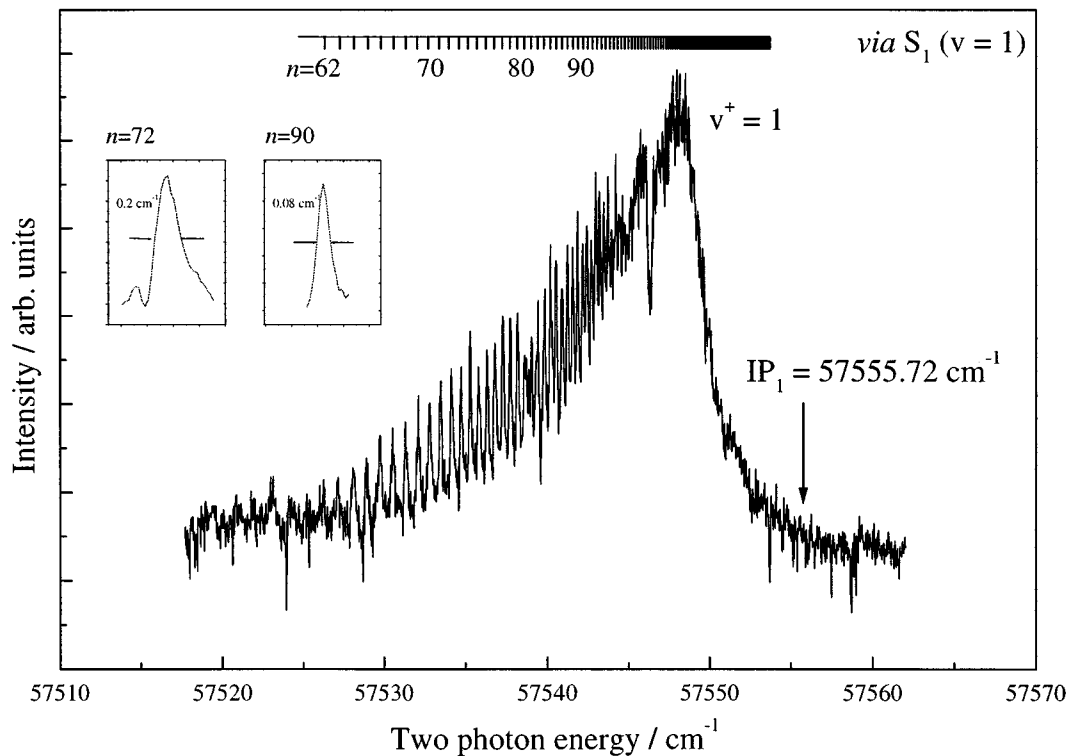
$$n = 30; \ell = n - 1 \text{ (circular)}; \tau = 2.3 \text{ ms}$$

ZEKE spectroscopy relies on the existence of metastable high- n molecular Rydberg states.

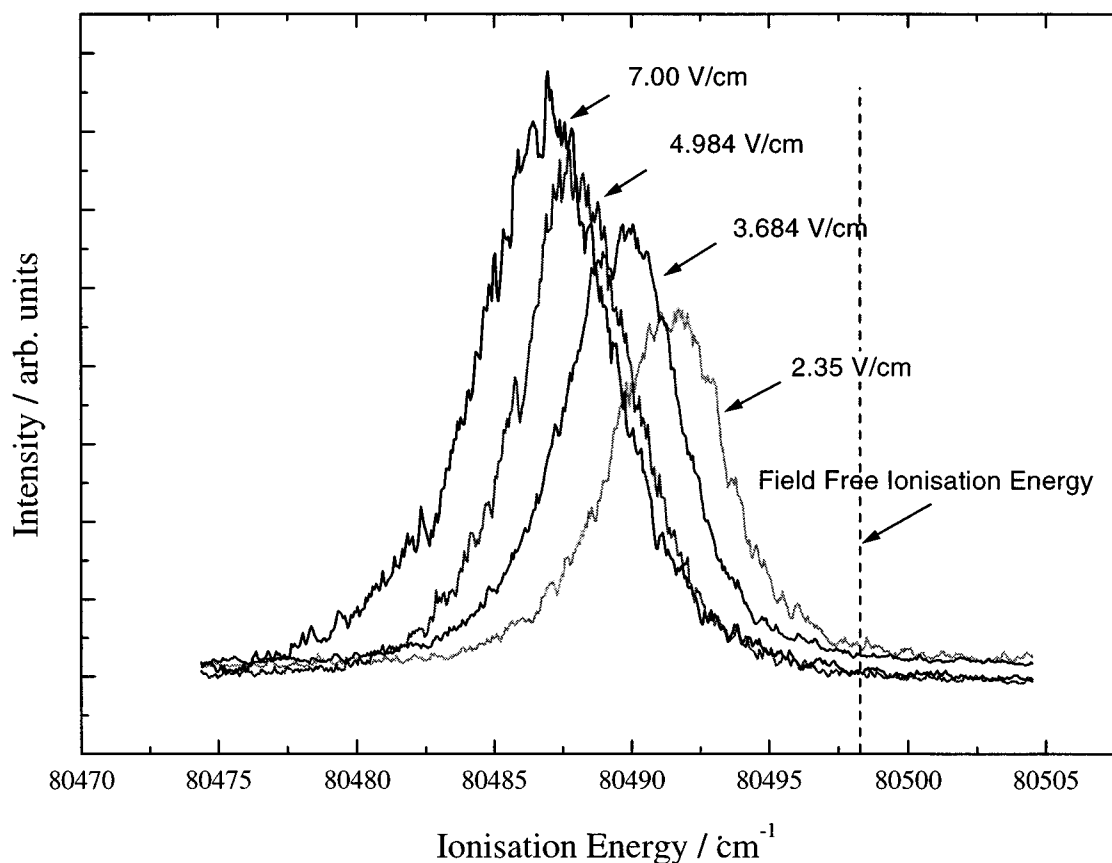
- ZEKE Rydberg states are high- n , high- ℓ , high- m_ℓ



- The signal comes from below threshold.

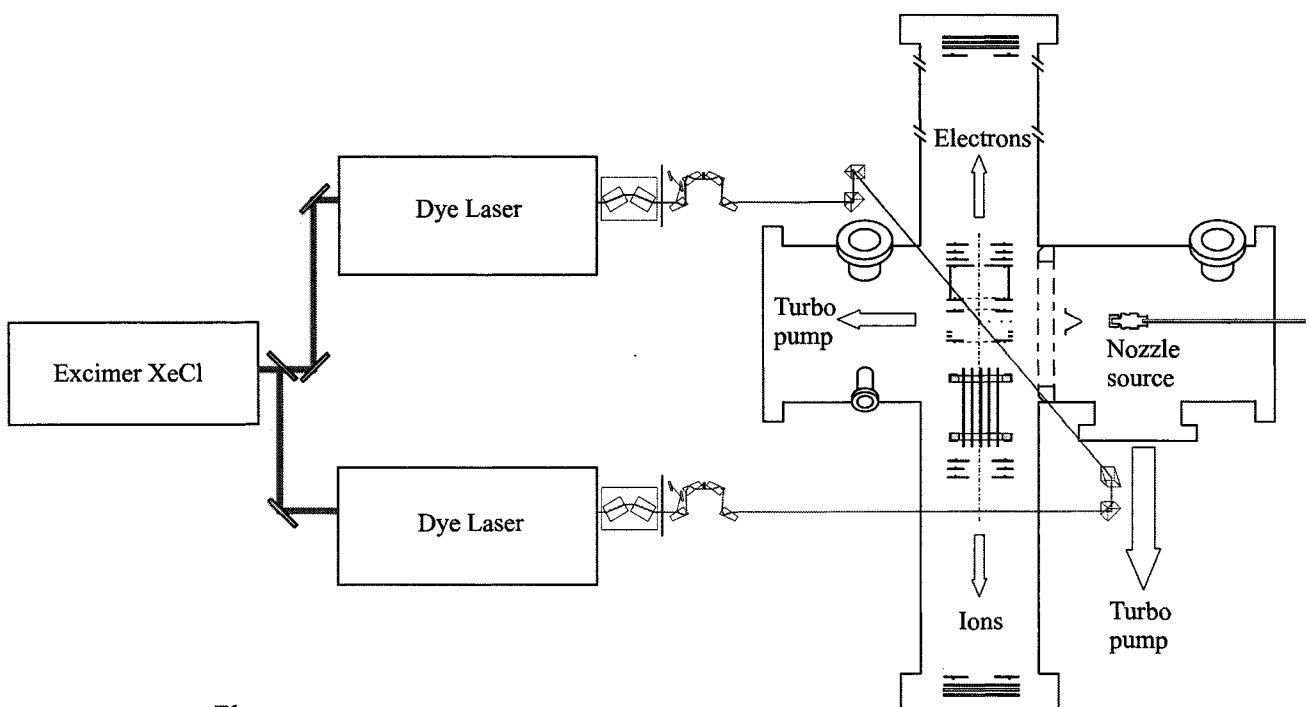


The position of a ZEKE band depends on field strength

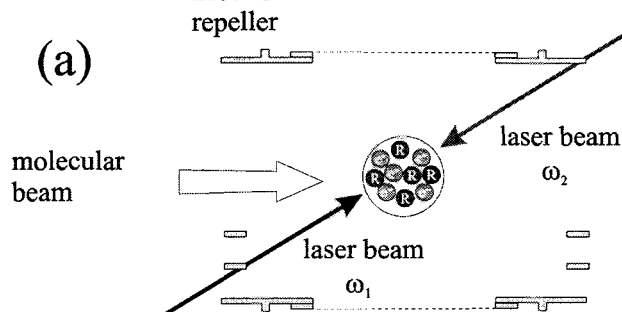


- The theoretical red-shifts for *pulsed* field ionisation are:
 - $-3.1\sqrt{V}$ cm^{-1} for *diabatic* ionization measured at the band maximum
 - $-4.6\sqrt{V}$ for *diabatic* ionization measured at the low wave number on-set of the band.

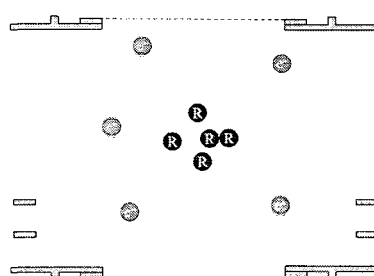
A typical ZEKE experiment



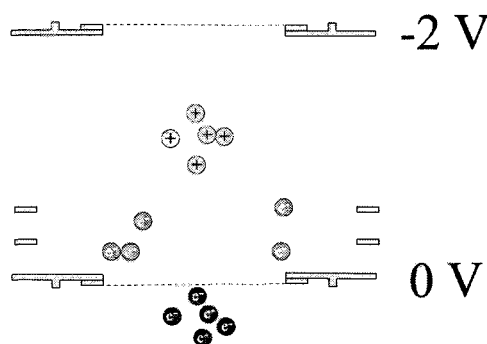
(a)



(b)



(c)



Improving the resolution

- Slow Rise-time and Stepped Pulses ($< 0.25 \text{ cm}^{-1}$)¹⁰

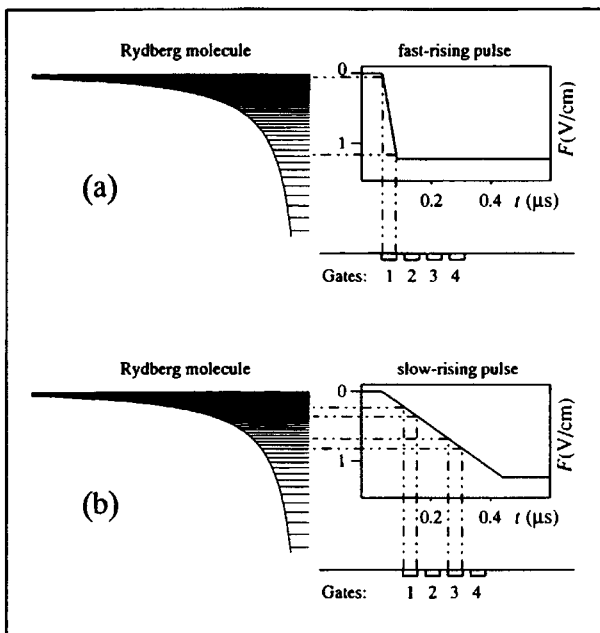


Figure 2.13 Pulsed field ionization of long-lived Rydberg states using a fast-rising (a) and a slowly rising (b) extraction pulse and collection within a certain time gate

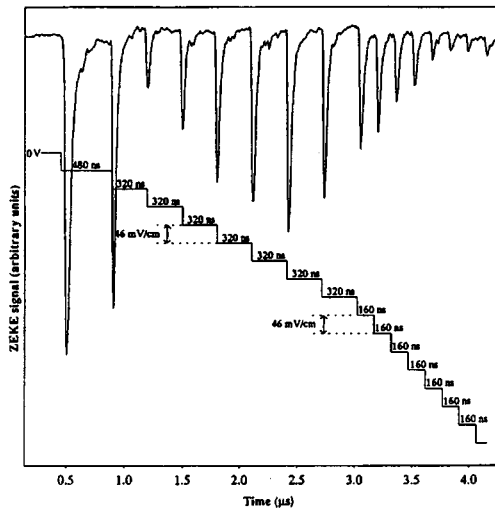


Figure 2.15 Shape of the multistep extraction pulse and resulting electron time-of-flight pattern. Each step changes the field strength by 46 mV/cm. The first laser populated the $S_1, 6^1 E_{1u}$ ($J' = 4, K' = 4, + l$) intermediate rovibronic level; the second laser was tuned to an energy of $35\ 948 \text{ cm}^{-1}$ (after frequency doubling). Each peak in the electron time-of-flight signal corresponds to a step of the extraction pulse. (Redrawn from Lindner *et al.*, 1994)

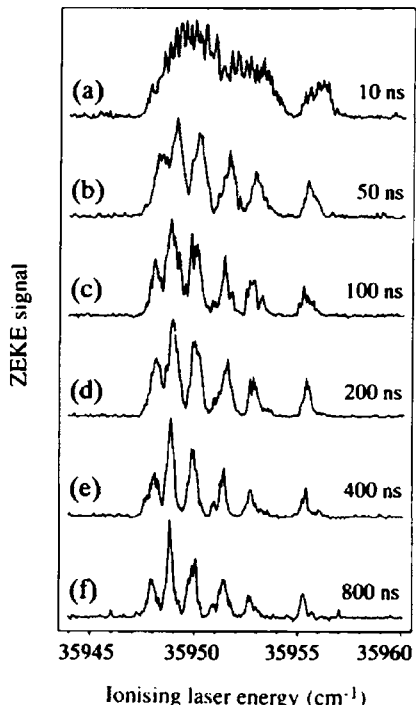
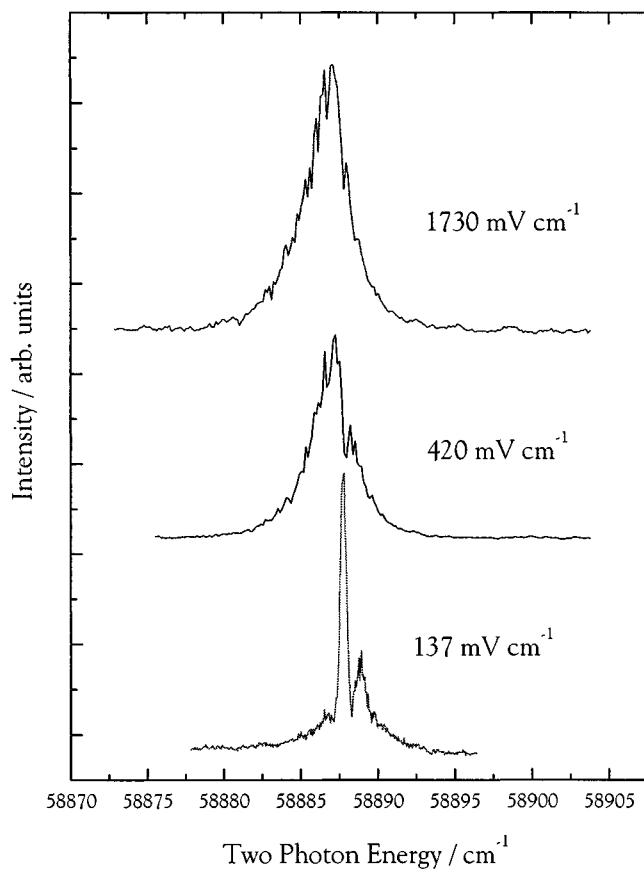
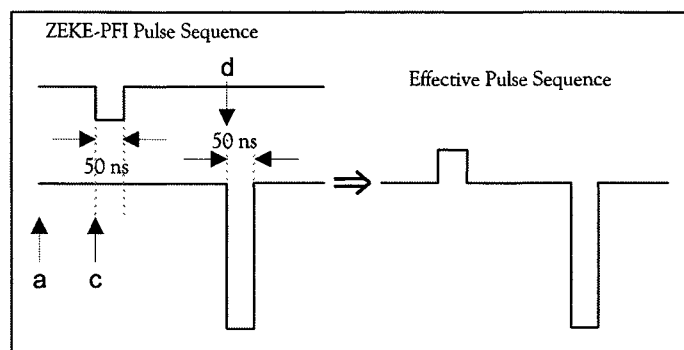


Figure 2.14 Spectral resolution of ZEKE detection as a function of the rise time of the extraction pulse. The spectrum of the $D_0, 2^2 E_{1g} \leftarrow S_1, 6^1 E_{1u}$ ($J' = 2, K' = 2, + l$) transition of benzene was recorded using 1 + 1'-two-colour-REMPI. The rise time was varied from 5 to 600 ns but the final field strength was kept at 600 mV/cm. The width of the detection time gate was kept constant (20 ns). (Reproduced from Lindner *et al.*, 1994)

¹⁰ R. Lindner, H.J. Dietrich and K. Müller-Dethlefs, *Chem. Phys. Lett.*, **228** (1994) 417.

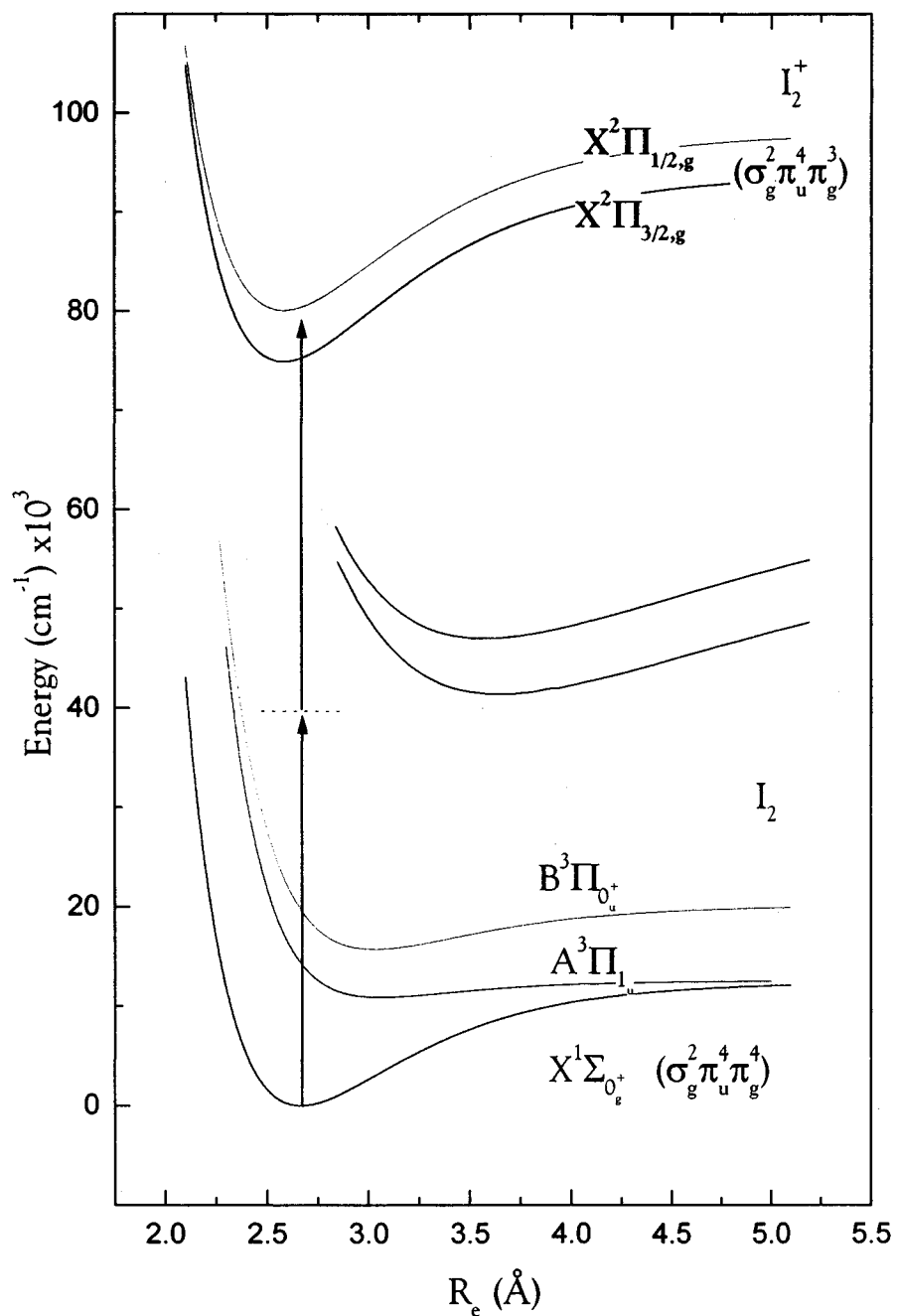
- Double inverted pulses ($< 0.5 \text{ cm}^{-1}$)

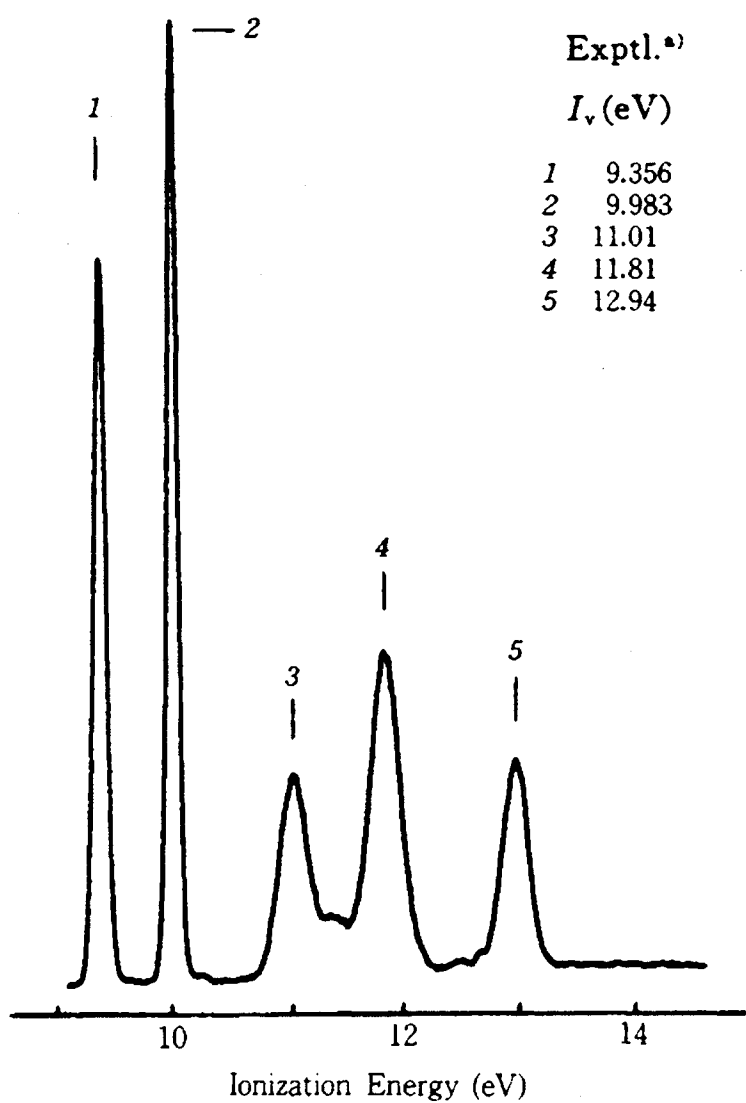


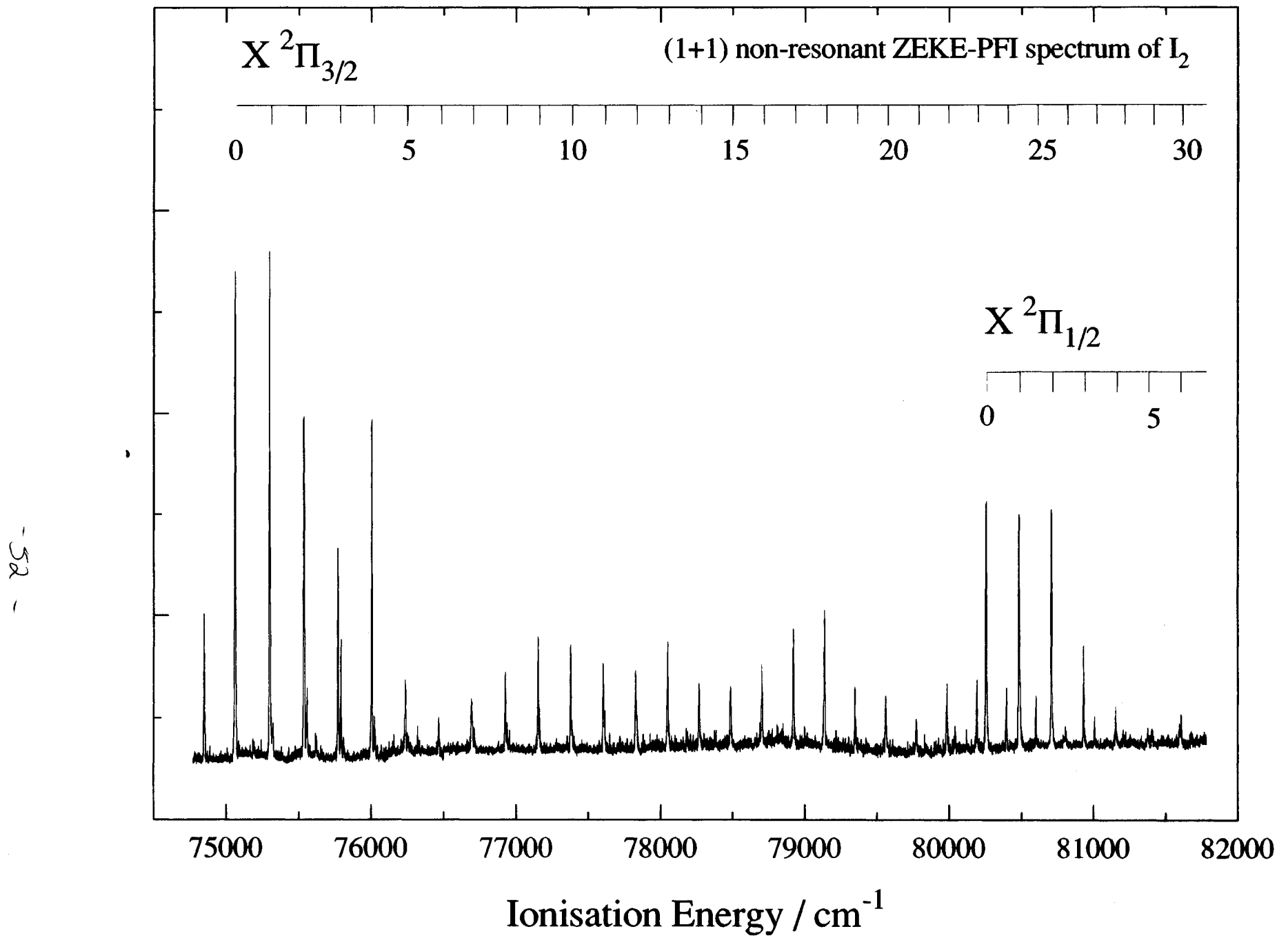
ZEKE spectra of DABCO¹¹ recorded at field strengths ranging from 137 mV cm^{-1} to 1730 cm^{-1} .

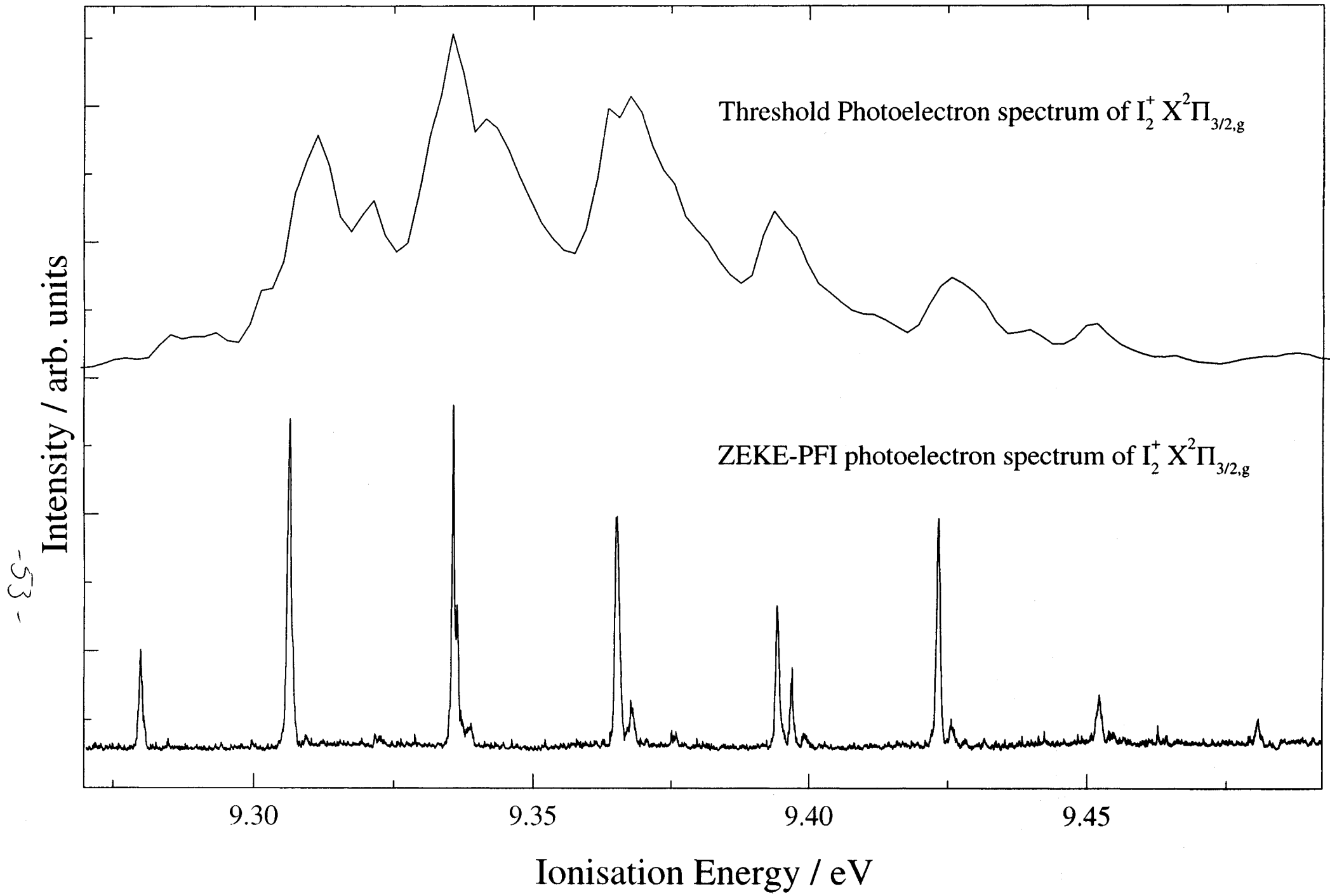
¹¹M.J. Watkins and M.C.R. Cockett, *J. Chem. Phys.*, **113** (2000) 10560.

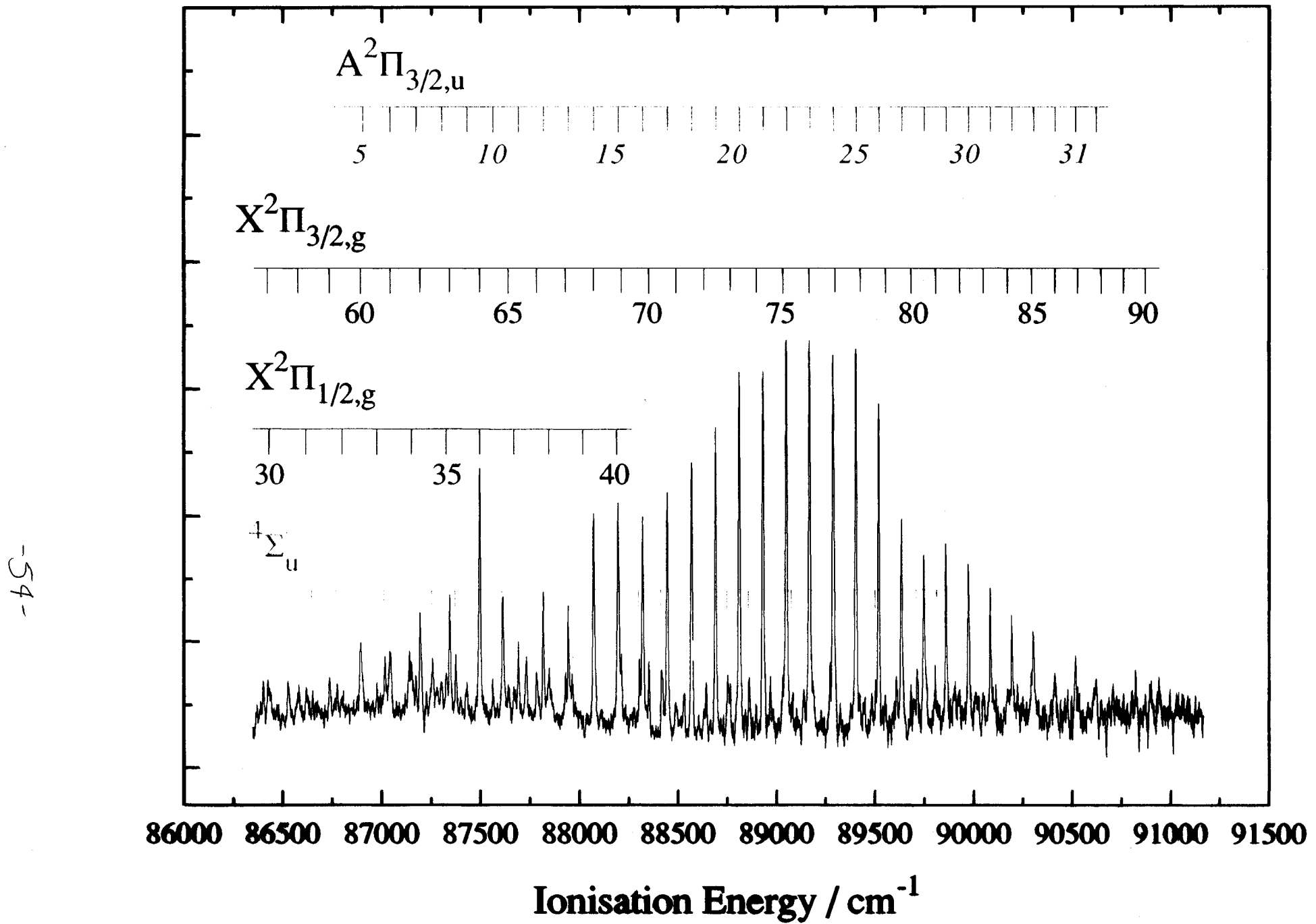
Non-resonant multiphoton ionisation: The ZEKE spectrum of Molecular Iodine

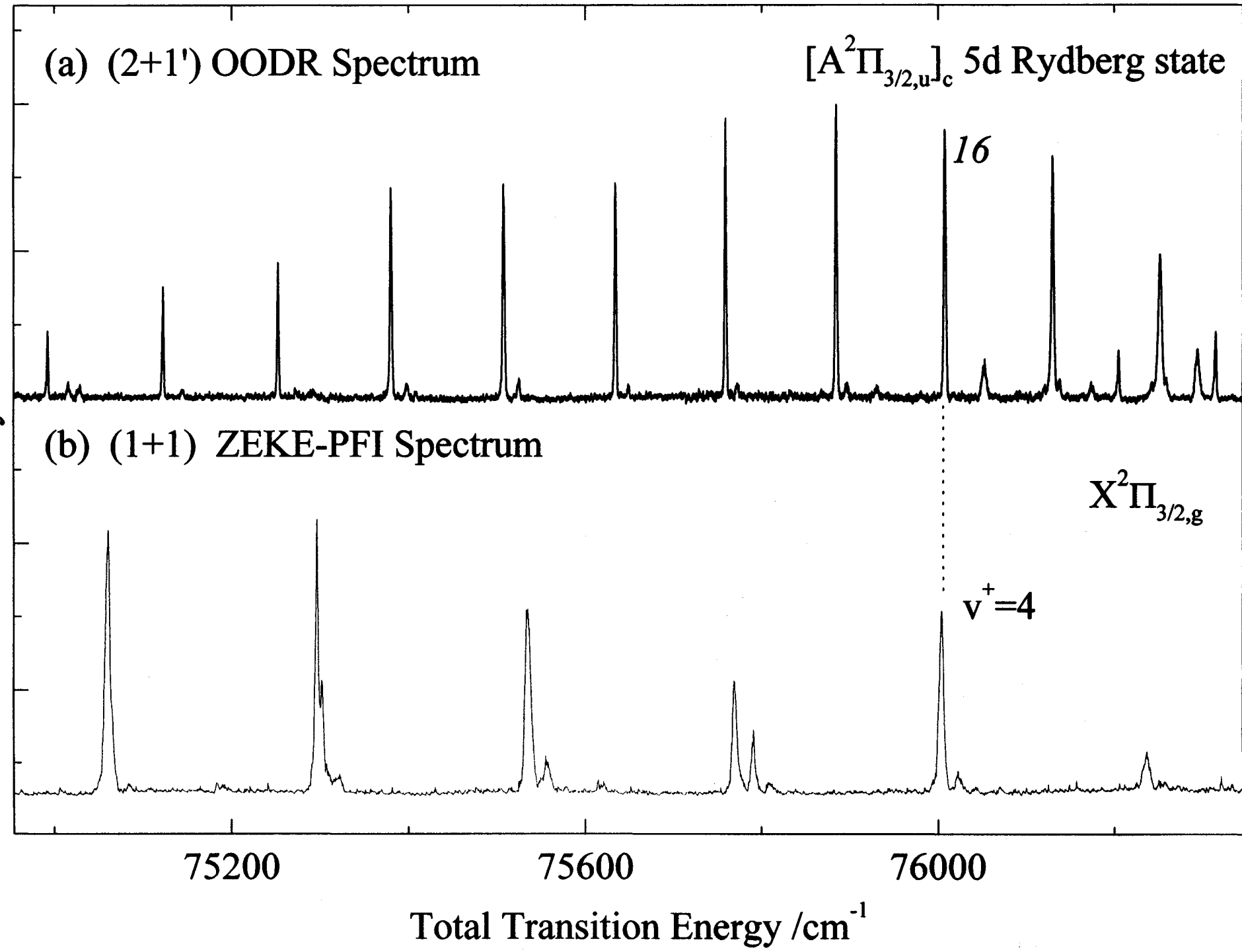


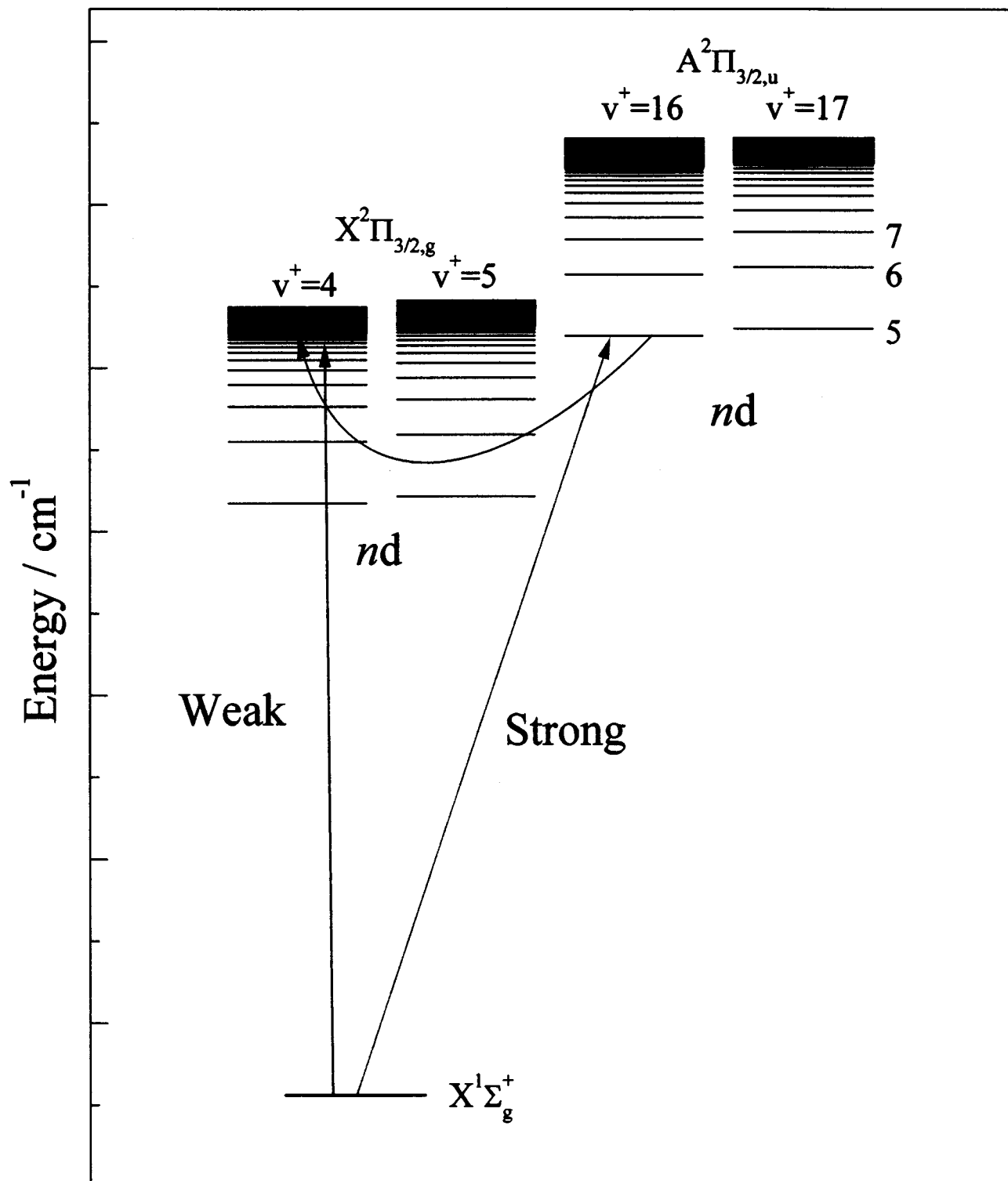






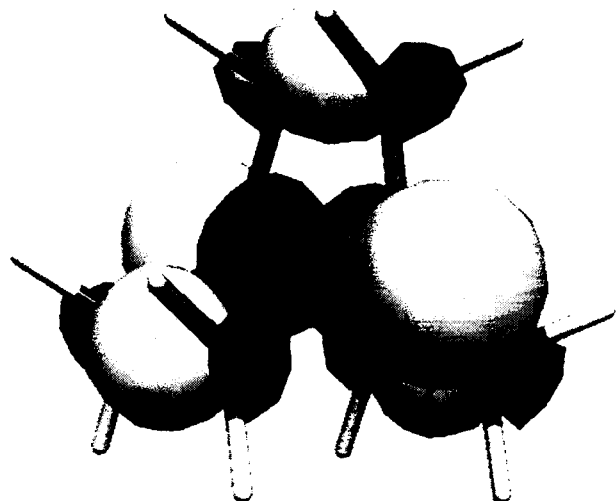






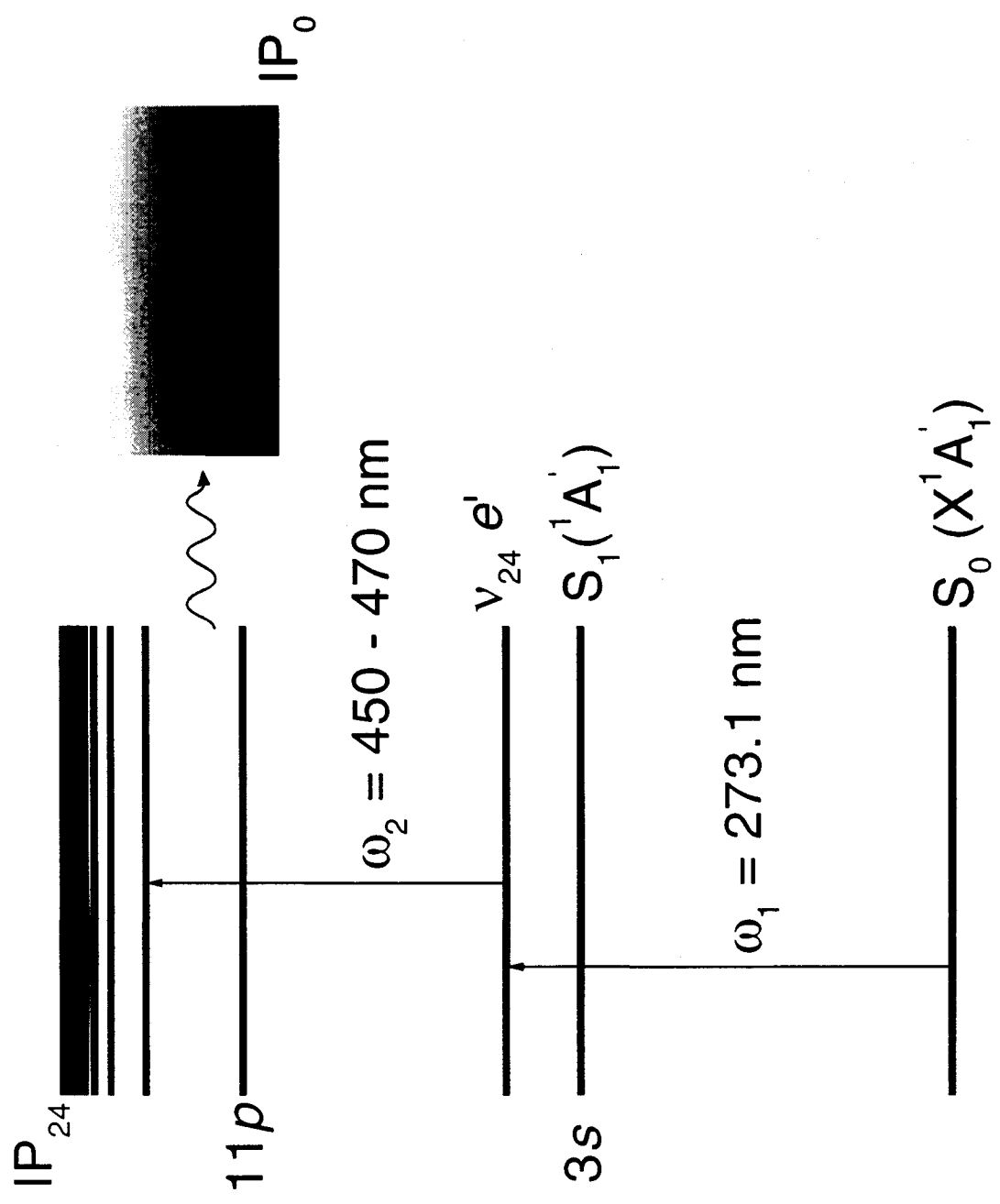
DABCO (RHF cc-pvdz)

HOMO

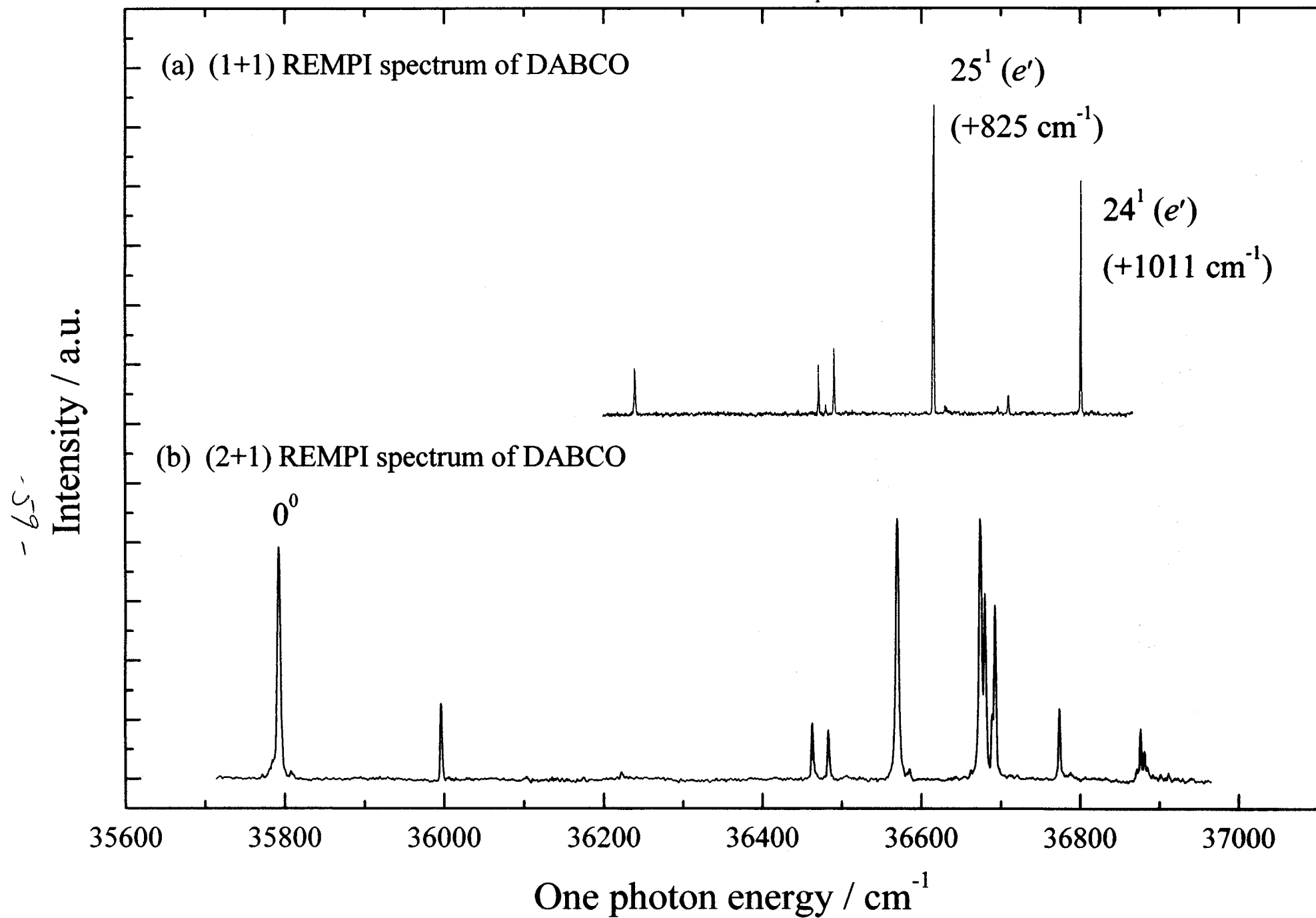


LUMO

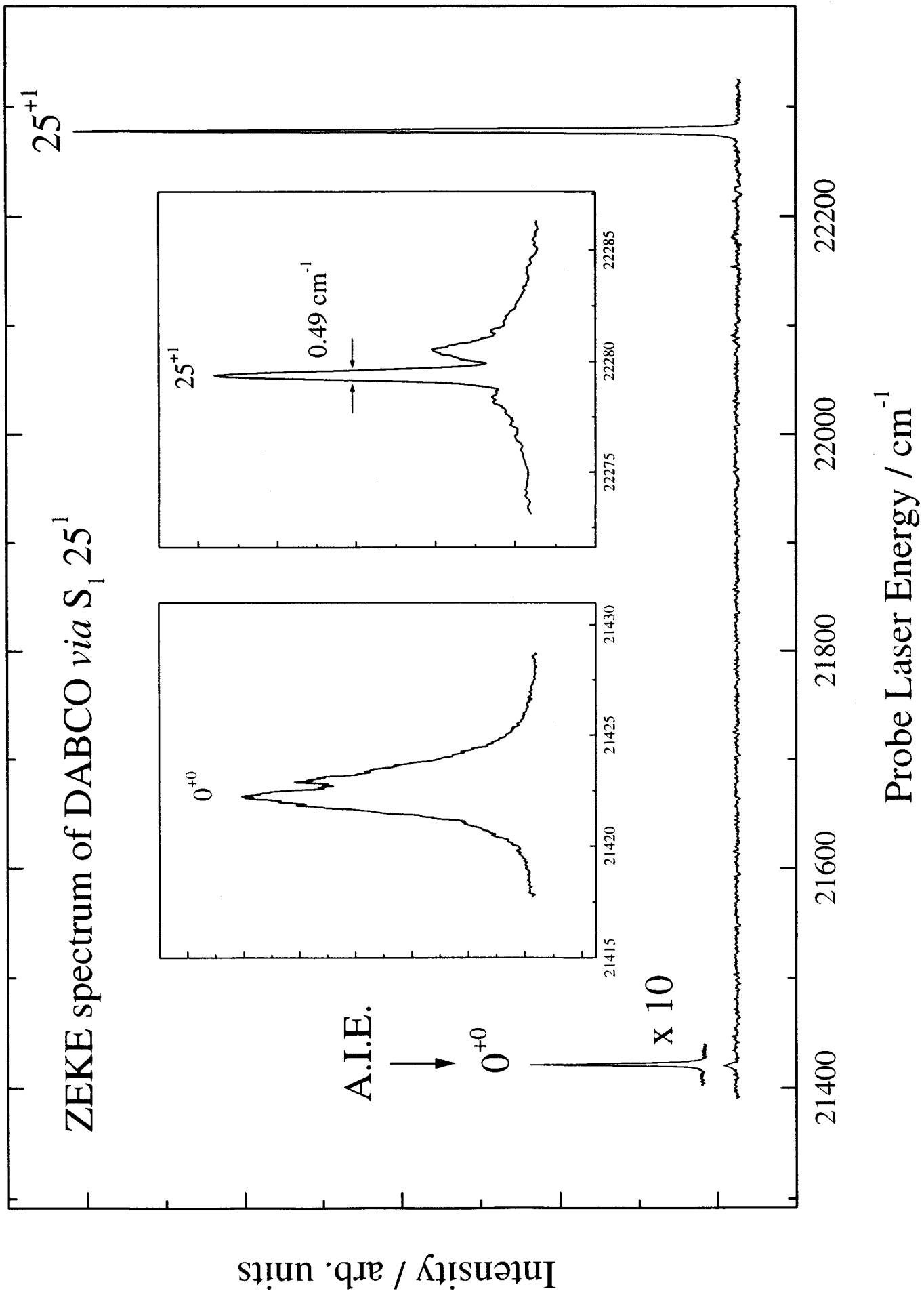


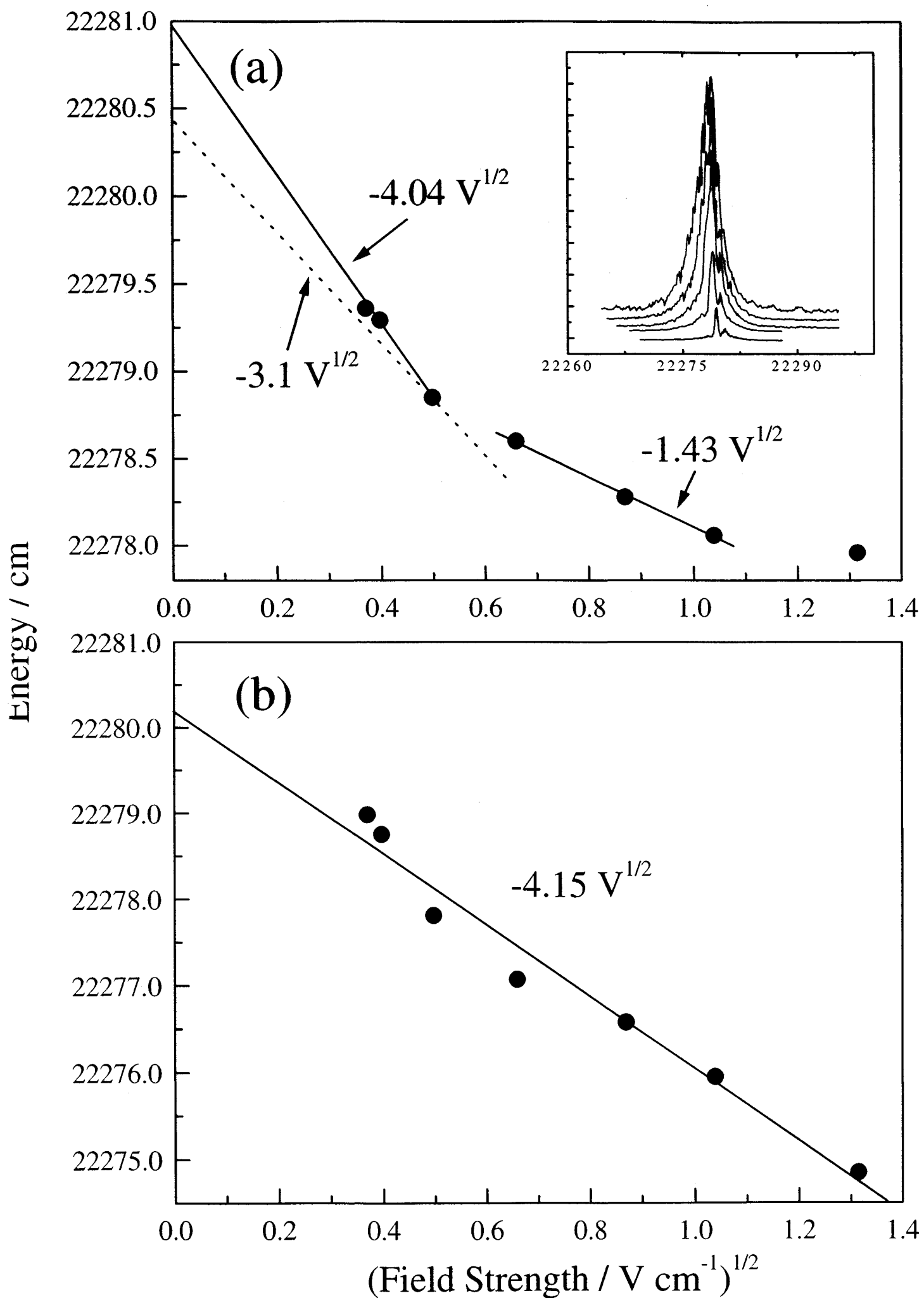


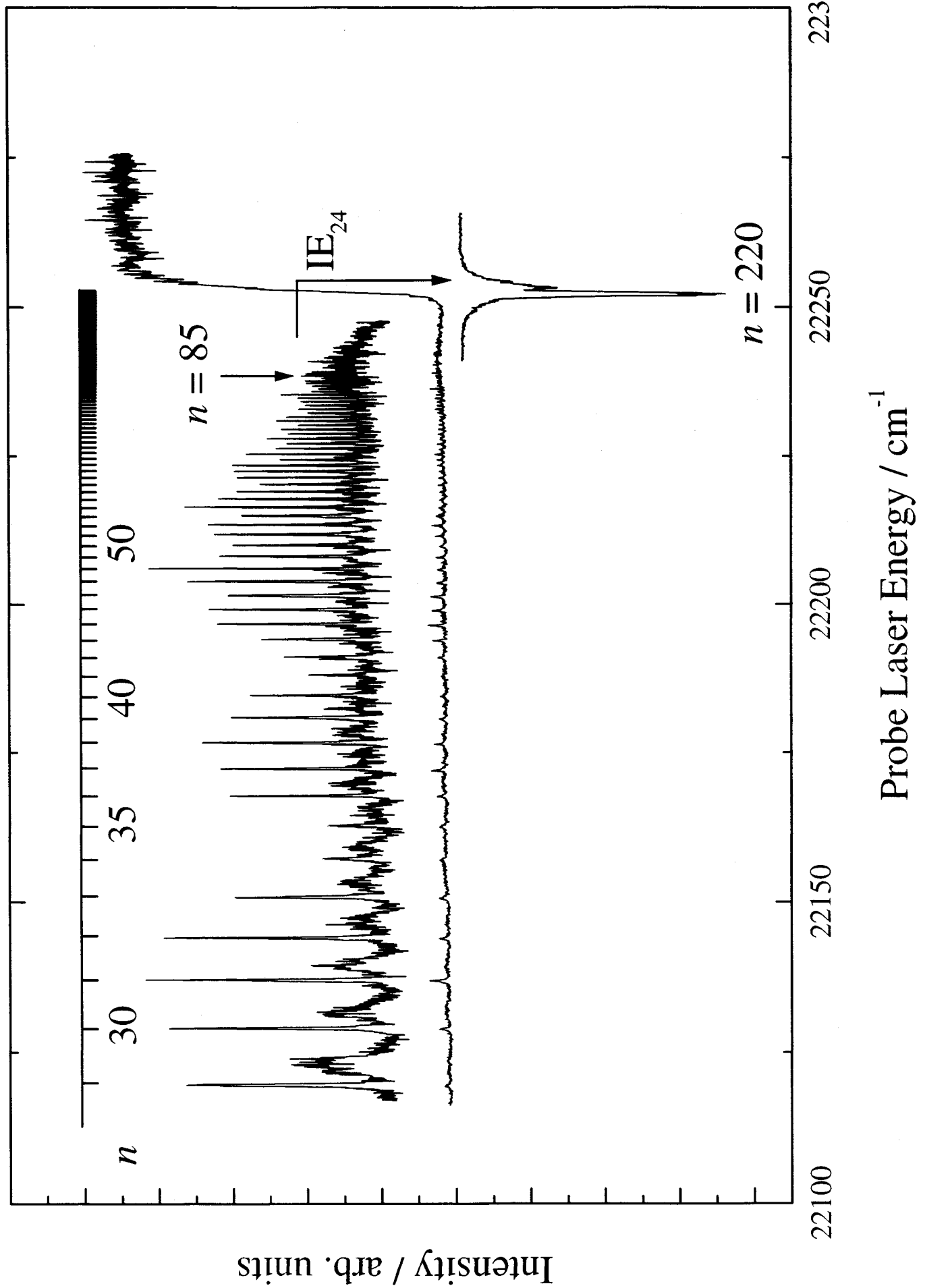
One and two photon REMPI spectra of DABCO 1A_1 (3s+)



ZEKE spectrum of DABCO via S_1 25^1

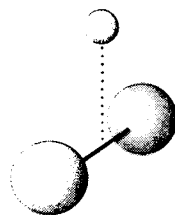






The van der Waals Interaction

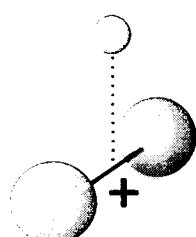
The Neutral



The dominant attractive force between neutral species is the Dispersion Interaction

$$V = -\frac{3}{2} \frac{\alpha' M \alpha' Rg}{r^6} \left(\frac{I_M I_{Rg}}{I_M + I_{Rg}} \right)$$

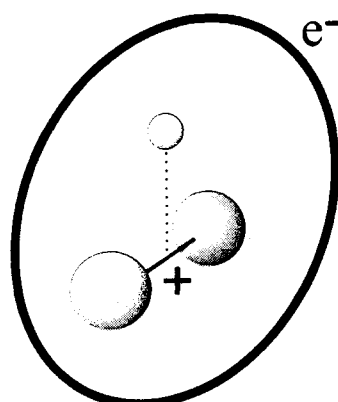
The Ion



In addition to the dispersion interaction, charge induced dipole forces assert themselves

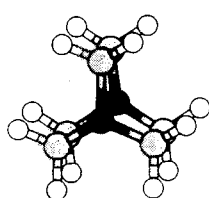
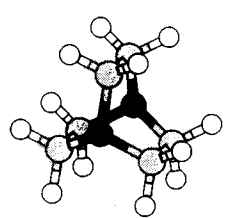
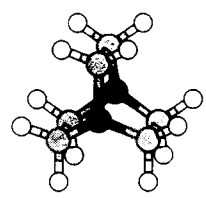
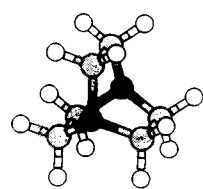
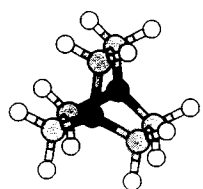
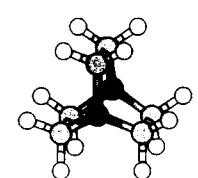
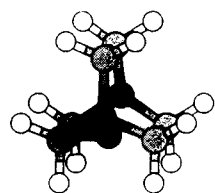
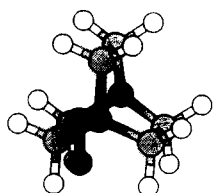
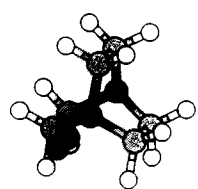
$$V = -\frac{\alpha Rg}{2} \left(\frac{e^2}{(4\pi\epsilon_0)^2 r^4} \right)$$

Rydberg States



Depends on n, l

HOW?

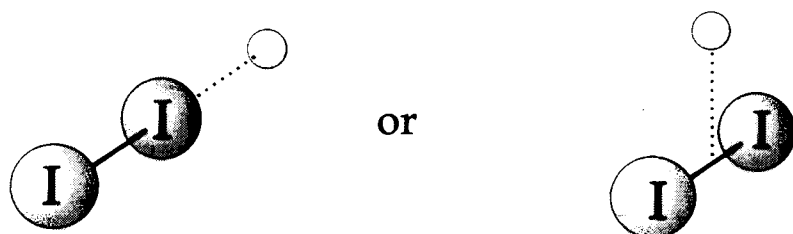


QUESTIONS

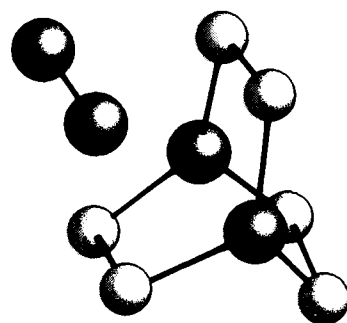
- What is the relationship between n and ℓ of the Rydberg electron and the binding energy of the complex?
- Can the formation of different isomers help us to learn more about the interaction?
- How stable are very high- n Rydberg states to solvation?

EXAMPLES

(a) I₂-Ar

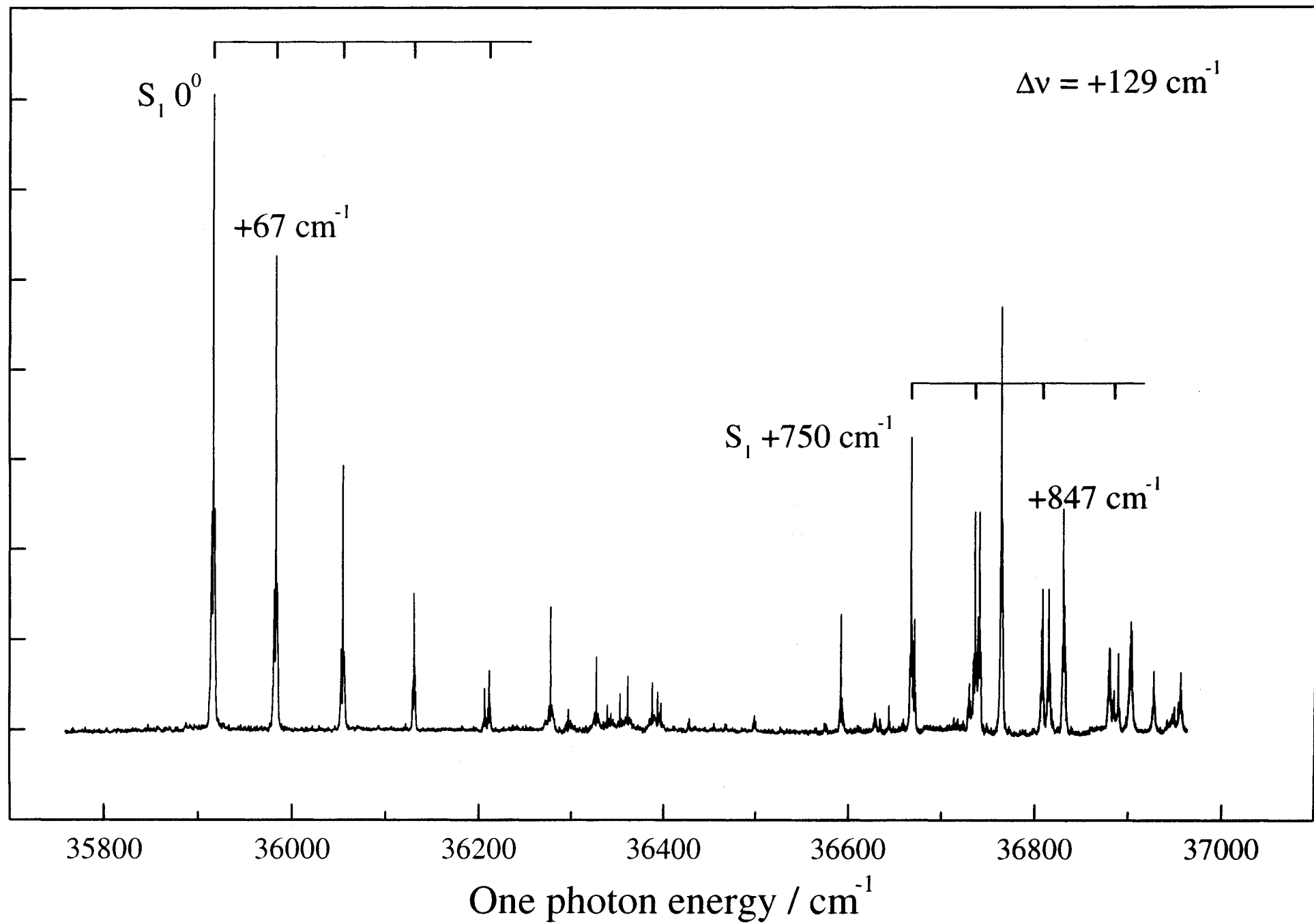


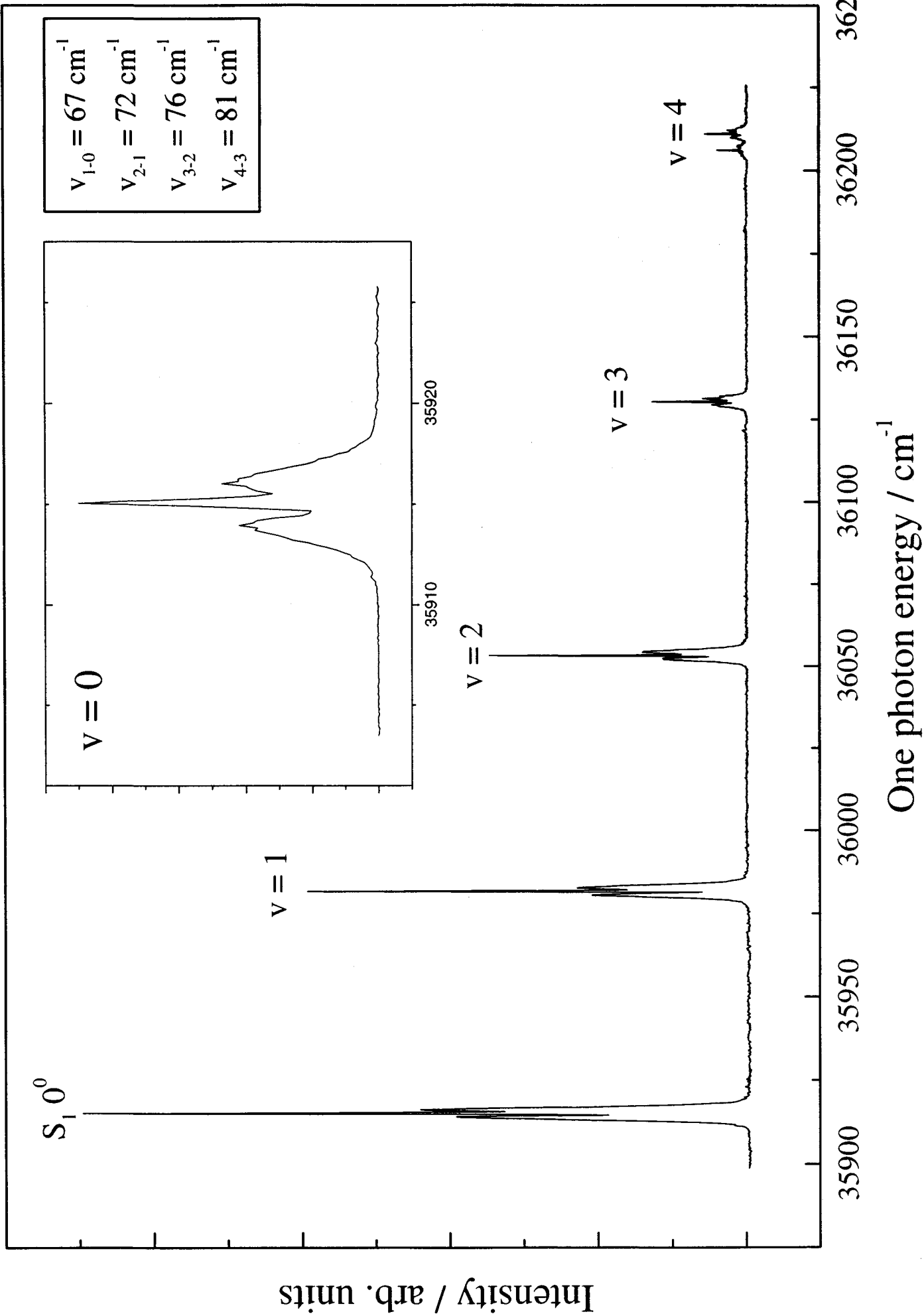
(b) DABCO-N₂



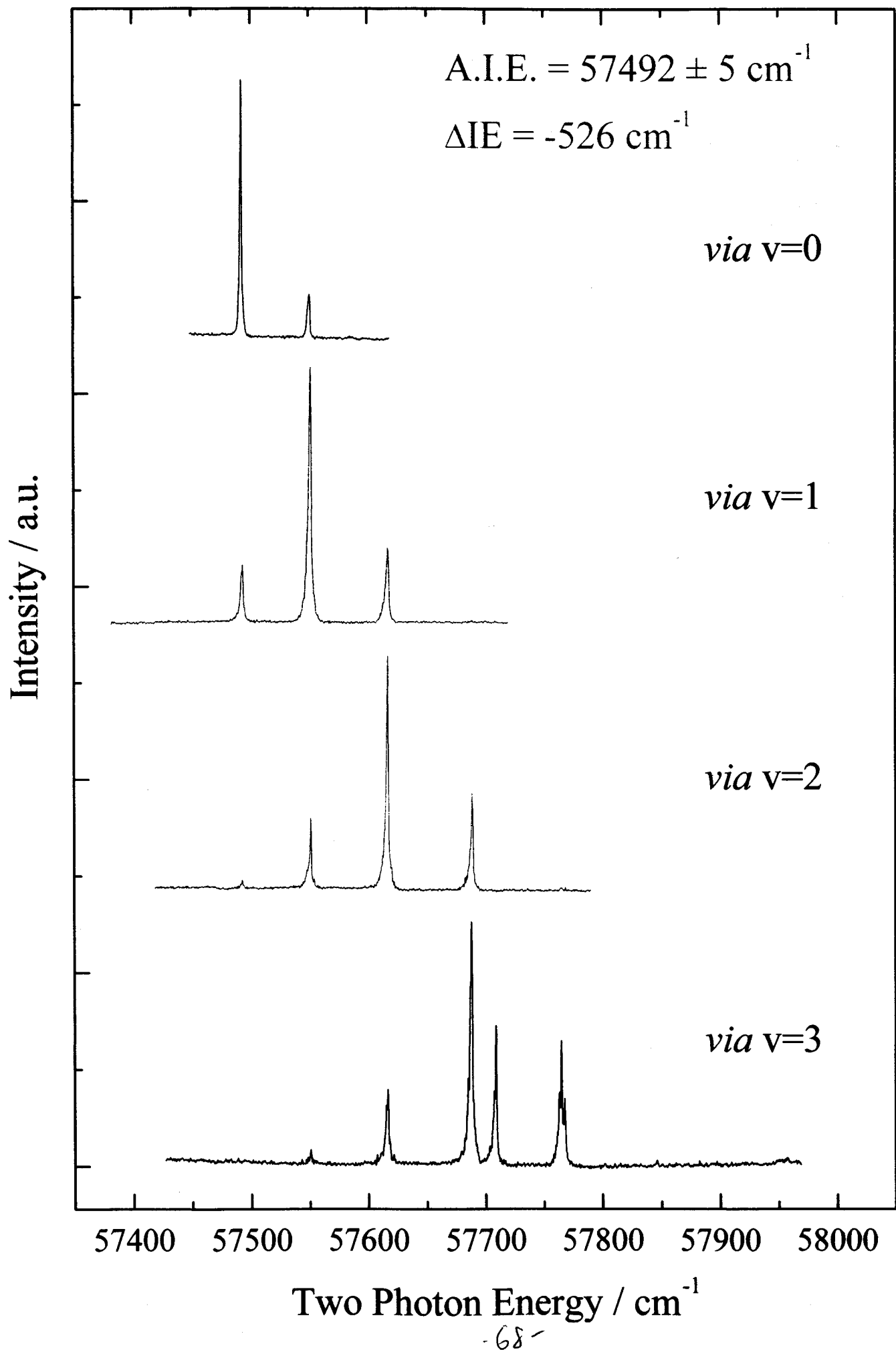
DABCO-N₂ (1+1') REMPI spectrum

- 97 -





DABCO-N₂ zeke spectra *via* $^1A'_1$ (3s+)



via S_1 ($v = 3$)

$V_{1-0} = 58 \text{ cm}^{-1}$
$V_{2-1} = 66 \text{ cm}^{-1}$
$V_{3-2} = 72 \text{ cm}^{-1}$
$V_{4-3} = 77 \text{ cm}^{-1}$
$V_{5-4} = 81 \text{ cm}^{-1}$

$v^+ = 3$

$v^+ = 3$

+ 217 cm^{-1}

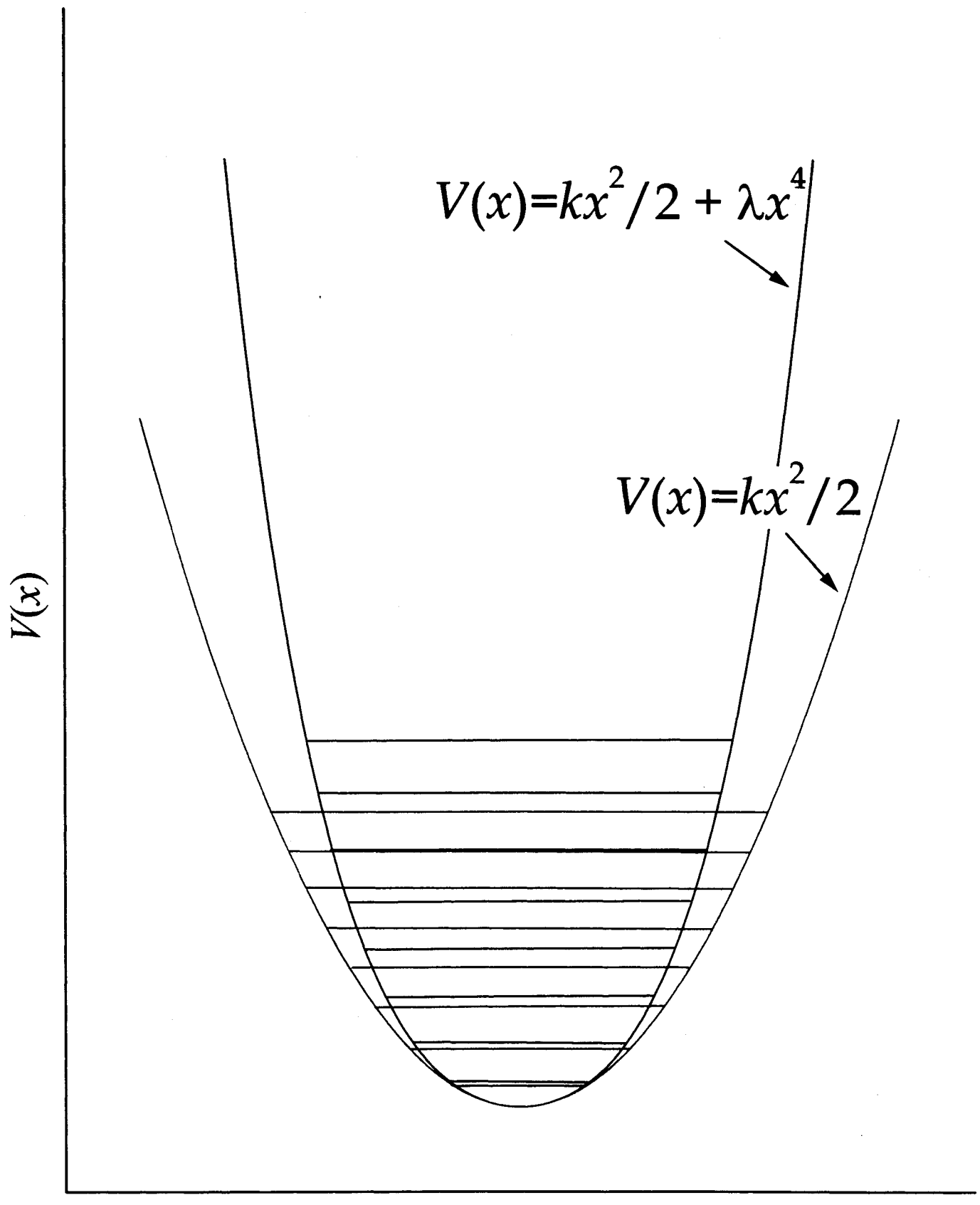
$v^+ = 4$

Intensity / arb. units

IP_0

+ 465 cm^{-1}

Two photon energy / cm^{-1}



THE UNIVERSITY *of York*

Acknowledgements

York
Mark Watkins
Klaus Müller-Dethlefs

Edinburgh
Jon Goode
Robert Donovan
Kenneth Lawley

and

££
The Royal Society
The University of York
The EC Science Programme
EPSRC